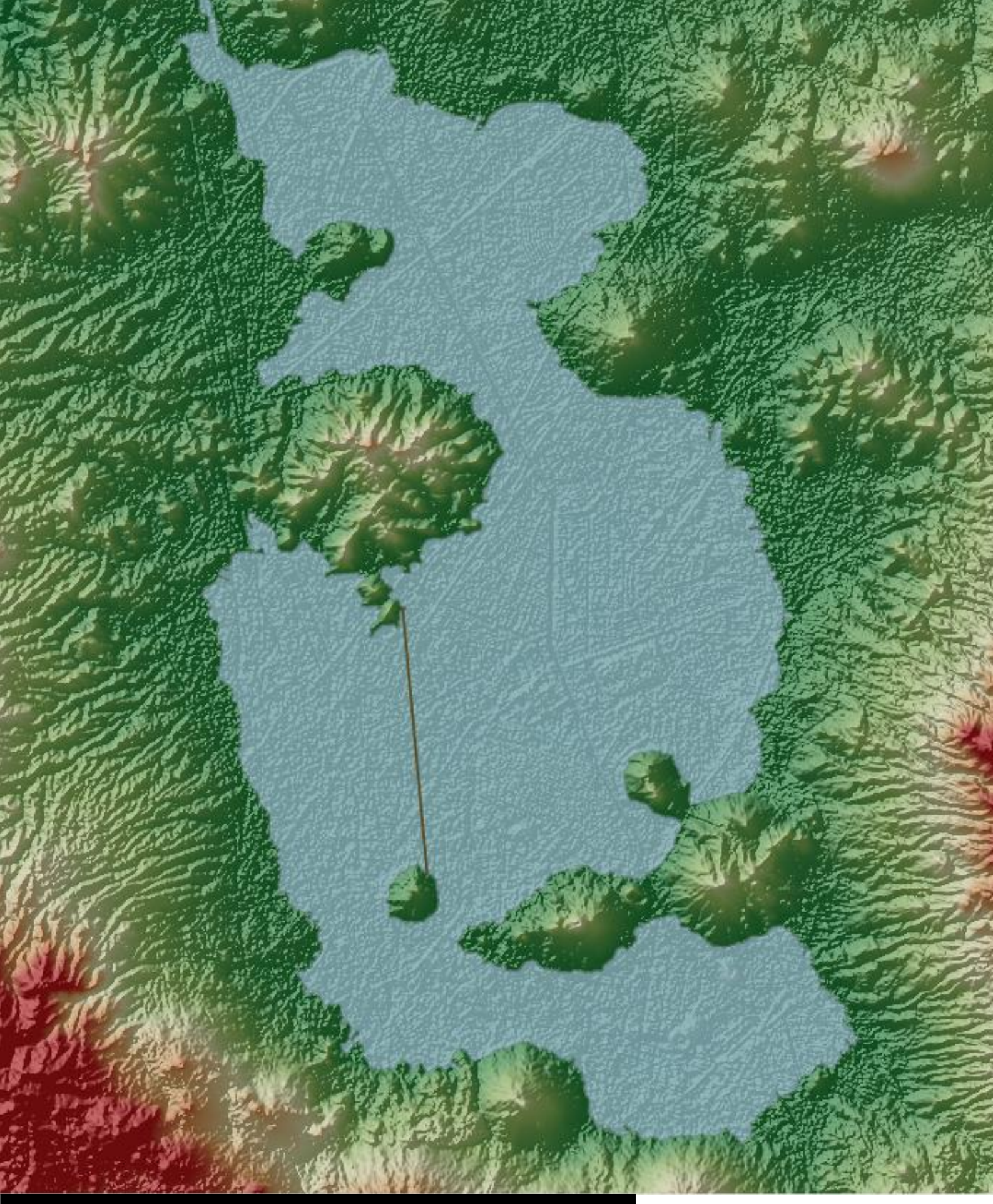

# Reliability Analysis of the Nezahualcoyotl Dike in the Aztec City of Tenochtitlan

G.A. Torres Alves

TU Delft

# Reliability Analysis of the Nezahualcoyotl Dike in the Aztec City of Tenochtitlan

By

GINA ALEXANDRA TORRES ALVES

in partial fulfillment of the requirements for the degree of

**Master of Science**
in Civil Engineering (Track Hydraulic Engineering)

at the Delft University of Technology,
to be defended publicly on Friday, October 12th, 2018, at 09:30 AM.

Thesis committee:

| | |
|---|---|
| Dr. Ir. O. Morales-Nápoles | TU Delft, chair. |
| Dr. Ir. B. Hofland | TU Delft |
| Prof. Dr. Ir. S.N. Jonkman | TU Delft |

# Preface

This thesis is the last step to achieve my Master's degree in Hydraulic Engineering at the TU Delft, with a specialization in Hydraulic Structures and Flood Risk. These past two years in the Netherlands have been a continuous learning experience in every aspect of my life.

First of all, I would like to acknowledge the funding through the "Becas de Excelencia 2015" Scholarship, from the Ecuadorian Secretary of Superior Education, Science, Technology and Innovation (SENESCYT).

This MSc thesis represents the first outcome from a challenging but very fun research that took place in the last months of my Master studies. I would like to thank my daily supervisor and chair of the thesis committee dr. ir. Oswaldo Morales Napoles for inviting me to participate in this thesis and his support during this whole process. His trust in my work helped me to get through the moments where I doubted myself the most. I appreciate all the conversations and advice. I'm glad that I did not only got a great supervisor but also a colleague and a mentor. Also, I would like to thank Dr.ir Bas Hofland and Prof. dr. ir. Bas Jonkman for being so enthusiastic about this thesis, for helping me to look at different perspectives and for their knowledge and experience. Finally, I would like to thank Prof. dr. ir. Markus Hrachowitz for helping me understand the complex nature of hydrology, which was a vital part of this work.

During my time in The Netherlands, I realized the value of true friendship and love. I learned how distance can lead people to grow apart but also how some bonds grow so much stronger. Distance is the true teacher in life. The support from my family and friends in Ecuador was vital when I was feeling homesick or defeated after my intense study sessions. Their messages, videos, photos, and good wishes were the fuel to keep me going. This thesis is dedicated to my mom, sister, and brother. I'm grateful that we never passed a day without talking even though at some point we all were in different parts of the world. Thank you for the long calls and the infinite laughs that have always characterize our family, but most of all, I would like to dedicate, not only this thesis but these last two years to my dear Dad, my "Cachito", who I hope is watching me from heaven and feeling proud of me. That would be my biggest achievement of all.

Finally, I would like to thank all the friends I made during my time in Delft. We went through the saddest winters and the happiest summers, we spent long nights studying but also we shared so many happy memories that I will always keep with me. I want to specially address this lines to my closest friends in Delft or as I like to call them "My Mexican family": Gaby, Arturo, Efra, Wendy and Gaby P. Thank you for the home-cooked meals after school, thank you for the "novela" nights, thank you for the long conversations, for listening when I was troubled, for seeing me cry but also for lifting me up and believing in me. Thank you for teaching me so much about the Mexican culture and history, which is the heart of this thesis. Thank you, my dear friends, we were all in this together and we managed to make it through successfully. I'm sure our friendship will last forever and I hope we could see each other soon.

Gina Torres Alves
Delft, October 2018

# Abstract

Before the Spanish conquest of Mexico, around the year 1519, the Valley of Mexico was a closed basin. As a result, at the bottom of the valley, an extensive system of shallow lakes, lagoons, and swamps was formed due to precipitation and permanent river's discharge from the Sierra Nevada mountains. This lacustrine system occupied around 1.000km$^2$ of the total surface of the valley. Lakes Zumpango, Xaltocan, Chalco, Xochimilco, Texcoco, and Mexico were distinguished. The capital of the Aztec empire, Tenochtitlan, was founded and built on an island in the middle of Lake Mexico.

The Aztecs were known for their impressive constructions and hydraulic structures. At the time of the Spanish conquest, they had a complex system of approximately 95 hydraulic structures (Palerm, 1973), of which the most impressive one was the Nezahualcoyotl dike. This structure was roughly sixteen kilometers long, eight meters' height and three and a half meters' width. Its principal function was to protect the city of Tenochtitlan from high water levels in Lake Texcoco.

Nowadays, there are no remains of the dike and most of the lakes were drained. The purpose of this thesis is to characterize the lacustrine system and the Nezahualcoyotl at the time of the Spanish conquest of Mexico City dike by using historical documentation and present-day climate and terrain data. This in order to assess the reliability of the dike as a flood defense mechanism and to compare it to modern safety levels. The dike was tested for one failure mechanism: Overflow. A Markov chain and Copula models are proposed in order to create a synthetic time series of precipitation and evaporation. Through a hydrological balance, the water elevation at Lake Texcoco was obtained. In this way, it was possible to provide an estimation of the water level fluctuation in the lake each year during the wet season. In total, a thousand years of synthetic data were generated.

The results of this work show that the water levels in the lake system presented by Palerm (1973) and Bradbury (1971) match the water levels obtained from a spatial analysis applied to the region. The model was able to reproduce to a good extent the hydrology of the system resulting in a 0.003 probability of failure (PF) for the dike. In other words, a 0.3% chance of being overflown in any one year. Additionally, the model used to assess the reliability of the dike showed to be very sensitive to the tributary area of the basin, and to the existing water level in Lake Texcoco at the beginning of the wet season. It is also recommended to extend this research by taking into account the possibility that the dike could have had gates that would have allowed to control water levels to a certain extent and also to take into account the role of the water level fluctuations at the other five lakes. Ultimately a full analysis that characterized to the best possible manner the complexity of the lake system and its highly intervened nature would be desirable to understand the engineering capabilities of the Aztecs.

To the author's knowledge, this is the first time that an attempt is made to compare the Aztec design criteria with present time standards. This research illustrates, from an engineering point of view, the possible design criteria of the Nezahualcoyotl dike and the uncertainties surrounding it. This work can be used as a guideline to assess the reliability of other ancient structures or present-day constructions all over the world whose design is largely based on informal criteria where information for the reliability assessment is scarce.

**Keywords:** Nezahualcoyotl, Texcoco, Tenochtitlan, dike, overflow, copulas, hydrological balance, water level, synthetic time series.

# Contents

# List of Figures

# List of Tables

# 1. Introduction

## 1.1 Background

Many centuries ago in Mexico, the first people to inhabit the country were the ones that managed to live near the banks of the rivers, lakes or lagoons. By finding ways to take advantage of the water and to defend themselves from it, hydraulic engineering in Mexico was born. This thesis is focused around the XVII century when one of the most formidable cultures of Mesoamerica flourished in central Mexico: The Aztecs.

The capital of this empire was Tenochtitlan and it was built in islands surrounded by a system of lakes in what is today Mexico City. The first inhabitants of the city depended on the lake and the closest springs, however as the population grew and the urban area expanded, the existent sources of water were not enough anymore so they were forced to get water from other places. For this reason, the necessity of hydraulic structures was inevitable (Peña Santana & Levi, 1989).

It follows that the evolution of hydraulic engineering in Mexico is directly related to the evolution of the country itself. Therefore by exploring the problems the Aztec's population had to deal with (floods), together with the necessities they had to satisfy (water supply), it is possible to determine the circumstances that lead to the surge of their impressive hydraulic structures (Peña Santana & Levi, 1989).

Among the structures built by the Aztecs and that were fully operational until the time of the Spanish conquest, the following can be distinguished (Rabiela, Ruiz, Licea, & Social, 2009): Dikes, walkways-dikes, canalized rivers, canals, aqueducts, irrigation ditches, drainage works, drawbridges, piers, ponds, pools and navigation channels. The purpose of these constructions was to avoid floods, to regulate the water levels in the lakes, to control the drainage in the catchment, irrigation, navigation, transport, and even war.

The Mexico Basin has an area of 9600 $km^2$ and the land that surrounded the lakes was once covered with forests, bushes, pastures, and water. In the XV century six historic lakes laid in this valley: Chalco, Xochimilco, Texcoco, Xaltocan, Zumpango and Mexico, the latter was an artificial lake (Medina A, 2010). In the islands within the lakes and in its shores, many villages were established: The Chalcas, Xochimilcas, Tepanecas, Mexicas, Toltecas, Chichimecas and the Acolhuas.

Around 1447, Moctezuma I, the ruler of the city of Tenochtitlan, asked Nezahualcoyotl, the lord of Texcoco, to build a levee that could contain the waters from Lake Texcoco to avoid floods in the city (Medina A, 2010). Nezahualcoyotl was known as the biggest constructor of hydraulic structures and landscaping at local and regional scale in the Mesoamerican era. Following Moctezuma's orders, he designed and supervised the construction of the levee that was named after him and which became one of the most extraordinary infrastructure developments at the time.

The Nezahualcoyotl dike had a length of approximately 16 Km and divided Lake Texcoco from north to south, forming Lake Mexico at its west side. The dike prevented trespassing of the saline water from Lake Texcoco towards Lake Mexico where the city of Tenochtitlan was located.

This research will analyze levee failure mechanisms commonly considered in risk and reliability assessments in the Netherlands and other countries. That is Overflow, Wave overtopping, sliding of the inner slope, shearing, sliding of the outer slope, micro-instability, and piping. Focus will be given to the most relevant to the Nezahualcoyotl's dike (overflow) in order to perform the reliability analysis and compare its design criteria to present day hydraulic structures.

## 1.2 Problem Statement

Floods are considered the most common natural hazard and third most damaging globally after storms and earthquakes (Wilby & Keenan, 2012) they are defined as a temporary covering of water outside its normal confines (FLOODsite-Consortium, 2005; cf.Munich Reinsurance Company, 1997). This natural hazard has been a matter of concern for humans since ancient times and the Aztec Empire was not an exception. However, during the Mesoamerican era, people did not count with the advanced tools and techniques of which we rely on nowadays, for example, international normative for construction of dikes, measurement, and processing of environmental data, complex computer software, modern machines for the construction of the dikes, etc.

The layout of the dike and the water levels at the lakes are uncertain, consequently, information about the performance of the dike, and flood events in the region is limited. This thesis will, therefore, investigate the possible design criteria of the Aztecs' hydraulic infrastructure.

## 1.3 Research Objectives

In particular, this thesis aims at performing a reliability analysis on the Nezahualcoyotl dike in order to assess the level of safety and the design criteria of this structure as a flood defense and compare it to modern safety standards.

For this main goal the following thesis objectives arise:

- To reconstruct the dike by characterization of its materials and construction techniques.
- To analyze the levee failure mechanisms applicable to the Nezahualcoyotl dike.
- To generate water levels at Lake Texcoco using a copula model considering present-day data of precipitation and evaporation.
- To perform a reliability analysis considering the most relevant failure mechanism of the dike.
- To identify which factors or variables have the largest influence on the reliability.
- To compare the reliability of the dike with modern safety standards.

## 1.4 Contribution of this Study

The Nezahualcoyotl dike was one of the most impressive hydraulic structures of the Mesoamerican Era in Mexico, yet very little or nothing is known about how safe it was. Therefore, this thesis aims, by means of a reliability analysis, to assess the design criteria employed by the Aztecs in the Nezahualcoyotl dike using probabilistic tools and estimations of different levee failure mechanisms. This analysis will allow gaining more information about the dike from an engineering point of view.

Nowadays, there are no remains of the Nezahualcoyotl dike in Mexico nor of the lacustrine system. Thus, information about its materials and construction techniques will be reconstructed from historical data and information of similar structures like the walkway-dikes or the aqueducts that used to surround the city of Tenochtitlan. To characterize the lake system, present-day data of precipitation, evaporation, topography, and wind will be used. However, information about the water levels in the lake is not available. The generation of this information is one of the many challenges presented in this thesis. In the following chapters, it will be shown how these problems were to a good extent overcome.

The methodology and results from this thesis can be used as a starting point for further and more complex assessments in the Nezahualcoyotl dike and its functionality. Furthermore, as this thesis is directly linked to anthropology, it will contribute to bringing awareness of the historical context of this dike. In particular, this thesis contributes to the understanding of Aztec engineering.

Moreover, the methodology presented in this thesis can be used as a guide to performing safety assessment in several structures from ancient cultures. It may be used in present-day structures around the world designed largely in an informal manner. This with the goal of understanding the criteria under which such structures are conceived and possibly illustrate the understanding of acceptable risk for humans in different times or parts of the world.

## 1.5 Research Methodology

To fulfill the main objective of this thesis, four main steps are proposed as shown in Figure 1-1:

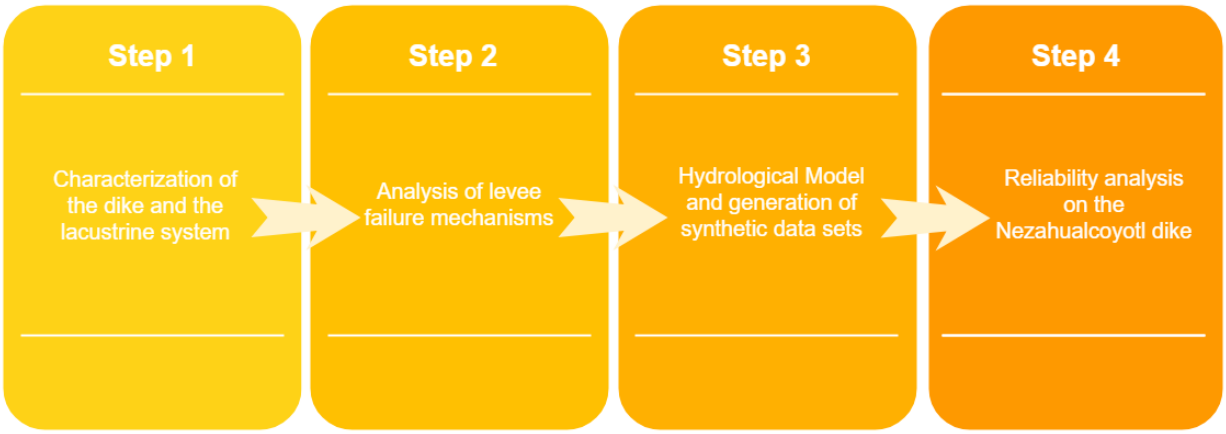


**Figure 1-1 Steps to be completed in this research.**

In step 1, a schematization of the characteristics of the dike under investigation and the lacustrine system was built from several historical sources and with present-day data. Then, in step 2, an analysis of the levee failure mechanisms applicable to the Nezahualcoyotl dike is carried out. As result of this analysis, overflow is selected as a failure mechanism to investigate in further depth. Following, step 3 presents a hydrological model constructed to simulate the environmental conditions at the valley by creating one thousand years of synthetic data sets based on present-day measurements of the variables involved (precipitation and evaporation). Finally, the fourth step aims at performing a reliability analysis of the Netzahualcoyotl dike for the selected levee failure mechanism from step 2.

## 1.6 Report Outline

This thesis is organized as follows: Chapter 2 presents a literature review that contains the most relevant topics related to this research, while Chapter 3 presents a description of the area of study; the methodology is presented in Chapter 4. The final layout of the lacustrine system and the Nezahualcoyotl dike is presented in Chapter 5. Chapter 6 and 7 discuss the results of the hydrological model and the reliability analysis respectively. Finally, the main conclusions of this work and recommendations for further research are presented in Chapter 8.

# 2. Theoretical Background

## 2.1 Reliability

There are several definitions of reliability but the definition from Bagowsky (1961) is widely accepted:

*"Reliability is the probability of a device performing its purpose adequately for the period of time intended under the operation conditions encountered"*

This definition comprises four parts: probability, adequate performance, time and operating conditions. Probability refers to the numerical information for the assessment of reliability. Adequate performance refers to the functioning of the element without a failure. This performance has to be maintained during the lifetime or a period of time of the element under the operation conditions encountered during the proposed time.

According to the Eurocode (British Standards Institutions, 2001) reliability is the ability of a structure or structural member to fulfill the specified requirements, including the design working life, for which it has been designed. It covers safety, serviceability, and durability of a structure.

Reliability (R) can be measured as the complement of the probability of failure (PF) of an element or structure (Eq. 1)

$$R=1-PF$$

**Eq. 1**

Probability of Failure is defined as the likelihood that an element would fail at a given time (Jonkman, et al., 2016). When the load S (set of forces) acting on a structure during its lifetime is larger than its structural resistance Re (capacity of a structure or a structural element to withstand actions without mechanical failure) the probability of failure can be evaluated. Resistance and load effects are often random variables, resistance of elements can vary for different materials and the loads can have spatial and temporal variation.

Loads and resistance can be represented with a probability distribution function. In this case, the probability of failure is described by Eq. 2.

$$PF=P[S>Re]$$

**Eq. 2**

The calculation of the reliability of a structure aims at keeping the probability of failure as low as possible, however, a reliability analysis focuses on the assessment of the ability of a structure to withstand anticipated and future hazards and loads during its estimated lifetime by estimating the material properties and strength capacity of the elements of the structure (Skrzypczak, 2017). Lack of reliability means that a condition with certain probability was not fulfilled.

## 2.2 Monte Carlo Simulations

In this thesis, the determination of the reliably of the Nezahualcoyotl dike will be carried out using Monte Carlo Simulations. With this method, the probability of failure is calculated exactly provided enough samples of a joint distribution may be generated. The idea behind the Monte Carlo simulation method is to use random sampling to study the properties of a system in which its components behave stochastically (Lemieux, 2009).

The Monte Carlo method is applied with the following steps:

1. The system is already described by a model, including a description of the joint probability distributions for the random variables in the system.
2. A program is created to implement this model and therefore simulate the behavior of the variables over a certain period of time.
3. Use the program to create a sample of observations.
4. Perform statistical inference on the samples to determine if the model works.

The previous is known as stochastic simulation (Lemieux, 2009).

## 2.3 Flood Defenses

### 2.3.1 Levees

A levee (or dike) is an elongated naturally ridge or an artificial fill or wall that regulates water levels (Petroski, 2006). The most important function of a dike is to retain water, so it needs to be sufficiently high to be able to withstand high water levels and wave run-up (Figure 2-1), additionally it has to be resistant to wave attack and overtopping and also needs to be stable and impermeable (Jonkman, et al., 2017).

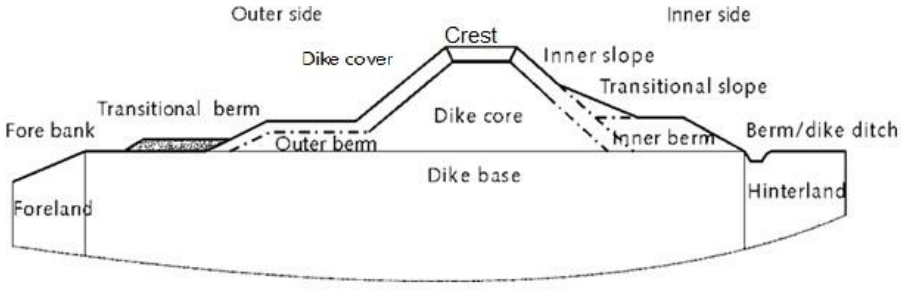


**Figure 2-1 Parts of a modern levee. (Jonkman, et al., 2017)**

One of the most important variables in a dike is the crest level, it must be high enough to withstand extreme water levels and in order to withstand wave attack dikes are covered with revetments of different types: Grass, concrete elements, stones or asphalt (Jonkman, et al., 2017).

A modern dike is composed of a combination of materials: a core of sand and a cover layer of clay. Also, modern dike design is based on design loads that change if the dike is located near the sea, a river or a lake. Additionally, the subsoil conditions, material availability, cost, local traditions, and experience are taken into account when designing a dike.

### 2.3.2 Hazards

When analyzing the reliability of a levee the first step is to identify the relevant hydraulic-hydrological conditions in the natural system, each location in the world is subjected to different phenomena, so the importance of knowing the natural system is vital. For the case of this thesis, focus will be given to the hazards that a dike can face at a lake, where high water levels and waves caused by wind set-up in combination with inflow from rivers are the main hydraulic loads (Jonkman, et al., 2017).

Hazard refers to unusual or severe events, for example anomalous environmental conditions, insufficient strength or resistance (British Standards Institutions, 2001). Hazards can originate from the natural environment or from human activity. If different hazards occur together in time and space, a situation more dangerous than one with a single hazard can emerge (Schneider, 2006). For civil structures, such hazard scenarios are common, so this concept has to be taken into account when assessing safety.

When analyzing the reliability of a structure the first step is to identify the relevant loads (S) that can act on a structure, considered as hazards.

In this thesis, the main loads for the Nezahualcoyotl dike are identified in section 3.5.

### 2.3.3 Failure Mechanisms

A modern levee system is generally composed of several elements that include levee segments and other structures (wall, spillways, gates, etc.) at system scale. Its main function is to reduce flood risk, thus, failure can be defined as the unintentional inundation of the leveed area. This failure can be either hydraulic or structural. Structural failure can induce by hydraulic failure and vice versa (CIRIA, 2013).

- Hydraulic failure (non-structural) occurs if water ingress into the leveed area (by through-flow, overflow overtopping of the levee), it occurs before the planned protection level is reached and without prior damage to the system element.
- Structural failure: Occurs by a breach in the levee system that results from damages affecting at least one system segment.

In the Netherlands, the most commonly encountered failure mechanisms are listed below. Next, a brief description of each one of them is presented according to (Jonkman, et al., 2017).

- Overflow
- Wave overtopping
- Sliding inner slope
- Shearing
- Sliding outer slope
- Micro-instability
- Piping
- Erosion outer slope
- Erosion first Bank
- Settlement
- Drifting Ice
- Collision

Overflow
Occurs when the still water level (without waves or the average level considering waves) is higher than the crest level of the flood defense and water flows to the protected area.

Wave overtopping
Occurs when the still water level is below the crest level and overtopping is purely due to waves running up the slope of the dike or directly overtopping vertical structures like flood walls. The limit state of this mechanism is based in terms of critical discharge, which depends on the sensitivity of the inner slope to erosion.

Instability of the inner slope
It is the most common mechanical stability problem in dikes. Usually analyzed with classical limit-equilibrium methods for slope stability such as Bishop or Spencer.

Shearing (Horizontal sliding)
It can occur at the base of the dike body; the main driving force is the horizontal force of the water exerted on the outer slope.

Instability of the outer slope
Occurs when the outside water level drops very quickly. The pore water inside the dike body cannot follow at the same pace and the pressure of the water inside the dike causes the outer slope to slide towards the water, this failure does not lead directly to flooding because the water level is decreasing but in a second water level rise, it can lead to flooding.

Micro Instability
Occurs when seepage water causes the phreatic surface to rise and reach the inner slope of a dike.

Piping
This failure mechanism starts to develop at the land side of the dike, if the hydraulic gradient in the subsoil towards the land side is sufficiently high, soil particles start eroding, leading to the formation of cavities or channels in the subsoil, also known as pipes, these pipes can grow till the water-side of the dike, undermining its foundation which can lead to collapse or sliding of the dike body.

Erosion of the foreshore
Occurs due slopes becoming steeper by erosion processes due to river currents or tidal currents in estuaries. Actual failure is not an erosion process but a flow-slide. Two main processes can take place in flow slides, alone and together: Liquefaction and unstable breaching.

Settlement
Certain soils are highly compressible and susceptible to consolidation, creep and settlements. After the construction of a dike, it often settles in the years after the construction. This is not a failure mechanism but needs to be taken into account in dike design.

As part of testing the reliability of a dike, is necessary to know which failure mechanisms apply to the dike. Table 2-1 shows when is required to evaluate each mechanism according to standard in The Netherlands.

| Failure Mechanism | When Evaluated? |
|---|---|
| Overflow and Wave overtopping | All levees should be evaluated on their crest height. |
| Piping | All levees with a potential piping vulnerable soil profile (Impermeable/sand boundary) |
| Macro Instability landside | Important for all levees |
| Macro Instability waterside | Important for levees that deal with extreme water level fluctuations. |
| Micro-instability | Important for levees that contain sand |
| Instability of the revetment | For levees vulnerable to wave erosion with a slope protection |
| Instability by infiltration and erosion at overtopping | For all levees, evaluated in combination with overtopping or stability of the revetment. |
| Heave | For situations with vertical sheet piles in the levee base |
| Horizontal Sliding at foundation | When peat forms a substantial part of the levee; in combination with landslide stability evaluation. |

**Table 2-1 Failure Mechanisms important in the Dutch evaluation. Modified from Ammerlaan (2007).**

Section 5.1 presents a discussion of the failure mechanisms applicable to the Nezahualcoyotl dike.

## 2.4 Markov Chains

A Markov chain is a stochastic model that describes the sequence of possible events in which the probability of each event depends only on the state attained in the previous event (Oxford Dictionary, 2018). In terms of climate data occurrence, such as precipitation, it means that the probability of rain on any day depends only on whether the previous day was raining or not. So, given the event on the previous day, then the probability of rain is assumed independent of events of further preceding days (R. Gabriel & Neumann, 1962). This model is known as a Markov chain whose parameters are the two conditional probabilities:

$$P_{11} = P\left\{wet\_day \middle| previous\_day\_wet\right\}$$
$$P_{10} = P\left\{wet\_day \middle| previous\_day\_dry\right\}$$

**Eq. 3**

As shown by the sub-indices in Eq. 3, the occurrence of a wet day is represented by the number 1 while a dry day is represented by a zero. Thus, a Markov Chain can be described by a transition matrix $P$ of the form:

$$P = \begin{bmatrix} P_{00} & P_{01} \\ P_{10} & P_{11} \end{bmatrix}$$

**Eq. 4**

Where:

- $P_{00}$ : Probability that it will not rain given that the previous day was dry (no rain).
- $P_{01}$ : Probability that it will not rain given that the previous day was wet (rain).
- $P_{10}$ : Probability that it will rain given that the previous day was dry (no rain).
- $P_{11}$ : Probability that it will rain given that the previous day was wet (rain).

Further details about Markov chain theory are presented in section 4.4.1. The results from the application of this model are shown in section 6.1

## 2.5 Copulas

When testing the reliability of a structure, environmental variables need to be considered given that they influence its analysis. Environmental variables are values of measurements for different random processes (Precipitation, evaporation, etc.)

In reality, environmental measurements can have uncertainties due to measurement limitations, therefore, data can be limited, not available or unreliable, thus, modeling of such data is needed in most cases. In nature, environmental variables are dependent on each other and this dependence also needs to be taken into account.

In the past, joint distribution models were developed using classical families of bivariate or multivariate distributions, like the bivariate normal, log-normal, gamma and extreme values distributions. However, the main limitation of these models was that the individual behavior of the considered variables must be characterized by the same parametric family of univariate distributions (Genest & Favre, 2007), therefore, in this thesis, copulas are considered as better alternatives to perform bivariate analysis on environmental variables because they avoid the restriction mentioned previously.

Copulas consist of functions that join multivariate distribution functions to their one-dimensional marginal distribution functions. They are multivariate distribution functions whose one-dimensional margins are uniform on the interval [0,1] (Nelsen, 2006). Sklar's theorem (Sklar, 1959) states that any multivariate joint distribution can be written in terms of the univariate marginal distribution functions and a copula which describes the dependence between the random variables. For the bivariate case:

$$H_{XY}(x,y) = C\{F_X(x),\ G_Y(y)\}\ x,y \in \mathbb{R}$$

**Eq. 5**

Let $H_{XY}(x,y)$ be a joint distribution with marginal distribution $F_X(x)$ and $G_Y(y)$ that lie in the interval [0,1] and a copula $C$ on the unit square $I^2$ ([0,1] x [0,1]) such that for all ( $x$ , $y$ ) Eq. 5 is satisfied. If $F$ and $G$ are continuous then $C$ is unique.

There are many copula families available, which usually have parameters that describe the strength of dependence between the variables. In this thesis the most common copulas are considered:

**Gaussian Copula:** This copula is parametrized by $\rho$, is part of the Gaussian family. It is also called the normal copula. See Eq. 6.

$$C_\rho(u,v) = \phi_\rho\left(\phi^{-1}(u), \phi^{-1}(v)\right)$$

**Eq. 6**

Where $\phi$ is the bivariate standard normal $\phi^{-1}$ is the inverse standard normal function and $\rho$ is the (conditional) product moment correlation.

**Clayton Copula:** Parametrized by $\alpha > 0$, is part of the Archimedean family and is defined by Eq. 7. This copula captures lower tail dependence.

$$C_\alpha(u,v) = \left(u^{-\alpha} + v^{-\alpha} - 1\right)^{\frac{-1}{\alpha}}$$

**Eq. 7**

**Gumbel Copula:** The Gumbel copula is parametrized by $\delta > 1$, is part of the Archimedean family. It presents upper tail dependence (See Eq. 8 below)

$$C_\delta(u,v) = \exp\left\{-\left(\left[-\ln(u)\right]^\delta + \left[-\ln(v)\right]^\delta\right)^{\frac{1}{\delta}}\right\}$$

**Eq. 8**

Copulas can be used to model various tail dependencies. Upper tail dependence is mathematically defined by the coefficient $\lambda_U$ for random variables $X_i$ and $Y_i$ such that:

$$\lambda_U = \lim_{u\to 1} P\left(X_i > F_{X_i}^{-1}(u) \middle| X_j > F_{X_j}^{-1}(u)\right) = \lim_{u\to 1} P\left(U > u \middle| V > u\right)$$

Following this definition, Gumbel copula has upper tail dependence ($\lambda_U = 1 - 2^{\frac{1}{\delta}}$) while the Gaussian copula has no tail dependence ($\lambda_U = 0$) therefore has a symmetric dependence in both tails. Finally, the Clayton copula has lower tail dependence which can be defined similarly to the upper tail dependence but for the lower quadrant. The methodology and results from the application of copulas can be found in section 4.4.2 and section 6.2 respectively.

In order to perform statistical inference, the data needs to be fitted into a copula in order to find the one that best represents the data. A way to do so is by non-parametric measures of dependence, such as Spearman's rho correlation coefficient or Kendall's tau, both refer to the ranks of the data achieving scale-invariant estimates (Schmidt, 2007). In this thesis, Spearman's rho is defined in terms of a copula as:

$$r_s(X,Y) = 12\iint_{I^2} uv\,dC(u,v) - 3 = 12\iint_{I^2} C(u,v)\,du\,dv - 3$$

The validation of the copula fitting process is performed using two types of tests: The sum of the square differences based on the Cramer von Misses statistics and the Semi-Correlations. These are introduced in the next section.

## 2.6 Statistical Tests

### 2.6.1 Sum of the square differences based on Cramer von Misses statistics

Cramer von misses statistics refers to the calculation of the sum of the square differences between the empirical $C_n$ and the parametric copula $C_{\theta_n}$ (for an example of its application see Leontaris, Morales-Nápoles & Wolfert, 2016). The empirical copula is a non-parametric estimator of the true copula and summarizes the information of the pseudo-observations, that is the transformation of original variables to [0,1] uniforms through empirical margins. For the bivariate case with two random variables ($u_1$, $u_2$) the empirical copula is defined as:

$$C_n(u) = \frac{1}{n+1}\sum_{i=1}^{n} 1\left(U_1 \le u_1, U_2 \le u_2\right),\ \mathbf{u} = \left(u_1, u_2\right) \in \left[0,1\right]^2$$

**Eq. 9**

The Cramer von Mises statistics for an empirical process $A_n = \sqrt{n}\left(C_n - C_{\theta_n}\right)$ is defined as (Remillard, 2010)

$$S_n = \int_{[0,1]^d} A_n^{\,2}(u)\, dC_n(u) = \sum_{i=1}^{n}\left\{C_n\left(U_{i,n}\right) - C_{\theta_n}\left(U_{i,n}\right)\right\}^2$$

**Eq. 10**

This procedure is applied between the empirical copula and every copula under consideration, the copula with the smallest value should be preferred.

### 2.6.2 Semi correlations

This test is related to the calculation of the Pearson correlation coefficient for the upper and lower quadrant of the actual measurements transformed to standard normal margins (Leontaris, Morales-Nápoles, & Wolfert, 2016). Let $\phi$ denote the standard normal cumulative distribution function, then $Z_j = \phi^{-1}\left(U_j\right)$ for j=1…,d are the standard normal transforms of the pseudo-observations (Joe, 2014).

The data, as standard normal transforms of observations, is divided into four quadrants, for positive correlation the upper semi-correlation is defined as (Leontaris, Morales-Nápoles, & Wolfert, 2016):

$$\rho_{ne} = \rho(Z_1, Z_2 \,|\, Z_1 > 0, Z_2 > 0)$$

**Eq. 11**

and the lower semi correlation is defined as:

$$\rho_{sw} = \rho(Z_1, Z_2 \,|\, Z_1 < 0, Z_2 < 0)$$

**Eq. 12**

The upper and lower quadrant correlations indicate whether or not there is tail asymmetry. If there is tail asymmetry, an obvious difference is present for the two semi correlations (Joe, 2014). Moreover, these values can be compared to the product moment correlation of all the quadrants $\rho$ and if the values of semi-correlation are larger than the overall Pearson correlation, then there is an indication of tail dependence.

Section 6.2 shows the results from the statistical tests presented previously.

# 3 Area of Study

In this section, a description of the Valley of Mexico is given for the time before the Spanish conquest. Additionally, a background about the Aztecs and their relationship with water management, hydraulic structures, and floods, is presented. Finally, a description of the lacustrine system and hydrological conditions in the region is provided.

## 3.1 Temporal and Geographical Position

Officially named the United Mexican States, the country of Mexico is a federal republic in the southern region of North America. To the north it limits with the United States of America, to the south and west with the Pacific Ocean, to the southeast with Guatemala, Belize, and the Caribbean Sea; and to the east with the Gulf of Mexico (Merriam-Webster, Inc, 1997)

The valley of Mexico is located in the Trans-Mexican Volcanic Belt in the Mexico Basin (Figure 3-1) and is the highest valley in the region at an altitude of approximately 2200 meters above sea level (LEAD, 2004). Its total surface area including high mountains is 9.600km$^2$ (Lombardo de Ruiz, 1973). Surrounding the valley there are several valleys of smaller sizes that have natural resources and ecological situations different from each other (Palerm, 1973). This highland plateau was the center for several pre-Hispanic civilizations: Teotihuacan, Toltec, and the Aztecs.

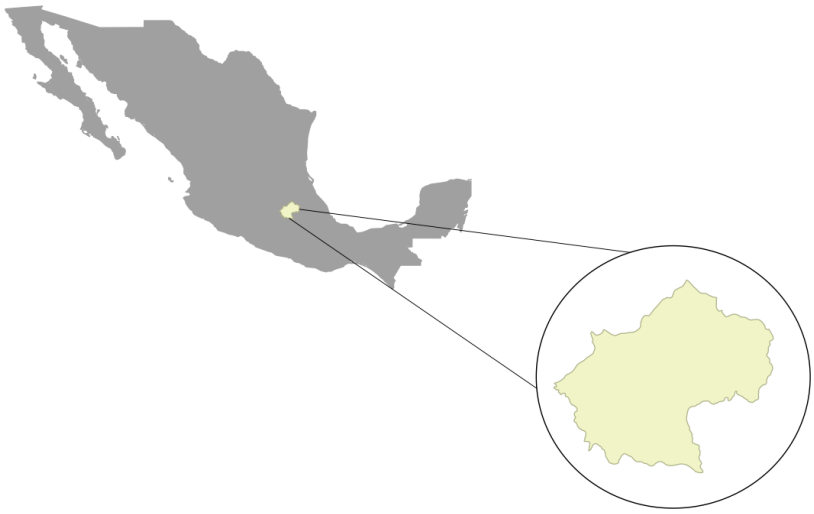

**Figure 3-1 Mexico Basin**

This thesis is focused in present-day Mexico City before the Spanish conquest around 1519 at the peak of the Aztec empire. At that time, the lakes, lagoons and swamps of the basin covered around 1000km$^2$ of the total surface of the Valley of Mexico (if the contour line of 2250 meters is taken as the high watermark of the lakes) in which the lakes of Chalco, Xochimilco, Texcoco (saltwater lake), Xaltocan, Zumpango, and Mexico (also known as Tenochtitlan) are distinguished (Figure 3-2).

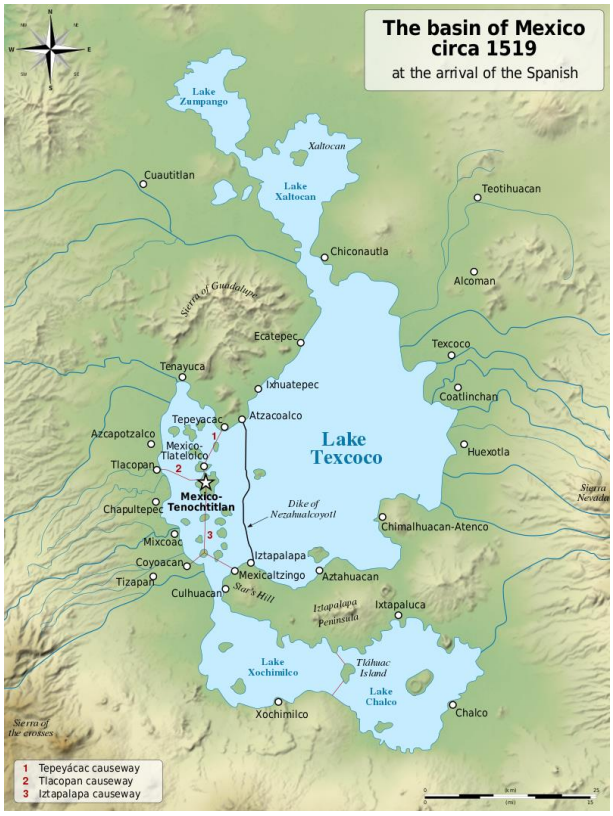


**Figure 3-2 Mexico Valley in 1519. (Niederberger, 1987)**

The capital of the Aztec empire, Tenochtitlan, was built at the west region of the lacustrine system, in Lake Mexico (Figure 3-2). The extensive hydraulic intervention in the lakes, allowed to intensify agriculture which resulted in highly populated urban centers.

The tributary area that contributed to the formation of the lakes corresponds to the Lake Texcoco sub-basin, located within the Mexico basin and has a total area of 4959.8 $Km^2$, as shown in Figure 3-3.

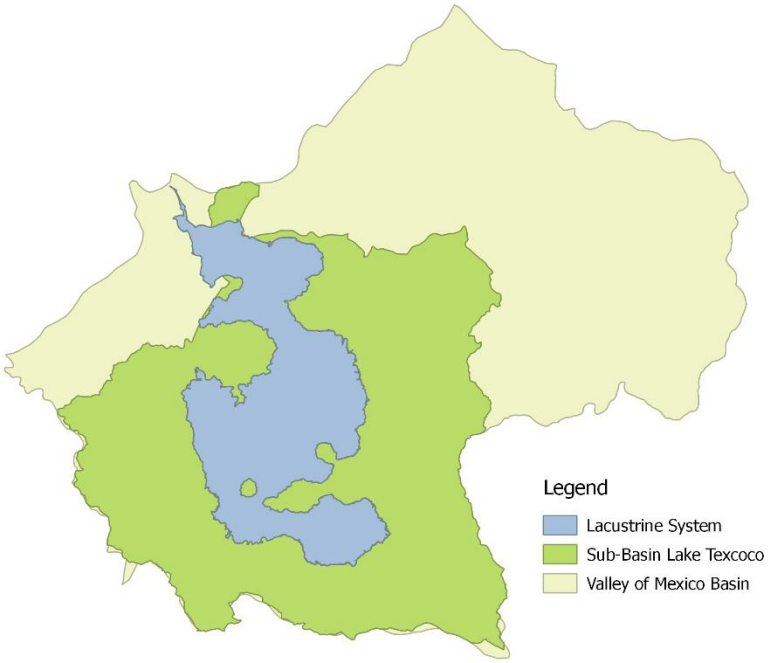


**Figure 3-3 Lake Texcoco Sub-basin.**

## 3.2 Hydrology of the Region

The Mexico Valley basin has a high-altitude and temperate climate. Most of the moisture reaching the area is associated with the easterly trade winds that bring summer rainfall. The weather in the valley is determined by several factors like humidity, vegetation, topographic differences, among others (Muciñio, 2001)

According to Caballero & Ortega Guerrero (1998), the basin ranges from semi-arid in the northeast (400mm/yr.) to sub-humid in the southwest (700-800mm/yr.). The temperature in summer ranges from 25°C to 28°C. The highlands are moister and cooler and precipitation can be greater than 1000 mm/yr. In general, the weather in the Valley of Mexico can be classified as subtropical, mild, semi-dry and without a well-defined winter season. The average annual temperature is 15°C approximately (Muciñio, 2001).

The wet season in the basin occurs generally between the months of May and October (Muciñio, 2001). Precipitation events at other times of the year are considered isolated events. During these months 80 to 90% of the annual precipitation occurs. The average annual precipitation is between 385 and 1400mm. The rain events are intense and of short duration, in just one storm, 7 to 10% of the average annual precipitation can be registered and from the total of rain registered in a single event, more than the 50% occurs within the first half hour (Muciñio, 2001).

The Mexico Valley basin was an endorheic (closed) basin, thus, the growth of the lacustrine area was limited by intense evaporation (Palerm, 1973). The annual evaporation rates range from 72% to 79% of the precipitation rates (Birkle, Torres, & González-Partida, 1998), sometimes evaporation rates can exceed precipitation rates to 1800-2200 mm in the Texcoco lake (Muciñio, 2001). Due to the geographic characteristics and the precipitation pattern in the basin, most of the rivers are defined as torrential with discharges of short duration (Muciñio, 2001)

### 3.2.1 Water Balance

A hydrological balance is the basic concept of conservation of mass with respect to water fluxes (Fitts, 2013). This balance requires:

$$I - O = \Delta S \qquad \textbf{Eq. 13}$$

In which:

- $I$ : Fluxes in
- $O$ : Fluxes out
- $\Delta S$ : Rate of change in water stored within.

The units used in Eq. 13 are $[L^3/T]$, therefore, this is a volume balance. A hydrological balance is useful for estimating unknown fluxes, for the case of this thesis the water level is the unknown variable, given that the lacustrine system no longer exists. Nowadays, the following fluxes are considered for the basin of the Valley of Mexico (Gómez-Reyes, 2013):

Fluxes in:

- Precipitation $Q_{rain}$
- Springs $Q_{springs}$
- Ponds $Q_{ponds}$
- $Q_{external}$

Fluxes out:

- Evapotranspiration $Q_{ET}$
- Infiltration $Q_{Infiltration}$
- Outlet $Q_{Outlet}$

Consumption:

- Urban use
- Losses
- Residual water used by PTAR (Water treatment plants)
- Reuse of the residual water
- Filling of water bodies

Re-entry:

- Residual water
- Treated residual water
- Surface exploitation

At the time of the Spanish conquest, several of the previously listed fluxes did not exist, for example, fluxes from consumption and re-entry; $Q_{oulet}$ refers to the drainage works in the basin and $Q_{external}$ refers to the water from a hydric system of storing, conduction, purifying and distribution of water to Mexico City and the State of Mexico. In section 4.4.3, an analysis of the relevant fluxes for this thesis is presented.

## 3.3 Lacustrine system

The lakes in the Valley of Mexico and its artificial compartments worked as communicating receptacles. The central lake, Texcoco, extended over a big area in the southern half of the valley. Its water was saline due to the nature of the mountain range in the surroundings and it was the lowest of all the lakes. It received the water surplus from all the other lakes. Zumpango and Xaltocan were the highest ones (6 and 3 meters higher than the Texcoco lake respectively); Xochimilco was higher than Texcoco and Chalco was even higher (3 meters above Lake Texcoco approximately) (Caballero & Ortega Guerrero, 1998; Rabiela, et al., 2009).

According to Birkle, et al., (1998) the lakes were considered as individual lakes during the dry season, however, they were joined as one body of water during high water levels. Usually after the wet season. The lakes connected when the water level reached approximately 6 meters above the basin elevation, around 2236 m.a.s.l (Lewis & Torres, 2013). However, Bradbury (1971), suggests that the lakes connected at elevation 2242 m.a.s.l and proposed that the bottom levels for the lakes were:

| Lake | Elevation at the bottom of the lake (m.a.s.l) |
|---|---|
| Texcoco | 2230 |
| Mexico | 2230.85 |
| Xochimilco | 2233.5 |
| Chalco | 2233.5 |
| Xaltocan | 2233 |
| Zumpango | 2236 |

**Table 3-1 Elevations of the lacustrine system.**

Moreover, Bradbury (1971), provided a map (Figure 3-4) in which the minimum, mean and maximum levels of the lacustrine system are drawn but does not provide the corresponding numerical value for each delineation.

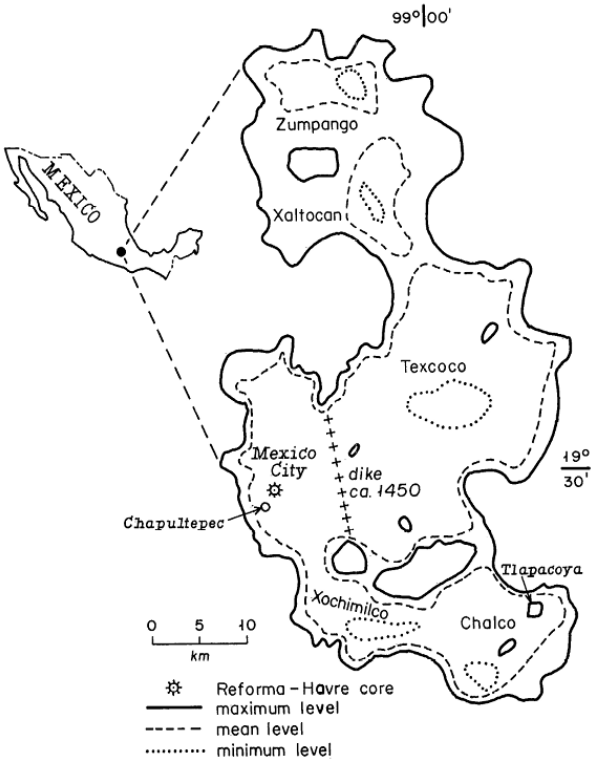


**Figure 3-4 Map of the lakes in the Basin of Mexico. Adapted from J.L. Lorenzo in Mooser et al. 1956. (Bradbury, 1971).**

The water feeding system between the lakes (Figure 3-5) is described by Rabiela, et al., (2009) as follows:

Lake Chalco constantly received fresh water from the rivers of the mountains and from springs. Xochimilco was fed by Lake Chalco and its own springs. Lake Mexico received water from the south and from some seasonal and perennial rivers, and from Lake Texcoco. Finally, Lake Texcoco was the deposit of the waters of all the lakes and torrential rivers.

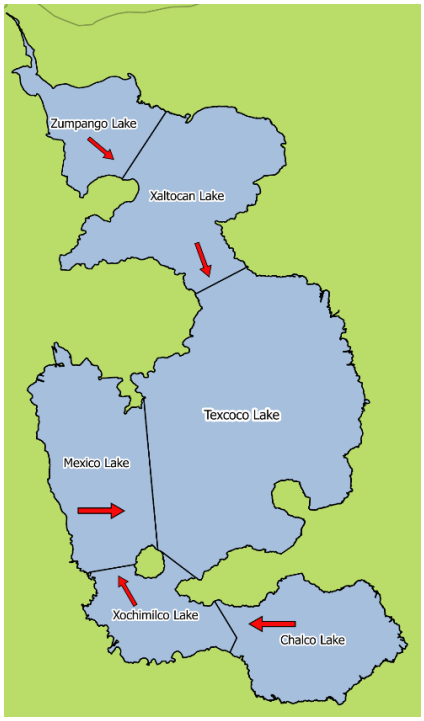


**Figure 3-5 Water feeding system in the lakes.**

According to Palerm (1973), this communication was closely related to the rain and hydrographic regime in the zone. During the dry season, the lakes were almost dry and resembled swamps. During the wet season, severe floods could occur in this lacustrine system. The connection between the lakes was characterized by overflow: Once the highest lakes were full, its surplus of water flowed towards Lake Texcoco.

Sometimes the water level at Lake Texcoco would overcome the water level in Lake Mexico or even the water level at Lake Xochimilco. Given that the water from Lake Texcoco was saline, its intrusion into Lake Mexico represented a bigger threat to the chinampas (Refer to section 3.4).

In order to deal with this climate seasonality and extreme differences between dry and water surplus conditions, the Aztecs had to come up with hydraulic structures. One of them was the Nezahualcoyotl dike, which divided Lake Texcoco in two from north to south: Lake Mexico to the west and Texcoco to the east. Its goal was to prevent water intrusion from Lake Texcoco towards Lake Mexico.

According to Armillas (1971), the high water mark in the lake system stood near the 2240-meter elevation since several centuries ago. Palerm (1973) states –based on historical anecdotes- that the high water mark stood near the 2250m contour line. Another important event described by the Spanish conquers, and presented by Palerm (1973) was that the water level growth in Lake Texcoco resembled a movement similar to the tides in the ocean. An extract of his book provides the following description: "…and because this big salt-water lagoon grows and has its tides as the sea does, water flows from it towards the fresh-water lake so strong as if it were an abundant river".

Palerm (1973) indicates that the Spanish could have confused seeing "tides" with the growth of the lakes during the wet season or perhaps there were currents created as a result of wind action. Nevertheless, this illustrates the movement of water between the lakes, which also explains why the Nezahualcoyotl dike and the walkway dikes were created (Section 3.4).

Nowadays, the floor levels might have been raised through silting but this effect may have been compensated by subsidence of the ground after the desiccation of the basin in the following centuries after the Spanish conquest. However, based on old maps and archaeological evidence, Armillas (1971) states that the changes in the floor relief through the last 600 years have been of minor consequence. Therefore, current topography of the site can be used to characterize the area of study.

## 3.4 The Aztecs and the Hydraulic Culture

In 1325 a nomad tribe from Aztlan was established in an islet where the people believed to have found the promised signal from their God Huitzilopochtli -an eagle over a prickly pear cactus devouring a rattlesnake- this settlement marked the beginning of the capital city of the Aztec empire: Tenochtitlan.

At first, people used the water from the lagoons or springs. However, as the population grew and the urban area expanded, they were forced to obtain water from other places, which led to the birth of hydraulic structures in Mexico (Peña Santana & Levi, 1989).

At the moment of the Spanish arrival, there were three fundamental types of hydraulic organizations in the agriculture of the Valley of Mexico. These organizations were in full operation and still expanding by the time of the Spanish arrival (Palerm, 1973):

1. Small irrigation systems: Usually situated next to springs and combined with terraces.
2. Big irrigation systems: Use of permanent and semi-permanent rivers by building dams, big deviation canals and an extensive network of ditches.
3. Hydraulic systems of the lacustrine area: The chinampas, dikes, walkway-dikes, defense structures against floods and drainage works, construction of artificial soils for agriculture and population, conduction of fresh water through canals, ditches and aqueducts and formation of artificial lagoons and swamps.

The technique that the Aztecs used to construct urban and agricultural soil in the lakes was called "chinampa" or also called floating gardens (Figure 3-6). This technique refers to the compaction of layers of soil partly extracted from the bottom of the lakes (Legorreta, 2006).

**Figure 3-6 Chinampas Model.**
*Source: https://www.flickr.com/photos/22887580@N06/2489191297/in/photostream/*

The chinampas extended from the lakes of Chalco- Xochimilco covering most of their surface and were expanded towards the central Texcoco-Mexico salt lake, around Tenochtitlan and several other places (Palerm, 1973).

The construction procedure of the chinampas, either for agricultural or urban development was very similar and is described as follows (Palerm, 1973; Rabiela, et al., 2009):

- Closure of an isolated area of the salt water body.
- Take advantage of rain and drought cycles to drain the area.
- Exploitation of the connection with canals, rivers, and aqueducts to convert the area into a zone of fresh water.
- For agricultural use: Construction of the chinampas by piling up of soil, mud, and conglomerate of aquatic vegetation to form a platform above the water level.
- For urban development: Placement of rows of posts as vertical piles in the bottom of the lacustrine bed, then filled with soil.
- All the elements used for the construction of the chinampas came from the lacustrine system.

The chinampas formed an intensive agricultural system as never seen before in the Mesoamerican era. By the XVI century, the chinampas in the Chalco-Xochimilco lake system extended for over 9500 hectares and were able to sustain around two hundred thousand people (Rabiela, et al., 2009). Such system required certain control of the water levels in the lake and also control of intrusion of salt water from Lake Texcoco. Therefore, the chinampas held a close relationship with the hydraulic structures (Rabiela, et al., 2009)

## 3.5 History of Floods

The city of Tenochtitlan, now known as Mexico City has a long history of floods. The city was located two meters above the level of the Texcoco lake (2232 m.a.s.l. See section 5.2), and during the wet season, it was prone to floods. Next, a brief recapitulation of the floods in the city -based on the report from the Water System in Mexico (2012)- is presented.

The first documented flood occurred in the year 1446 when abundant water coming from rain elevated the level of the lakes until they almost reached the level of the treetops, completely flooding the city.

After this event, Moctezuma (second Aztec emperor, fifth king of Tenochtitlan and first of such name) asked Nezahualcoyotl, Lord of Texcoco, for a solution to prevent new floods. Nezahualcoyotl recommended building a fence out of wood, stone, and mud, crowned by a strong wall of masonry that will contain the flow of water from the Texcoco lake. In this way, the Nezahualcoyotl dike was born. Its gates allowed to extract water from Lake Texcoco in the dry season and to contain it during the wet season. The construction of the Nezahualcoyotl dike began around the year 1450 (Palerm, 1973; Daou, 2011).

The dike was also known as the “Old dike” or “Dike of the Indians”. It cut Lake Texcoco from north to south forming two lakes: Mexico (West) and Texcoco (East). This dike ran from the Santa Catarina Mountains in Tepeyac to the Sierra de la Catarina near Ixtapalapa.

Around 1486, during the reign of the eighth Aztec ruler, Ahuizótl (who enjoyed having gardens and orchards), the demand for water increased. Therefore, to cope with the supply of water, he ordered the construction of a new aqueduct directed toward the center of Tenochtitlan. After several warnings about the danger of the great amount of water that could flow through such aqueduct, he decided to build the structure anyway. Years later, in 1499, heavy rainfalls caused the overflow of the water in the aqueduct. This event indirectly took the life of Ahuizótl himself due to a strong impact in his head when he was trying to escape from the water. Such flood led to the construction of another structure: The Ahuizótl dike (located within Lake Mexico).

In 1521, the Mexica civilization had already fallen against the Spanish conquers. This event represented an opportunity to relocate the city. However, by order of Hernán Cortés (leader of the expedition that started the conquest of Mexico), the new city was built in the same place. He ordered the destruction of a large part of the Nezahualcoyotl dike so his brigantines could sail during war, some canals were used for transport and commerce through canoes. Time after the conquest, the city continued to grow but its new governors did not understand the role of the hydraulic structures in the lacustrine system and its surroundings. Their activities increased soil erosion and sedimentation in the lakes, reducing its capacity to retain water during the wet season.

The first flood after the conquest happened the 17 of September of 1555. This disaster led to the construction of the San Lázaro dike in 1556 but in 1579 the city was flooded again.

By the year 1604, the viceroy Juan de Mendoza y Luna asked for a project to drain the lakes after a flood that occurred that same year. However, no offers were presented. Later, in 1607 a flood resulted from the overflow of the lake and the discharge of several springs that appeared in the streets of the city and inside of buildings. The water level grew so much that the city was at the edge of disappearing. Then, the viceroy at the time, Luis de Velasco II offered a reward for the person who proposed an effective way to drain the lakes.

Enrico Martinez proposed to drain the Cuautitlán river and the Zumpango lake trough the Nochistongo gash towards the Tula River. The project was approved on the 23 of October 1607. However, by 1615, Martinez had failed to execute the construction of the project properly. In 1623 the Viceroy Diego Carrillo Mendoza Pimentel ordered the destruction of some of the dikes built by Martinez. These dikes retained water from the Cuautitlán River that ran towards Lake Zumpango and then Lake Texcoco. The Viceroy wanted to test if the danger of doing so was as bad as people had warned him. This decision caused one of the biggest disasters ever occurred in the city. The resulting flood lasted six years, it destroyed most of the buildings and decreased the population considerably. After this, the Viceroy proposed to change the location of the city, however, the citizens were tired of the inexperience of the Viceroy and attacked the royal palace, forcing the Viceroy to run away.

By 1629, after a continuous rainfall of 36 hours, Mexico City was again flooded. The water level reached a mean of 2 and a half meters. Most properties were destroyed and approximately thirty thousand people died from drowning or starvation. In 1635 the Viceroy Lope Diez Aux de Armendariz ordered several works to repair the damage caused by the last flood and to resume the drainage works which lasted until 1789. The project suffered several modifications. The work was stopped and resumed several times during this period while the city still suffered from severe floods every 15 to 20 years approximately. The second drainage work was the “Gran Canal de Desagüe” (Big drainage canal), that started working in 1900. In this way, the lacustrine system was drained from the basin almost entirely.

It is important to notice that during the time from the construction of the Nezahualcoyotl dike until the arrival of the Spanish conquerors (70 years approximately) there is no mention of floods in the city of Tenochtitlan from an increase of water level in Lake Texcoco, while after the destruction of the dike the city was continuously flooded throughout the next 350 years. This fact provides insight into the importance of the dike in the city of Tenochtitlan and the experience of the Aztecs as hydraulic engineers.

## 3.6 Summary

In this chapter, the area of study and the history of floods in the region was described. The following bullets summarize essential information for the upcoming chapters.

- This thesis is focused in the Valley of Mexico for the time before the Spanish conquest when the Nezahualcoyotl dike was fully operational and the lacustrine system still existed.
- The capital of the Aztec empire, Tenochtitlan, was built in Lake Mexico. The Nezahualcoyotl dike protected this city from the rising water levels at Lake Texcoco.
- The area of the Valley of Mexico is 9600 $Km^2$ and the area of the sub-basin which contributed to the formation of the lacustrine system is 4959.8 $Km^2$.
- 80 to 90% of the annual precipitation in the region occurs during the wet season (May-October).
- The lakes worked as communicating receptacles of water. During the dry season they were considered as individual lakes and during the wet season, they were joined as one body of water.
- The relationship between the lakes was characterized by overflow. Once the highest lakes were full, its surplus of water flowed towards Lake Texcoco, which was the lowest lake of all.
- During the lifetime of the Nezahualcoyotl dike (70 years), there are no records of floods in the city, while after its destruction, the city was constantly threatened by floods.

# 4 Methodology

This chapter presents the details and steps of the methodology carried out throughout this research. First, the main assumptions and simplifications are presented, followed by the general framework employed in this thesis. Then, details about the construction of the models and the analysis of data are explained. Finally, a description of the procedure to assess the reliability of the dike is presented.

## 4.1 Assumptions and simplifications

To develop this thesis, important assumptions and simplifications were made and are listed below:

- The interaction between the lakes influenced the growth of the water level in Lake Texcoco. In this thesis, such complex relationship was not taken into account and only the water level fluctuation in Lake Texcoco was considered for analysis.
- Datasets of present-day information of precipitation and evaporation were used (In order to characterize the fluxes in and out of the basin in a hydrological balance). Additionally, wind data and topography were also employed.
- The hydrological model only considers measurements during the wet season.
- The presence of gates in the Nezahualcoyotl dike was neglected.
- The reliability analysis was performed for one levee failure mechanism: Overflow.

## 4.2 General Framework

To achieve the main objective of this thesis and to give answers to the research questions, four steps are proposed as shown in the flowchart of Figure 1-1:

- Step 1: Characterization of the dike and the lacustrine system.
- Step 2: Analysis of levee failure mechanisms.
- Step 3: Hydrological Model and generation of synthetic data sets.
- Step 4: Reliability analysis.

The development and results of the hydrological model depend on the failure mechanism to be tested. In the following sections, the methodology employed to carry out each step is presented.

## 4.3 Step 1: Characterization of the system

The aim of this step is to depict the Nezahualcoyotl dike and the hydrological conditions in the lacustrine system around the time of the Spanish conquest. The process was carried out as follows:

a. Gathering of information:
    1. Historical documentation from the lacustrine system and the dike.
    2. Current measurements of environmental variables and terrain data.
b. Data processing and analysis.
c. Representation of the system

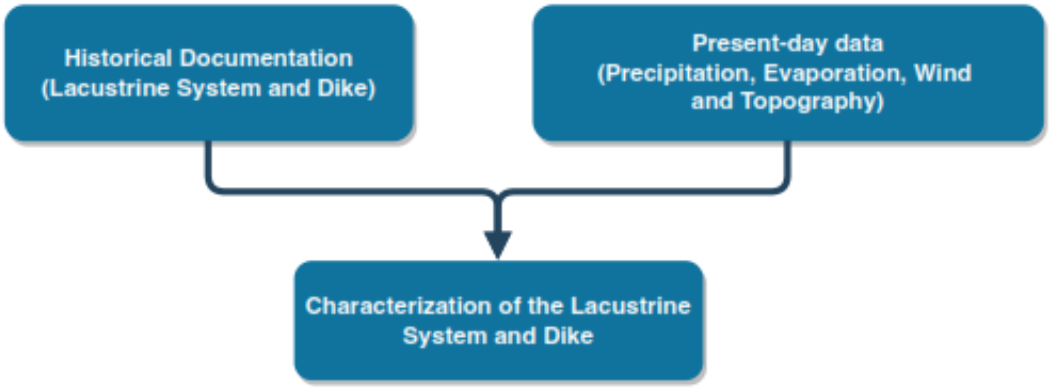


**Figure 4-1 Flowchart of the methodology employed to characterize the lacustrine system and the dike.**

Following the flowchart shown in Figure 4-1, the steps for each section are described as follows.

### 4.3.1 Gathering of information

Nowadays, neither the lacustrine system nor the Nezahualcoyotl dike exists anymore. Therefore, information about the area of study needs to be collected from historical sources. Several manuscripts were collected, studied and interpreted by Palerm (1973), most of the historical information in this thesis is based on his work and some other details from several other authors. The majority of the information gathered from these sources are related to the Nezahualcoyotl dike's materials, dimensions and appearance.

Meanwhile, in order to describe the hydrological conditions in the area of study, datasets of environmental variables and terrain information are required. The variables considered are shown in Table 4-1:

| Name | Description | Units |
|---|---|---|
| Precipitation | Maximum of daily precipitation. | mm/day |
| Evaporation | Maximum of daily evaporation. | mm/day |
| Wind Speed | Hourly measurements. | m/s |
| Wind Direction | Hourly measurements. | Degrees |
| Area | Area of the lakes in the lacustrine system | $Km^2$ |
| Topography | Contour lines of the area of study | m |

**Table 4-1 Name and description of the variables.**

The information presented in Table 4-1 were obtained from Mexico's national databases.

### 4.3.2 Data processing and analysis

The information from different historical sources was compared between each other in order to create an estimation of the dike's dimensions and its construction materials (Section 5.3) while present-day measurements of environmental variables were used to characterize the hydrology in the region and the growth of water levels in the Lake Texcoco. (Section 5.2). By combining these two types of information it is possible to create a description of the dike and the lacustrine system

at the time before the Spanish conquest. The steps followed to analyze such information are described as follows:

**Precipitation and Evaporation**

Measurements of these variables were obtained from Mexico's national database: CLICOM (Climate Computing Project- http://clicom-mex.cicese.mx/), in the form of maximum daily measurements. The climate stations are distributed throughout the State of Mexico and Mexico City.

A total of 409 stations were available. In order to reduce the number of stations that were used in this thesis, two filters were applied. The first filter was selecting the stations with more than twenty-five years of measurements to ensure the greatest amount of data possible. The second filter consisted of choosing the stations that were relevant according to their geographical position, meaning that only the stations surrounding the area once occupied by the lacustrine system were considered.

The data of the stations that met all the previous requirements were analyzed and processed. It is common that environmental measurements contain errors that arise from different causes, for example, damage in the equipment or a sudden interruption of the measurements due to maintenance, among others. These errors are usually represented as an unrealistic number within the dataset (for example -999). Faulty observations were not considered in the analysis.

Additionally, the time period of measurements for every climate variable needs to be equal, the final time period for each station was reduced to the time period in which all variables match. Finally, the information had to be converted from their original format (.csv) to a more manageable format for future computations (mat files). All these steps were carried out using a Matlab scripting.

**Wind speed and direction**

Wind data was obtained from the System of Atmospheric Monitoring of Mexico City "Aire CDMX" (http://www.aire.cdmx.gob.mx/default.php). This database is subdivided into different groups. For wind data, the corresponding database group is called REDMET (Meteorological network), which has information since 1986 in the form of hourly measurements.

The stations considered for this thesis were chosen based on their geographical location and their availability of data. As with climate data, wind stations presented different time periods of measurements between each other.

In order to determine if wind data is relevant for this study, the predominant wind direction needs to be computed for each station. According to their geographical location, it can be determined if the wind blows in direction of the Nezahualcoyotl dike. Additionally, in lakes, wind can influence the water level considerably by heading up the water (wind set-up), this increase of water level can be determined as follows (Molenaar & Voorendt, 2016):

$$\frac{dS}{dx} = C_2 \frac{u^2}{gd}$$

**Eq. 14**

In which:

- $S$ : Total wind set-up [m].
- $C_2$ : Constant $\approx$~$3.5*10^{-6}$ to $4.0*10^{-6}$
- $d$ : Water depth [m].
- $u$ : Wind velocity [m/s].
- $x$ : Fetch [m].
- $g$ : Gravity Acceleration [$m/s^2$]

The previous equation shows that wind set-up increases with increasing wind velocity and fetch and for decreasing water depth. If the set-up is in the order of a few centimeters or less, the influence of wind can be neglected.

In this thesis, wind set-up is not characterized using probabilistic models, instead, it will be added as a deterministic variable (Considering the highest wind speed measured at a given station as the worst case scenario) to the water levels resulting from the hydrological model.

**Geographical Information and Terrain**

Terrain data is an important variable for the lacustrine system because it helps to determine the elevation at the bottom of the lake, the maximum height that the dike could have had, the high water mark and the water level fluctuations. Terrain data was obtained from two different sources: Mexico's database INEGI (National Institute of Statistics and Geography) and HydroSHEDS (Lehner, Verdin, & Jarvis).

Resolution of the data is a key factor to take into account given that differences in altitude in any given point can be in the order of several meters depending on the source. In order to select the best topography, all the sources were compared by creating a cross section in Lake Texcoco, from the generated profile views it was possible to observe the difference in altitude from each source at this transect.

Additionally, a combination of historical documentation and terrain data was employed to assess some characteristics of the dike, such as its orientation and total length (Section 5.3).

**Volume-Elevation Curve**

The lacustrine system was drained almost entirely, therefore, there is no information about the water levels in Lake Texcoco or its corresponding volumes. However, it is possible, by using terrain and topographic data to get a rough estimation of the volume and surface area of the lake at certain depths, these are called the Volume-Elevation and Volume-Area curves respectively.

The procedure starts with the selection of an adequate topography. Next, by using a spatial analysis software like ArcGIS it was possible to obtain the volume and surface area of water in the lake at different depths.

## Step 2: Analysis of levee failure mechanisms

In order to determine which levee failure mechanisms are the most relevant for the Nezahualcoyotl dike, it is necessary to identify the hazards that the city of Tenochtitlan faced during the wet season. Section 3.5 presented a description of the flood history in the region and it was used as the main source of information for the selection of the most relevant failure

mechanism. From such analysis, overflow was selected as the most relevant failure mechanism for the Nezahualcoyotl dike (Section 5.1). This mechanism takes place when the water level at the lake exceeds the crest of the dike. Thus, is described by the water level fluctuation at Lake Texcoco. Consequently, overflow was the base for the development of a hydrological model that aims to estimate the fluctuation of water level in Lake Texcoco.

## 4.4 Step 3: Hydrological Model

The methodology employed to develop the hydrological model is summarized in Figure 4-2. First, a probabilistic model (of Markov chains and copulas) was employed to construct the environmental time series. Then, the hydrological balance at Lake Texcoco was computed. Finally, by combining the results from the probabilistic model, the hydrological balance and the Volume-Elevation curve, the water levels at Lake Texcoco were obtained.

For this thesis, a Markov chain model was selected because it is able to characterize the rain pattern in a location based on probabilities. This information will describe the occurrence of rain during the wet season. While the Copula model determines the values of precipitation and evaporation for such pattern based on the dependence between those three variables. More details about this process are presented in the following sections.

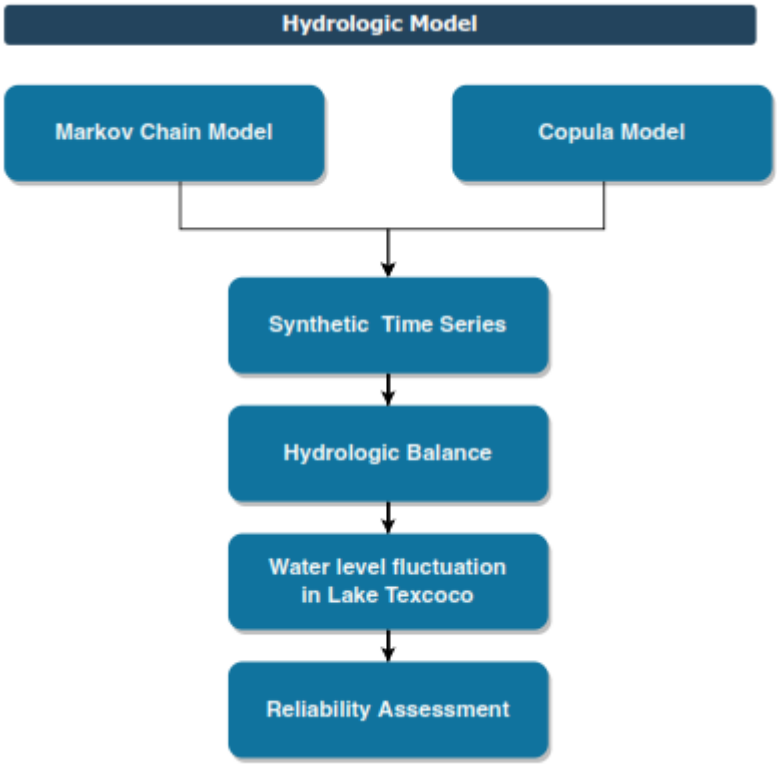


**Figure 4-2 General flowchart of the Hydrologic Model.**

The model only considered conditions during the wet season (May to October) because during that period is where most of the rainfall is registered throughout the year (Muciñio, 2001). The modules from the flowchart shown in Figure 4-2 are described as follows.

### 4.4.1 Markov Chain Model

The hydrological model starts with a Markov Chain Model. As mentioned previously, the measurements of precipitation and evaporation were considered only for the wet season (From May to October). The aim of this first submodel is to define the rain pattern during this period.

A Markov Chain is described by a transition matrix $P$ as mentioned in section 2.4. Such matrix relies on the current state to predict the next state. In this thesis, two states are considered, wet and dry days, represented by the number 1 and 0 respectively. The transition probabilities can be estimated directly from the observed transitions in the data. For instance:

$$P_{01} = \frac{N_{01}}{N_0^*}$$

Where $N_{01}$ is the number of observed transitions from state 0 to 1 and $N_0^*$ is the number of transitions that start from state 0. Thus, for the following sequence:

$$[0,1,1,0,1,0,1,0,0,1]$$

It is found that $N_{01}$=4 and $N_0^*$=5 which results in $P_{01} = 4/5$. The same procedure is applied for $P_{00}$, $P_{10}$, and $P_{11}$. Thus, $N_{00}$=1, $N_{11}$=1, $N_{10}$=3, and $N_1^*$=4 that results in $P_{00}=1/5$, $P_{10}=3/4$, and $P_{11}=1/4$. The resulting transition matrix is:

$$P = \begin{bmatrix} 1/5 & 4/5 \\ 3/4 & 1/4 \end{bmatrix}$$

This model is based in terms of occurrence and non-occurrence of rainfall on any day. Through the resulting transition matrix and the simulation tool in Matlab, a thousand years of wet seasons are generated (185 days each). Each wet season has the form of a sequence of zeros and ones like the example presented in this section.

A detailed summary of Markov theory is presented by Rip (2016). The estimation of the amount of rain for each wet day is explained in the following section.

### 4.4.2 Copula Model

Once the rain pattern has been generated by using the Markov Chain sub-model, the corresponding amount of precipitation and evaporation is estimated.

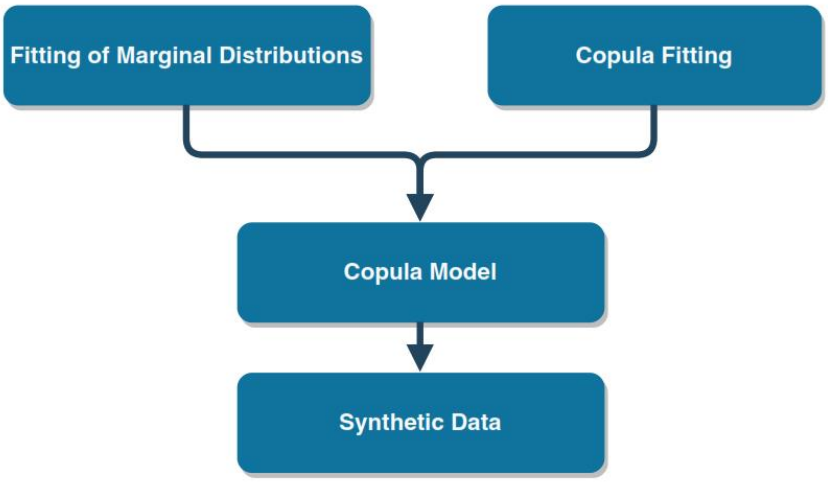


**Figure 4-3 General flow chart of the Copula Model.**

Climate variables are described as random processes. In order to have a better understanding and description of the data sets it is necessary to find a probability distribution that best describes their behavior. This process is called distribution fitting. The probability distributions were chosen based on the negative log-likelihood method (NLogL) which is equivalent to the maximum likelihood estimation (MLE). The distribution with the lowest value of NLogL was selected as the best fit. The results from this procedure are shown in section 6.1.

To create a realistic environmental time series, the dependence and observed autocorrelation between the variables have to be taken into account and a probability distribution does not consider these factors. In order to include dependence and autocorrelation, the joint probability distribution between the variables is described by bivariate copulas. Thus, the variables were analyzed in pairs. The process to find the copula that best describes data pairs is called copula fitting and is validated by two statistical tests: Sum of the square differences based on Cramer-von Mises and Semi-correlations (Eq. 10, Eq. 11 and Eq. 12). The results from this procedure are presented in section 6.2.

The pairs of data were divided into two groups according to two conditions: Wet days and dry days. The pairs for wet days are Precipitation-precipitation (PR-PR) and Precipitation-Evaporation (PR-E). The pair for dry days is Evaporation- Evaporation (E-E). See Figure 4-4.

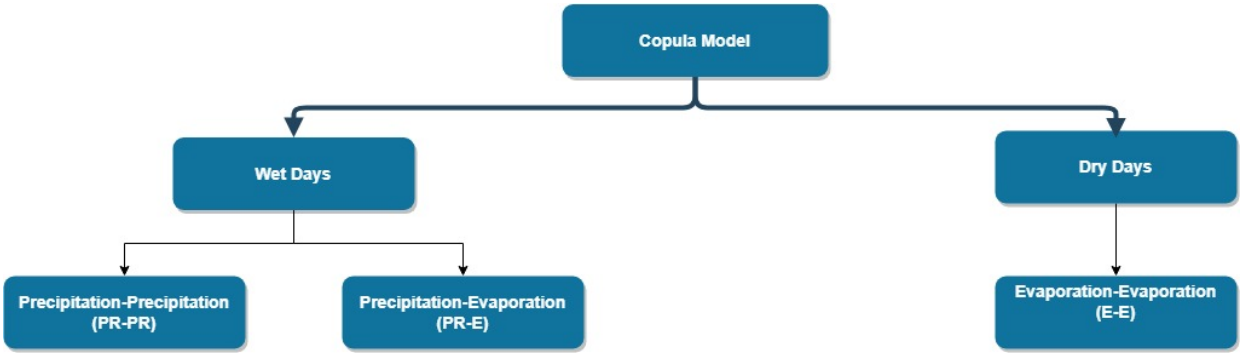


**Figure 4-4 Flowchart for the generation of synthetic data through a Copula Model.**

For the pairs, PR-PR and E-E, the relationship between these marginal distributions is described by autocorrelation which refers to the dependence of precipitation or evaporation with lagged versions of themselves. The same procedures described in section 2.6 may be used to fit copulas of a random variable with lagged versions of itself.

Once the copulas that describe the dependence and autocorrelation between the variables are known (Eq. 6, Eq. 7and Eq. 8), the synthetic time series can be produced. The time series is made up of two datasets: Precipitation and evaporation. Each copula generates data for a specific variable given the condition if it was a wet or dry day. This can be illustrated as follows:

The $PR-PR$ copula, where the conditional copula of precipitation in time $t$ given precipitation in time $t-1$ is denoted as $C\left(PR_t \middle| PR_{t-1}\right)$. One may sample from this conditional copula in order to generate data of precipitation given a wet day. The $PR-E$ copula, in which the conditional copula of evaporation in time $t$ given precipitation on time $t$ is defined as $C\left(E_t \middle| PR_t\right)$. This copula generates data of evaporation given a wet day.

Values for precipitation on dry days are not modeled as they are already taken as zeros. The generated dataset for evaporation given a dry day was generated based on the $E-E$ copula. Where the conditional copula of evaporation in time $t$ given evaporation in time $t-1$ is defined as $C\left(E_t \middle| E_{t-1}\right)$.

The previous procedure of random generation consists of the following steps:

Generation of data on wet days:

- The first value of precipitation ($PR_t$) is generated in [0,1] using a uniform random generator.
- The values of precipitation ($PR_{t+1}$) are calculated in [0,1] based on the previous value ($PR_t$) by solving the corresponding inverse conditional fitted copula.
- Next, the inverse of the corresponding conditional copula functions provides the value of evaporation ($E_t$) in [0,1] for each of the generated precipitation values ($PR_t$).

Generation of data on dry days:

- The first value of evaporation ($E_t$) is generated in [0,1] using a uniform random generator.
- The values of evaporation ($E_{t+1}$) are calculated in [0,1] based on the previous value ($E_t$) by solving the corresponding inverse conditional fitted copula.

The values of precipitation and evaporation are transformed back to their original units through the inverse cumulative distribution function of each separate variable. Finally, the resulting values are combined forming the time series for a wet season. In total, one thousand wet seasons were generated. All the algorithms were developed in Matlab.

### 4.4.3 Hydrological Balance and Estimation of Water Levels

Once the time series has been generated, the hydrological balance at Lake Texcoco can be carried out. The Valley of Mexico is a basin that has been severely intervened by humans for the last hundreds of years, therefore it is important to identify the fluxes relevant to the basin at the time of the Spanish conquest. In section 3.2 a list of the main present-day fluxes is presented.

From those, the fluxes from consumption and re-entry are neglected. $Q_{oulet}$ and $Q_{external}$ are not considered either. Additionally, the contribution from springs, ponds, and infiltration are also neglected in order to simplify the model. Therefore, based on the concept from Eq. 13, the final configuration of the hydrological balance at the time of the Spanish conquest is:

$$PR_i \cdot A_{Tributary} - E_i \cdot A_{lake_j} = \frac{dV}{dt}_{ij} \quad [\mathrm{m^3/Day}]$$

**Eq. 15**

In which:

- $PR_i$ :The ith value of precipitation on the lake surface [$m^3$/day].
- $E_i$ : The ith value of evaporation from the lake surface [$m^3$/day].
- $A_{Tributary}$ : Tributary area of the basin [m2].
- $A_{lake_j}$ : Surface area of the lake j [m2].
- $\frac{dV}{dt}_{ij}$ : The ith rate of change of volume at the lake at depth j [$m^3$/day].

As shown in the previous equations, the fluxes considered for the hydrological balance at Lake Texcoco are precipitation and evaporation. The tributary area of the basin was obtained using data from the Environmental Secretariat of the State of Mexico (2018).

There is no information about the water level in the lake at the start of the wet season, therefore the hydrological balance was computed for every meter depth from the bottom of the lake (2230 m.a.s.l) until the high watermark proposed by Palerm (1973): 2250 m.a.s.l (See section 3.3). In this way, the computed water levels are relative to the given initial water depth. Moreover, wind set up was incorporated into this model as a deterministic variable added to the computed water levels using Eq. 14 presented in section 4.3.2.

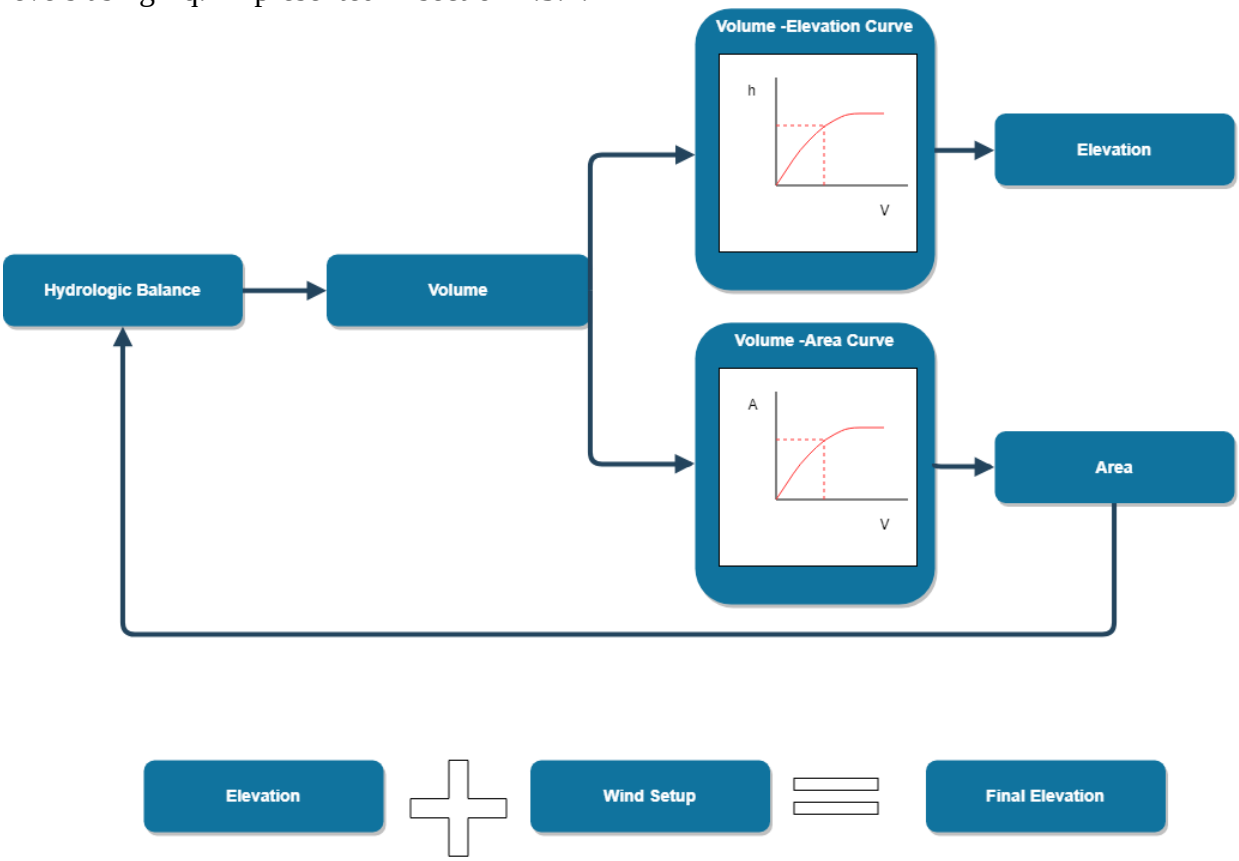


**Figure 4-5 Flowchart of the methodology for the computation of water levels.**

The general procedure for the computation of the water levels is shown in Figure 4-5 and is described in more detail with the following steps:

1. An initial water depth is established.
2. The hydrological balance equation is applied, the result is the volume fluctuation $dV$ given the climate variables used as input.
3. The volume at the lake is computed by adding the volume variation $dV$ to the volume corresponding to the initial water depth.
4. The surface area ( $A_{lake}$ ) and depth ( $h$ ) at the lake corresponding to the computed volume are obtained from the Volume-Area and Volume-Elevation curves.
5. The process is repeated from step 2 but now $A_{lake}$ correspond to the area computed in step 4. This procedure is repeated until the water levels have been computed for the entire wet season and for each initial depth (From 2231 m.a.s.l to 2250 m.a.s.l)
6. Once the water levels at the lake are obtained, the wind set up corresponding to each level is computed as a deterministic value. Finally, the wind set-up values are added to the water levels in order to obtain the final water elevation at the lake.

The previous procedure was applied to the thousand years of synthetic data. All the operations were developed using a Matlab script.

## 4.5 Step 4: Reliability Analysis

After the synthetic datasets have been produced and the corresponding water level fluctuations have been computed, the reliability of the dike has to be tested and only one dike failure mechanism will be considered (Overflow).

The first step to evaluate overflow on the Nezahualcoyotl dike is to extract the annual maxima water level of the generated water levels (Section 4.4.3). These data were then fitted to a probability distribution function in order to characterize its behavior. The criteria used to evaluate overflow on dike is based on the probability that a given water level in Lake Texcoco will exceed the height of the dike (PF) and its corresponding return period. This procedure was performed using a Matlab script. In this thesis, the aim is to make an assessment of the dike under the selected failure mechanism given such probability.

The results from this methodology are presented in chapter 7.

# 5 Final Layout of the System

In this section, the main hazards for the Nezahualcoyotl dike are evaluated in order to determine the most relevant failure mechanism of the dike, also, a characterization of the natural system in the Valley of Mexico is presented based on historical information and current data, including a description of the water level at the lakes. Finally, a layout of the Nezahualcoyotl dike is constructed.

## 5.1 Selection of Levee Failure Mechanisms

In this section, the selection of overflow as the most relevant failure mechanism is presented as an analysis between information from Table 2-1, section 2.3.3 and historical data from Chapter 3.

The flooding history of the city of Tenochtitlan (section 3.5) describes an increase of the water levels in Lake Texcoco that throughout the years caused saltwater intrusion into the city. At the time of the Aztec empire, several hydraulic structures were constructed in an attempt to avoid floods, one of them was the Nezahualcoyotl dike. However, as stated in section 3.4, even though these structures helped to keep the city safe, they also affected negatively other conditions in the lacustrine system by constraining the natural interaction between the lakes. After the Spanish conquest, the city was constantly affected by floods due to the lack of knowledge about the lakes from the new governors in charge.

Overflow takes place when the water level exceeds the crest height of the levee. As stated previously, this failure mechanism is constantly described throughout the history of the city of Tenochtitlan, making it the most recurrent failure mode in the dike according to historical sources. This research also considers the contribution of wind set-up at the lake given the questionable description that the lake was influenced by tides (section 3.3). It is interesting to mention such description, however, its accuracy is difficult to determine without adequate analysis. Wind waves could be a factor to take into account too (See results in Section 7.1 and 7.2).

The piping failure mechanism starts to develop at the land side of a dike by a large hydraulic head difference. This failure mechanism is relevant for cases of vulnerable soil profiles. For the Nezahualcoyotl dike, there was no land side, both sides of the dike had water, especially during the wet season. Thus, the difference in water levels from the Texcoco and Mexico side was not as large as it was by the end of the dry season when Lake Texcoco was assumed to be empty. The water in Lake Mexico could be assumed to remain more or less the same through the year given that it was necessary to maintain the chinampa system, approximately 2 meters water depth (section 3.5). Notice also that Lake Texcoco bottom level was lower than Lake Mexico (Table 3-1), therefore if piping were to occur, it would start at Lake Texcoco side, causing (in an advanced situation) flooding towards that side and it would not represent a flood hazard for Tenochtitlan. This same analysis can be applied to heave. Consequently, piping and heave are not relevant failure mechanisms for the Nezahualcoyotl dike given that would not cause damage to the city of Tenochtitlan nor the chinampa system.

Microinstability starts to develop at the land side of a dike. Occurs when the seepage water causes the phreatic surface to rise and reach the inner slope of the dike (Jonkman, et al., 2017). If the dike consists of permeable granular material, internal erosion can be initiated. The dike was constructed with sand, stones, and mud, so this failure mechanism could be possible during the dry season. However, there are no records of the dike failing this way, additionally, more

information about the construction materials are required in order to make a proper estimation of the likelihood of this failure mechanism.

Macro instability is important for levees with a steep slope in wet conditions, also it is important for levees that deals with extreme water level fluctuations. This research focuses on the wet season and it is known that the lake had big changes in water level due to precipitation events during this time. However, the study of this failure mechanism would involve a detailed analysis of the materials of the dike, which carry additional uncertainties. Therefore, to simplify the analysis, this method is not considered as the most relevant for the dike.

Horizontal sliding at the foundation occurs when the dike has a small freeboard (water level close to the crest). Especially when the dikes are made of a local lightweight material such as peat which can be found in lacustrine zones. The Nezahualcoyotl dike was constructed with materials from the bottom of the lake (same as the chinampas) so it is probable that peat was one of them. However, soil information at the site would be needed. This failure mode aggravates after periods of long droughts therefore if failure were to occur, water would have flown from Lake Mexico towards Lake Texcoco, not representing a flood danger for Tenochtitlan.

Finally, a failure mechanism that was not mentioned in Table 2-1 is the failure due to non-closure of gates. In historical sources is mentioned that the Nezahualcoyotl dike would have had gates to regulate the flow between the two lakes. The reliability of closure, the number of demands and the storage capacity of inflow water behind the dike has to be considered. This failure mode is not treated in this thesis in order to simplify the analysis, however, it is an important failure mechanism to take into account for future research.

From the previous analysis, it can be concluded that the most relevant failure mechanism for the Nezahualcoyotl dike is overflow, at which the reliability of the dike will be tested given the historical evidence about its occurrence through history.

## 5.2 Layout of the Lacustrine System

In order to characterize the lacustrine system, the hydrological conditions of the Valley of Mexico need to be understood. To develop this section, information from section 5.3 was employed and vice versa, thus, both sections feedback each other. A description of the results from data analysis and processing is presented next.

**Precipitation, evaporation**
Data from a total of 378 precipitation/evaporation stations was downloaded and classified as follows:

| Location | Number of Stations | |
|---|---|---|
| | Less than 25 years measurements | More than 25 years measurements |
| State of Mexico | 157 | 192 |
| Mexico City | 26 | 34 |

**Table 5-1 Number of stations for precipitation and evaporation data.**

By applying the filters to select data presented in section 4.3.2, a total of five stations were chosen to characterize the hydrological conditions surrounding Lake Texcoco. The stations are shown in Figure 5-1.

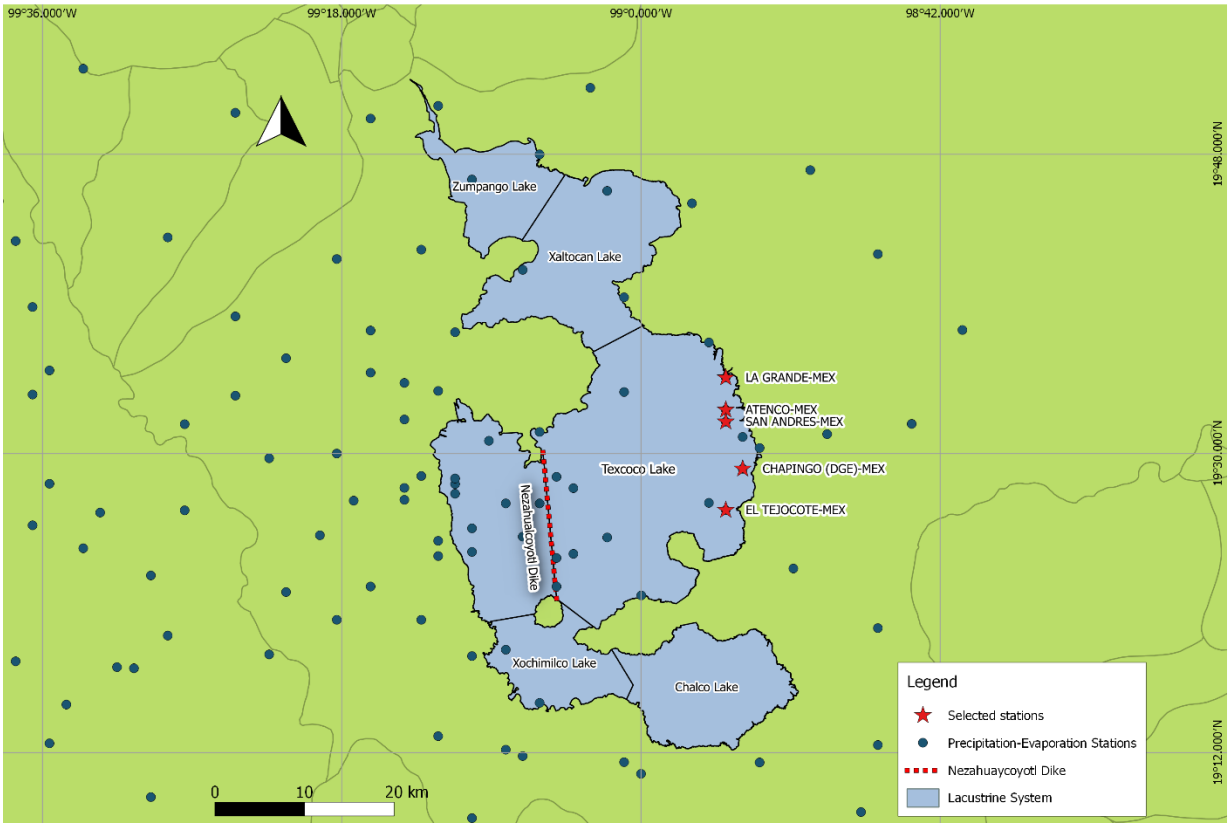


**Figure 5-1 Climate stations surrounding the lacustrine system.**

Table 5-2 provides an overview of the data:

| Code | Name | Coordinates | | Time Period |
|---|---|---|---|---|
| | | Longitude (dd) | Latitude (dd) | |
| 15008 | Atenco | -98.92 | 19.54 | 1/1/1961-22/8/2013 |
| 15044 | La Grande | -98.92 | 19.58 | 1/1/1964-31/8/2014 |
| 15083 | San Andres | -98.92 | 19.53 | 1/5/1967-31/12/2014 |
| 15167 | El Tejocote | -98.92 | 19.44 | 1/12/1957-1/1/2007 |
| 15170 | Chapingo (DGE) | -98.90 | 19.48 | 13/3/1957-1/1/2000 |

**Table 5-2 Summary of climate information per station.**

As part of processing the data, several values had to be deleted, thus, the measurements are not continuous. Additionally, each station had different time periods, therefore, the number of measurements varied from station to station. The time period between stations and variables were matched, in this way, the same number of measurements were obtained. Nevertheless, the total amount of data was still representative, all of them surpass 9 years of measurements for each station.

### Wind Data

In Table 5-3 and Figure 5-2, a total of eight wind stations surrounding the location of the Nezahualcoyotl dike are presented.

| Code | Name | Coordinates | | M.a.s.l (Meters above sea level) | Time Period |
|---|---|---|---|---|---|
| | | Longitude (dd) | Latitude (dd) | | |
| ACO | Acolman | -98.91 | 19.64 | 2198 | 01/07/2011-22/02/2018 |
| GAM | Gustavo A. Madero | -99.09 | 19.48 | 2227 | 01/12/2005-01/03/2018 |
| MON | Montecillo | -98.90 | 19.46 | 2252 | 01/02/1986-01/01/2006 |
| HAN | Hangares | -99.08 | 19.42 | 2235 | 01/01/2001-01/03/2018 |
| NEZ | Nezahualcoyotl | -99.03 | 19.39 | 2235 | 01/07/2011-01/03/2018 |
| UIZ | UAM Iztapalapa | -99.07 | 19.36 | 2221 | 01/03/1986-01/03/2018 |
| SAG | San Agustin | -99.03 | 19.53 | 2241 | 01/04/2015-26/02/2018 |
| XAL | Xalostoc | -99.08 | 19.53 | 2160 | 10/01/1986-01/03/2018 |

**Table 5-3 Wind stations.**

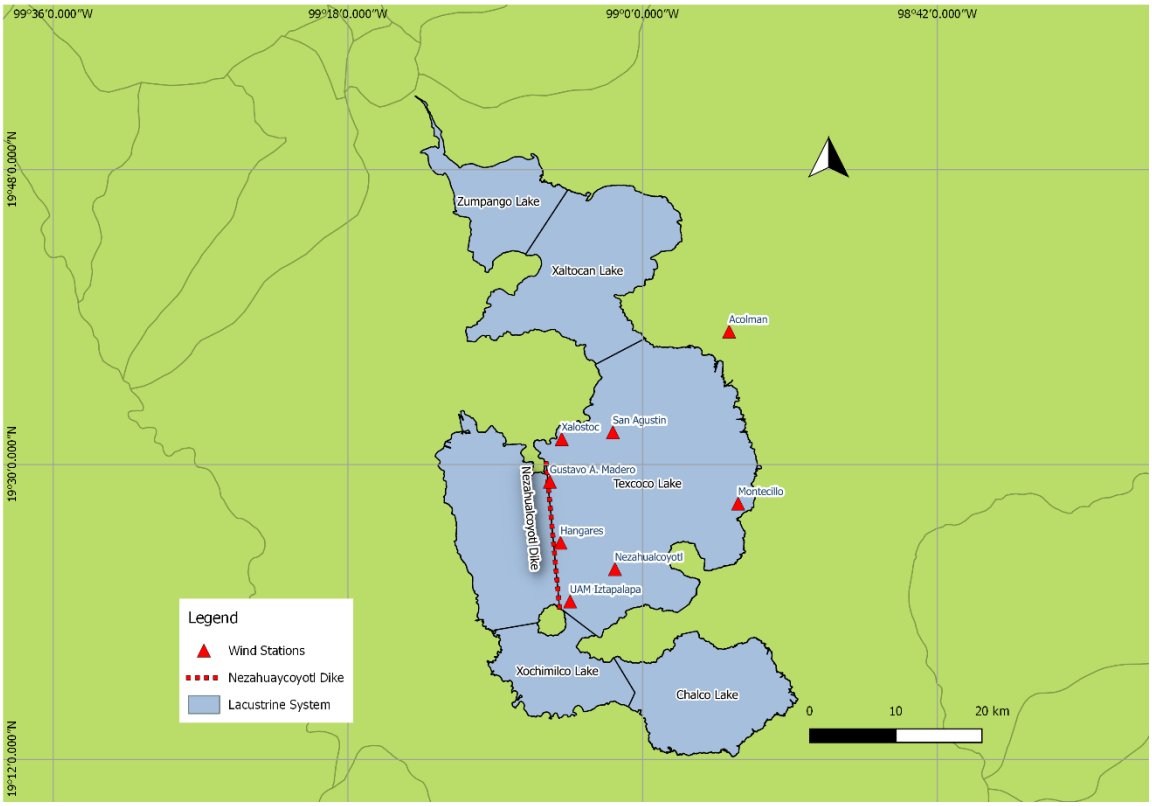


**Figure 5-2 Selected Wind Stations in the lacustrine system.**

The predominant wind direction was computed for each station using a Matlab script to plot wind roses by Pereira (2015). The result is shown in Figure 5-3.

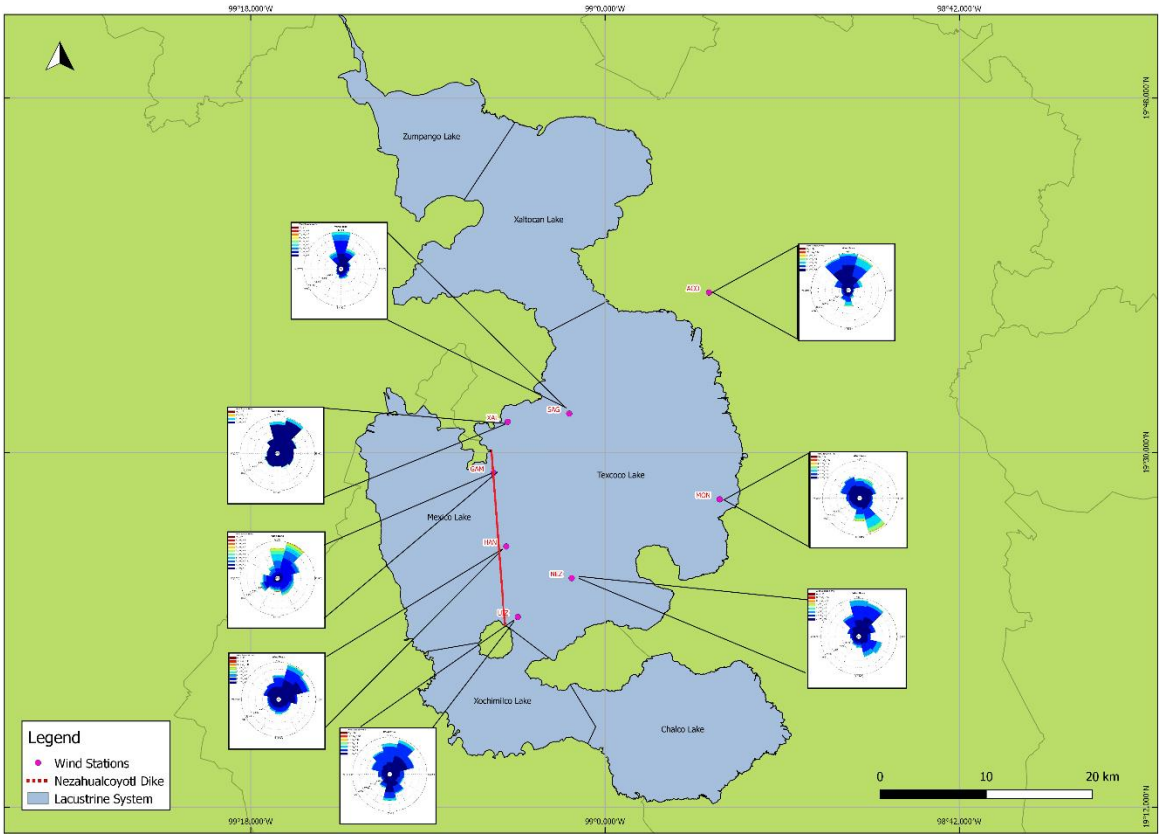


**Figure 5-3 Wind Rose map of the lacustrine system.**

In a wind rose, the frequency of wind over a time period is plotted according to wind direction. In this case, the considered time period was the entire length of the measurements as shown in Table 5-3. In Figure 5-3, the color bands show the wind speed ranges, and the direction of the longest radius determines the wind direction with the greatest frequency. The wind roses for all the stations are presented in Appendix A.

For Acolman, Nezahualcoyotl and San Agustin stations, the wind is predominantly directed to the south at a speed between 0 and 2m/s, 2 and 4m/s and 2 and 3m/s respectively. While for Gustavo A. Madero, Hangares, UAM Iztapalapa, and Xalostoc stations the predominant wind direction is directed towards the southwest at velocities ranging from 0 to 5 m/s. Finally, Montecillo station has a predominant wind direction to the north-west with velocities between 2 and 6m/s.

From the location of the stations and the data obtained from the wind roses, it is possible to determine the relevance of wind at the Nezahualcoyotl dike. As seen in Figure 5-3, none of the stations have their predominant wind direction towards the dike, however, most of the stations at the east side of the dike shows that the predominant wind direction is towards the south end of the dike, this factor is important because a long fetch favors wind set-up.

Wind set-up increases with increasing wind velocity and fetches and decreasing water depth, therefore, for its calculation, the worst case scenario will consider the set-up at the south end of the dike. The computation will contemplate the maximum velocities corresponding to its predominant wind direction at each station at the east. Figure 5-4 shows the results for the stations with the longest fetch towards the south end of the dike.

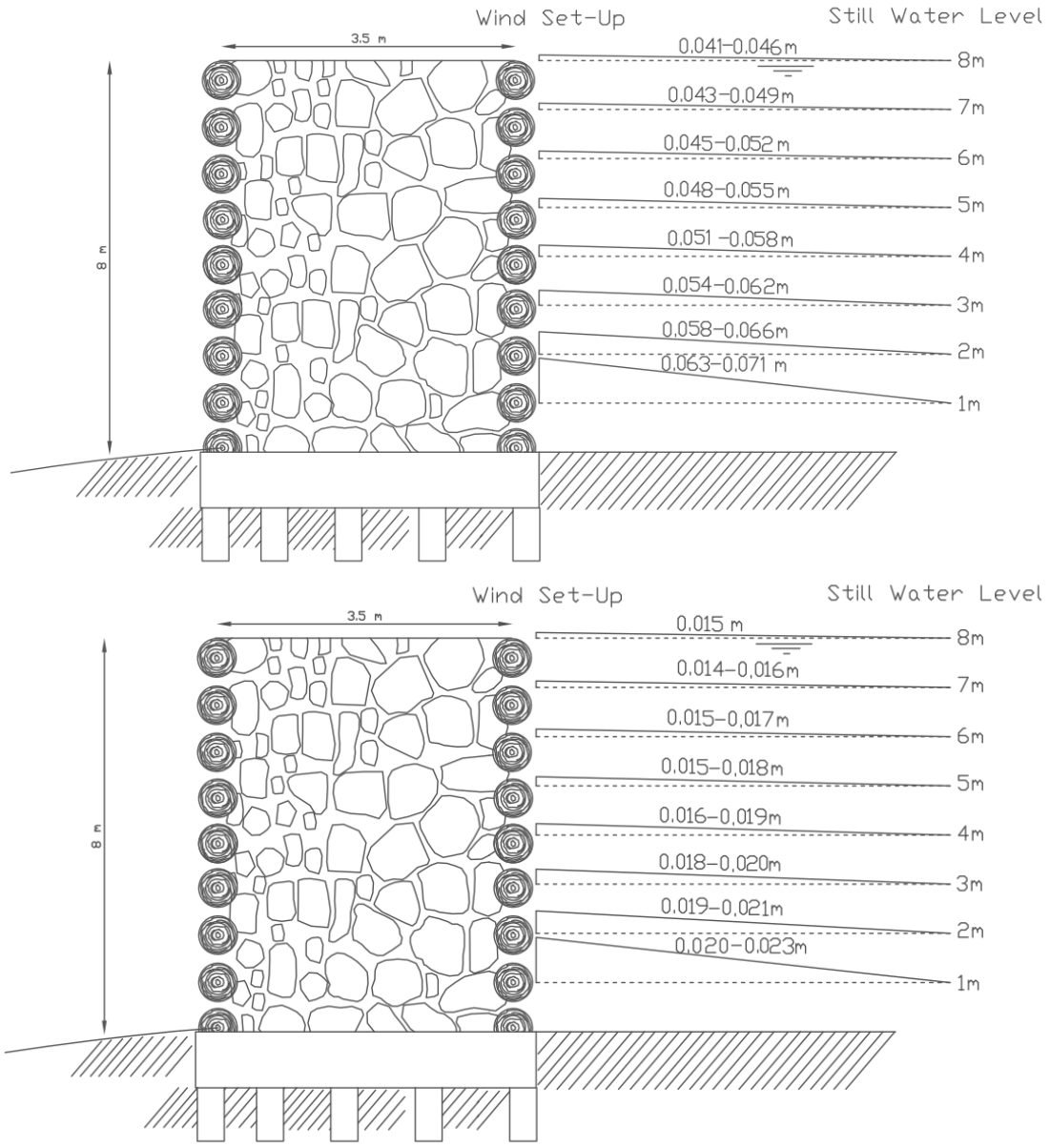


**Figure 5-4 Wind Set-Up and the south end of the dike for maximum velocities. Acolman Station (8m/s) (Upper figure). San Agustin Station (6m/s) (Lower figure)**

*Left side of the dike: Lake Mexico. Right side of the dike: Lake Texcoco.*

Figure 5-4 presents the layout of the Nezahualcoyotl dike (Too see how this layout was obtained please refer section 5.3) with different water depths at the foot of the structure. It is noticed that wind set-up does not represent a flood threat when the water level in the proximity of the dike is not equal to the height of the dike and as mentioned previously, the higher the water level, the smaller the wind set up. The values shown in Figure 5-4 correspond to the wind set-up for the maximum velocities recorded for Acolman and San Agustin stations, but the wind roses show that such velocities occur less than 1% of the time for both stations (Appendix A).

Velocities that occur most of the time (9% of the time approximately) do not exceed 4m/s and the corresponding wind set-up is 0.004 and 0.015m for a water depth of 8 meters for Acolman and San Agustin stations respectively.

However, the wind set-up needs to be considered also at the center of the Nezahualcoyotl dike given that this section corresponds to the deepest part of Lake Texcoco and it was also the location of the city of Tenochtitlan (See Figure 5-7). The stations with the longest fetch are Acolman and Montecillo and the corresponding wind set up at 8m depth is 0.1 and 0.15 meters respectively.

**Geographical Information and Terrain Data**

Geographic data were obtained from two different sources (INEGI and HydroSHEDS), in total, three topographies were gathered (Table 5-4). In order the characterize the terrain of the lacustrine system, a transect was drawn across the lake (including the dike) and a cross-section view was obtained for the three topographies. Figure 5-5 shows the position of the transect:

| Name | Resolution |
|---|---|
| HydroSHEDS | Mexico Void filled DEM 15 Arc-second resolution. |
| HydroSHEDS | Mexico Void filled DEM 3 Arc-second resolution. |
| INEGI | Contour lines 1:20000m scale. |

**Table 5-4 Geographical and Terrain data sources.**

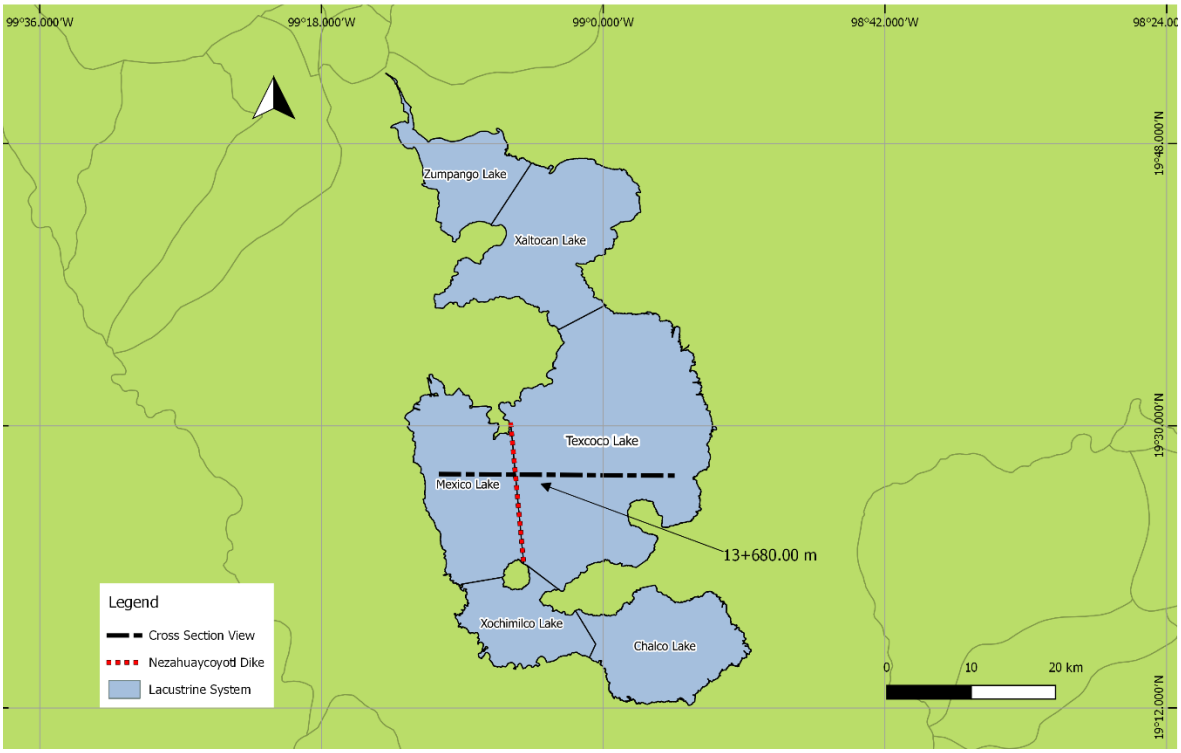


**Figure 5-5 Location of the dike and transect for cross-section view of the lake.**

The point at which the dike meets the transect corresponds to 13+680m (starting from the left side of the transect). At this point and its surroundings, the terrain for the 3 different topographies is compared as shown in Figure 5-6.

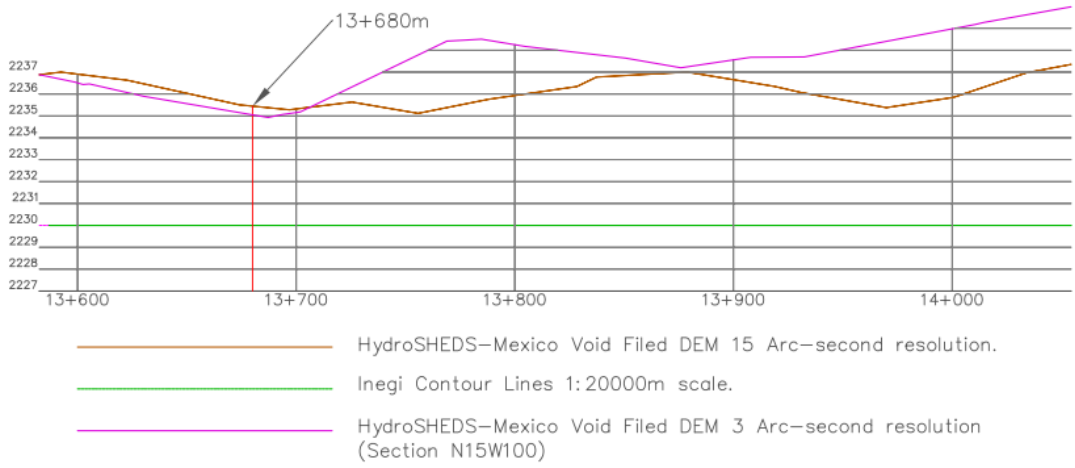


**Figure 5-6 Cross section view of the transect for the 3 topographies.**

Figure 5-6 shows that both profiles from Hydro-SHEDS agree with each other, while the profile from INEGI differs greatly (5 meters approximately). At first, the right choice would be to use one of the topographies from Hydro-SHEDS, preferably the one with the highest resolution (3 Arc-second). However, the data from INEGI was produced using techniques of photometry, generating contour lines every 10m, so it can be assumed that this source is more accurate than the Hydro-SHEDS sources.

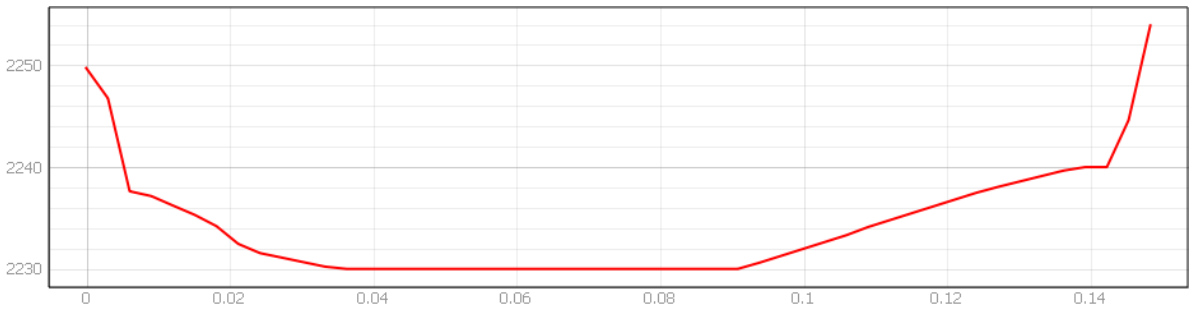


**Figure 5-7 Longitudinal Section of the Nezahualcoyotl Dike.**
X-axis: Meters above sea level. Y-axis: 0.01Km.

Notice from the previous figure, that the terrain in which the dike was constructed, did not have the same bottom level throughout the entire longitude of the dike. The middle part of the dike (3.5-9 Km) had a level of 2230 m.a.s.l while the north (Left end in Figure 5-7) and south (Right end in Figure 5-7) end are the highest ones (Between 2240 and 2250m). Thus, the middle section was the lowest of the entire dike, the risk of floods was bigger for this section which also was the place where Tenochtitlan was located approximately.

### Volume Elevation Curve

The Volume-Elevation curve was generated using a spatial analysis tool (ArcGIS) together with the topography from INEGI. The command “Surface Volume” in ArcGIS was used to perform this task. It calculates the area and volume of a Digital Elevation Model (DEM) above or below a given reference plane, as shown in Figure 5-8.

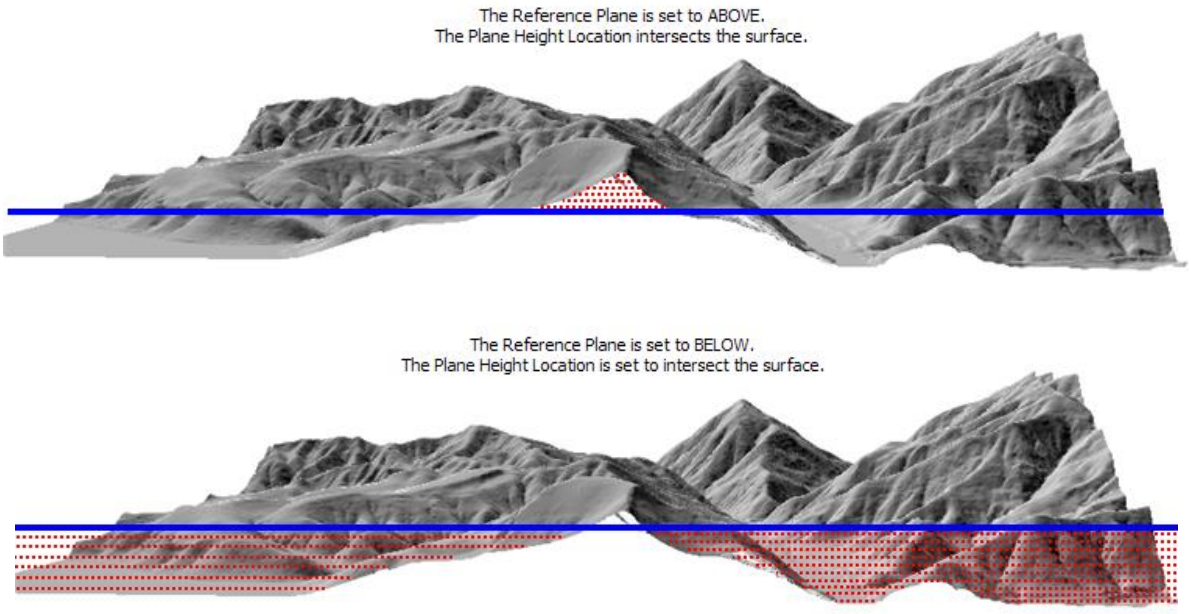


**Figure 5-8 Illustration of computation of Surface Volume tool in ArcGIS.**
*http://desktop.arcgis.com/es/arcmap/10.3/tools/3d-analyst-toolbox/surface-volume.htm*

The reference plane was set to BELOW in order to compute the volume of water at the lake system at different levels as shown in Figure 5-9.

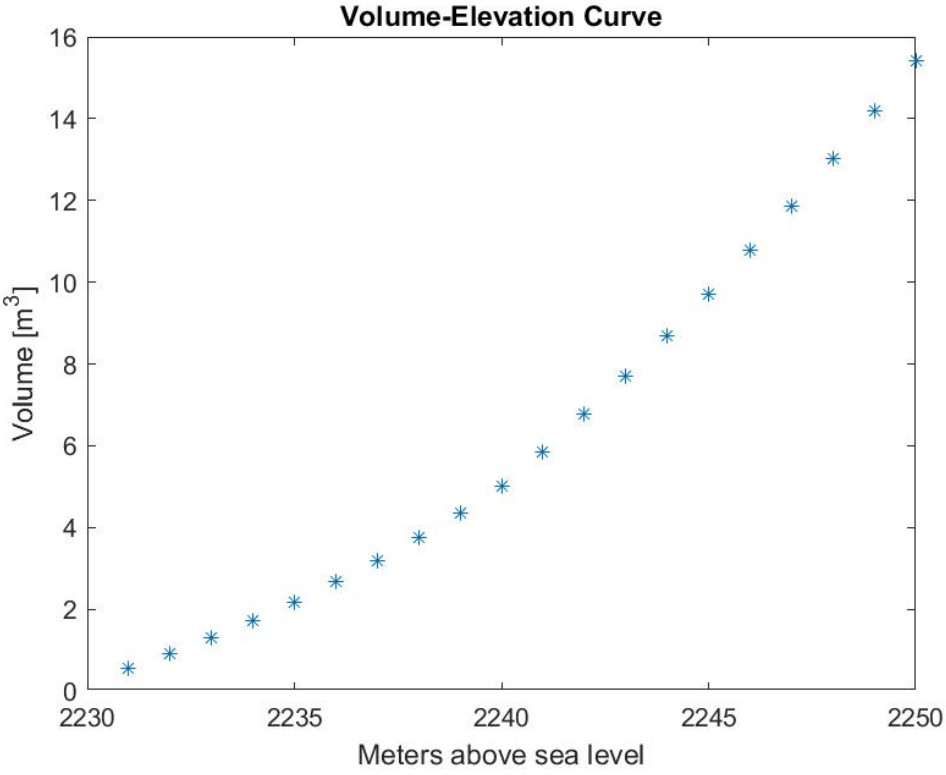


**Figure 5-9 Volume-Elevation Curve**

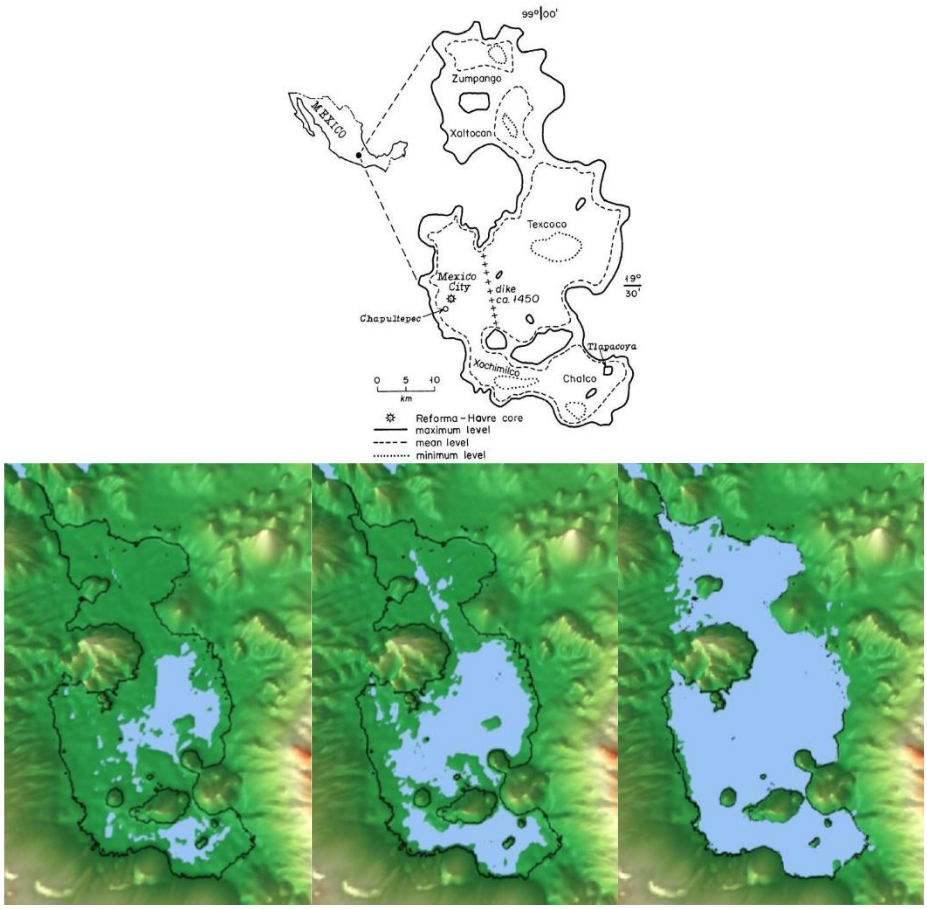


**Figure 5-10 (a) Water levels in the Basin of Mexico (Bradbury, 1971) (Top); (b) Lake at level 2231 m.a.s.l (Bottom Left); (b) Lake at level 2236 m.a.s.l (Bottom Center); (d) Lake level at level 2250 m.a.s.l (Bottom Right).**

In Figure 5-10, the map proposed by Bradbury (1971) and the results from the V-E curve are presented. A comparison between these figures was executed in order to determine a better estimation of the water levels in the lacustrine system. There is a clear difference between the minimum watermark of Figure 5-10a and Figure 5-10b, the surface area of water in the latter is much bigger than the amount of water shown in the first figure, this indicates that the lowest watermark proposed by Bradbury (1971) could have been lower than 2230 m.a.s.l, however, both figures coincide that the lakes are not joined together. Moreover, level 2230 is the level at the foot of the dike (Figure 5-7), therefore, it can be assumed the level 2231 m.a.s.l the minimum water level for this thesis. The complete evolution of the water level in Lake Texcoco is presented in Appendix B.

Figure 5-10a shows that at mean water level, Lake Texcoco has merged with the lakes from the south but not yet with the lakes from the north, a similar delimitation can be appreciated in the results from ArcGIS between levels 2236 and 2239 m (Figure 5-10c). The lakes from the north are merged with the rest of the lacustrine system at level 2240 m.a.s.l (Figure 5-11b) until the system is completely full at 2250 m.a.s.l (Figure 5-10d), the high watermark coincides with the description given by Palerm (1973) and Figure 5-10a.

The system was not filled with water beyond the high water mark of 2250 m.a.s.l given that at such level the water depth at the middle section of the Nezahualcoyotl dike would be of 20 meters (12 meters higher than the height of the dike. Refer to section 5.3), thus, higher water levels would not provide additional information to the reliability of the dike.

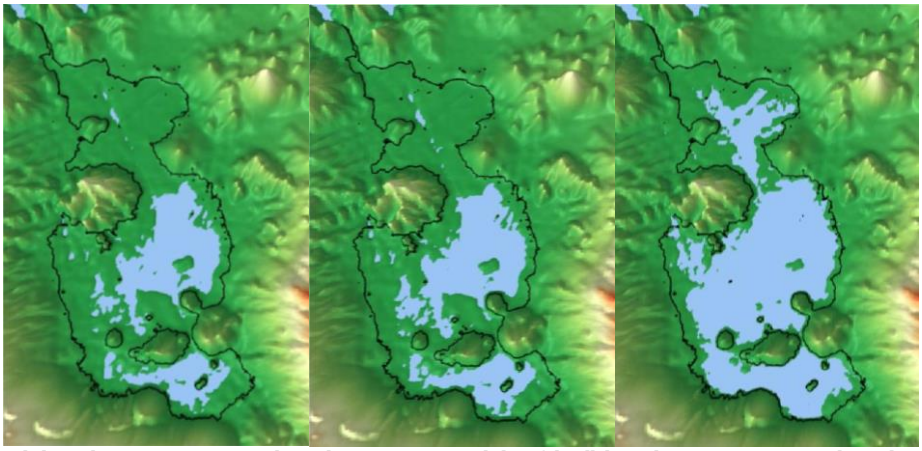

**Figure 5-11 (a) Lake Texcoco at level 2232 m.a.s.l (Left); (b) Lake Texcoco at level 2233 m.a.s.l (Middle); (c) Lake Texcoco at level 2240 m.a.s.l.**

Notice that in Figure 5-10b there is almost no water in Lake Mexico, while in Figure 5-11a and in Figure 5-11b (1 and 2 meters higher respectively), the water level in Lake Mexico starts to become noticeable. This indicates that Lake Mexico was higher than Lake Texcoco. Moreover, Lake Mexico was constrained to keep a constant water level throughout the year due to the chinampa system, thus, in order to estimate the water level in this lake, it was also necessary to obtain the elevation at the foot of the most important temple in Tenochtitlan: "Templo Mayor" (of which there are still vestiges in Mexico City) located in the center of the Aztec capital. See Figure 5-12.

**Figure 5-12 Templo Mayor. Top View (Left); Street View (Right)**
Source: Google Earth (2018).

The elevation at the red dot in Figure 5-12 is equal to 2232m. Thus, the water level in Lake Mexico could not exceed such height in order to avoid flooding the city.

Is important to keep in mind that the volumes presented in Figure 5-9 are a rough estimation of the system given that the procedure involved to generate such data is different from the actual filling process that the system had. In this scenario, the system was filled with water from the bottom of Lake Texcoco and up, while in reality, it was the other way around, the highest lakes filled first and the water surplus flowed towards Lake Texcoco. Finally, it was possible to compute the surface area of each lake in the system at the high water mark (2250 m.a.s.l) as shown in Table 5-5.

| Lake | Surface Area [Km2] |
|---|---|
| Chalco Lake | 175.38 |
| Mexico Lake | 207.52 |
| Texcoco Lake | 534.69 |
| Xaltocan Lake | 240.59 |
| Xochimilco Lake | 107.54 |
| Zumpango Lake | 107.09 |

**Table 5-5 Surface area of the lakes in the system at complete flooding.**

All together sum a surface area of 1372.83 $Km^2$ in which the Texcoco lake occupies 27% of the total.

## 5.3 Layout of the Nezahualcoyotl Dike

As described in section 3.5, the city of Tenochtitlan had to face multiple floods during its history. At one of them, around the year 1446, during the reign of Moctezuma I (Palerm, 1973; Lombardo de Ruiz, 1973), the water level in Lake Texcoco grew so much that flooded most part of the city and the population had to mobilize with canoes and small boats. Moctezuma did not know which solution apply to such a situation, so he sent his messengers to Texcoco and asked to the king of that land, Nezahualcoyotl, for ideas on how to avoid the flood to reach the entire city, because at that time many buildings had fallen or been completely destroyed.

After knowing this situation, Nezahualcoyotl went to Tenochtitlan and together with Moctezuma decided that the most effective solution was to construct a fence that could stop the water from reaching the city. The construction of the Nezahualcoyotl dike began around the year 1450 (Palerm, 1973; Daou, 2011).

The dike cut Lake Texcoco from north to south forming two lakes (Figure 5-13): Mexico (West) and Texcoco (East) and it crossed from the Santa Catarina Mountains in Tepeyac to the Sierra de la Catarina near Ixtapalapa.

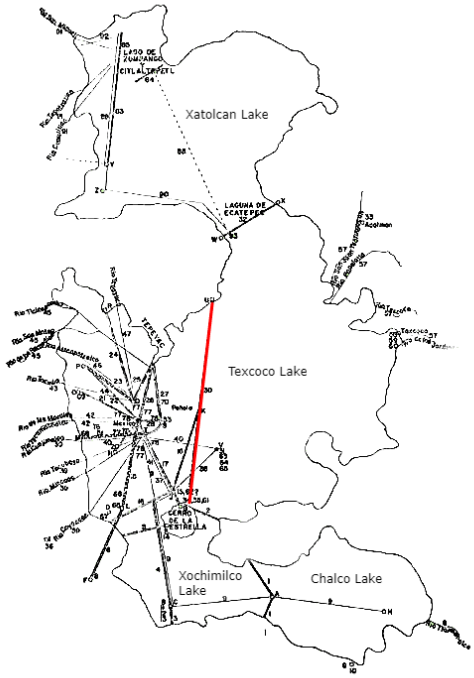


**Figure 5-13 Position of Nezahualcoyotl dike (Red). (Modified from Palerm, 1973)**

In Figure 5-13, not only the Nezahualcoyotl dike is appreciated (red line) but also the extent of all dikes and walkway-dike system developed by the Aztecs until the arrival of the Spanish. The walkway-dikes were cut by bridges to allow the navigation of canoes, however, there is no evidence that the Nezahualcoyotl dike had these cuts. Other sources mention openings that allowed to drain Lake Mexico (Palerm, 1973). If this were true, it had to exist a way to open and close such openings to allow the dike to function as a flood protection structure and as a separation between the Lake Mexico and Texcoco (Palerm, 1973). In this research, the presence of openings, gates and/or cuts will not be taken into account.

The following transformations in the system are attributable to the Nezahualcoyotl dike and the construction of the many hydraulic works in the western part of the Texcoco lake (Palerm, 1973):

a. Lake Mexico was salt-free which allowed a big extension of the chinampas, however, these constructions reduced even more the natural drainage and the capacity of storage of water in the lake.
b. By affecting the drainage of the freshwater lakes from the south (Chalco-Xochimilco) and of Lake Mexico towards Lake Texcoco, the cycle of flooding on the city of Tenochtitlan changed, sometimes due to the fresh water (due to lack of drainage) and other times due to saltwater (Invasions from the reduced Lake Texcoco).

Given that the dike no longer exists, its dimensions are based on historical reports and vary depending on the author. Table 5-6 presents a summary from several sources:

| Source | Length [m] | Height [m] | Width [m] |
|---|---|---|---|
| Lombardo de Ruiz (1973) (1) | 14484.1 | - | 7.3 |
| Lombardo de Ruiz (1973) (2) | 16000.0 | 4.0 | 9.0 |
| Palerm (1973)- First Sources of the Spanish Conquest | 16000.0 | - | - |
| Palerm (1973)- Spanish and Indigenous Sources of the First Period of Viceroyalty | 14484.1 | - | 7.3 |
| Palerm (1973)- Late sources of the Viceroyalty | 14484.1 | - | 20.1 |
| Legorreta (2006) | 16000.0 | - | - |
| Daou (2011) | 15000.0 | - | - |
| Hernández Cruz (2013) | 16000.0 | 8.0 | 3.5 |

**Table 5-6 Compilation of data for the Nezahualcoyotl dike.**

As seen in the previous table, the estimations from the authors have big differences, while others had not mentioned all the relevant dimensions. However, most of them agree that the dike was 16 km long. Most the sources are based on anecdotes by the first Spanish who arrived at the Valley of Mexico, they were not engineers or constructors, therefore, their appreciation of the dike could not have been accurate. According to Armillas (1971), the lacustrine system was shallow and this allowed the expansion of the chinampas in the lakes (This is true according to the water level in Lake Mexico). Therefore, it would be reasonable that the height of the dike could have been between 3.5 to 4 meters instead of 8m as some of the sources suggest. However, as shown in the previous section, the level at the bottom of Lake Texcoco was 2230 m.a.s.l and the mean water level fluctuated between level 2236 and 2239 m.a.s.l (Figure 5-10c). Thus, the dike would have needed to be higher than 6 meters in order to withstand above average water levels. The dimensions provided by Hernández Cruz (2013) in Table 5-6 seems reasonable.

Lombardo de Ruiz (1973) and Palerm (1973) provide a description of the materials used to construct the dike: “Thick wooden piles were stuck to the ground forming a hollow fence, inside the fence, big rocks and sand were deposited between the piles”. A representation of this description is shown in Figure 5-14.

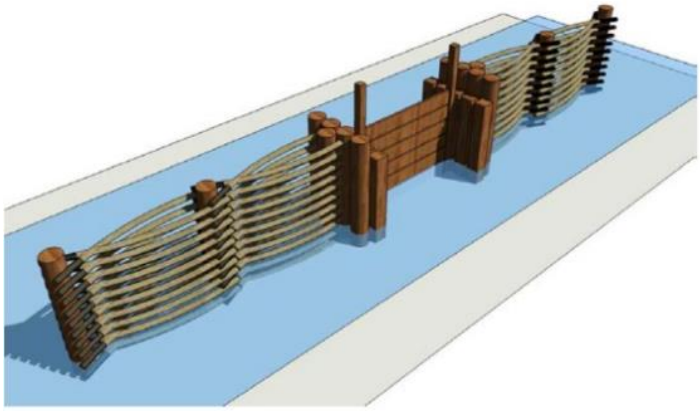

**Figure 5-14: 3D Graph of the construction base for the Nezahualcoyotl dike. (Olivas Solano, 2010)**

Similar structures can also provide information on the construction techniques and materials employed for the Nezahualcoyotl dike, one of them is the Chapultepec aqueduct, described as follows (Peña Santana & Levi, 1989):

In 1418, Nezahualcoyotl, Lord of Texcoco, designed an aqueduct that would transport water from the Chapultepec springs towards the center of Tenochtitlan. The first version of the structure was constructed using rafts of reeds that were stuck through posts to the bottom of the lake to form its base, then the rafts were sunk by loading them with grass, stones, and mud. The bases were

aligned leaving spaces for the circulation of water from the lake. On top of the bases, the pipes were constructed using compacted mud reinforced with wooden sticks. This first structure was weak and it finally disappeared in the big flood of 1446, such flood led to the construction of the Nezahualcoyotl dike in 1450.

The reconstruction of the aqueduct started in 1465 considering several changes on the construction techniques: The new version was built using masonry; this structure was very resistant and even survived for many years after the Spanish conquest. Figure 5-15 shows a cross-section of the aqueduct with its relevant dimensions:

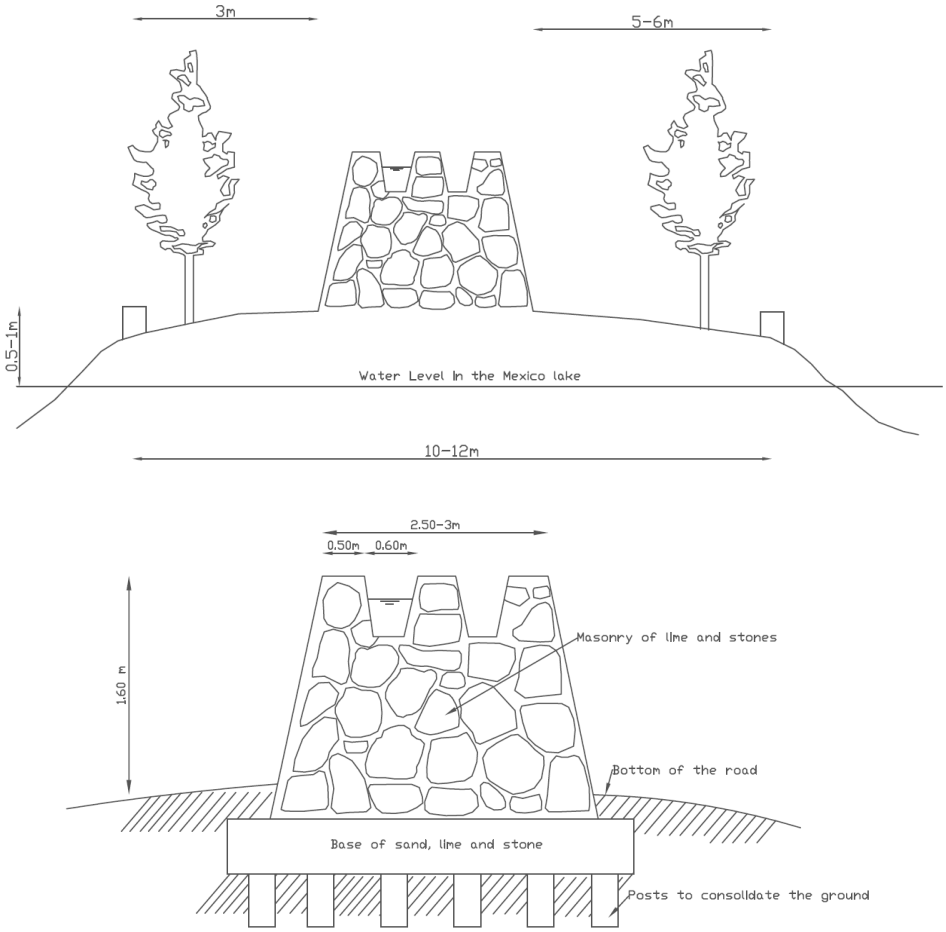


**Figure 5-15 Cross sections of the Chapultepec's aqueduct. Modified from Peña Santana & Levi (1989).**

From the descriptions of both structures, several points can be made: First, both were designed by Nezahualcoyotl. Second, the construction of the dike and the last version of the aqueduct started after the big flood in 1446, therefore, both structures needed to be designed to withstand floods and consequently, to have similar construction materials and techniques.

In Figure 5-13, Palerm (1973) determines the orientation of the dike (From the Santa Catarina Mountains to the Sierra de la Catarina near Ixtapalapa). By following this description, the dike was drawn and then measured in ArcGIS. It was found that it measured 21 Km approximately instead of 16 Km as most of the historical sources in Table 5-6 suggests. Two scenarios are possible:

a. The visual estimation of the Spanish conquerors was not reliable. After all, they did not have a background in construction or other related fields that would have allowed them to make a proper visual estimation.
b. The proposed orientation of the dike by Palerm (1973) is wrong.

Therefore, assuming that point b is true, another orientation for the dike is proposed. The north end of the dike was moved towards the west in order to comply with the 16km estimated by Palerm's (1973) historical sources.

Finally, the layout of the Nezahualcoyotl dike was characterized as follows:

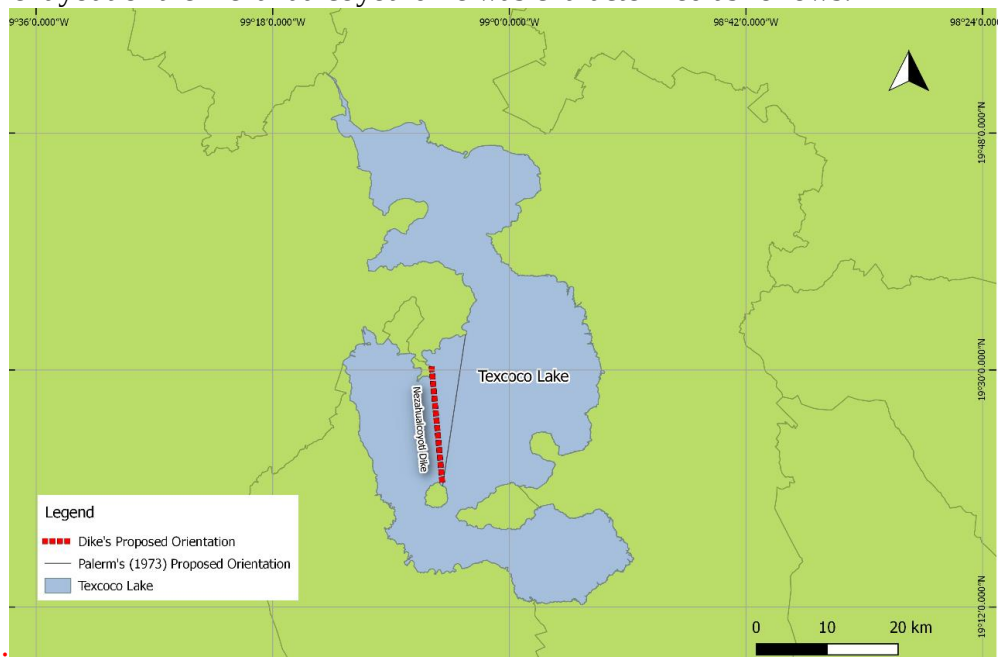


**Figure 5-16 Proposed orientation of the Nezahualcoyotl Dike. (Top View)**

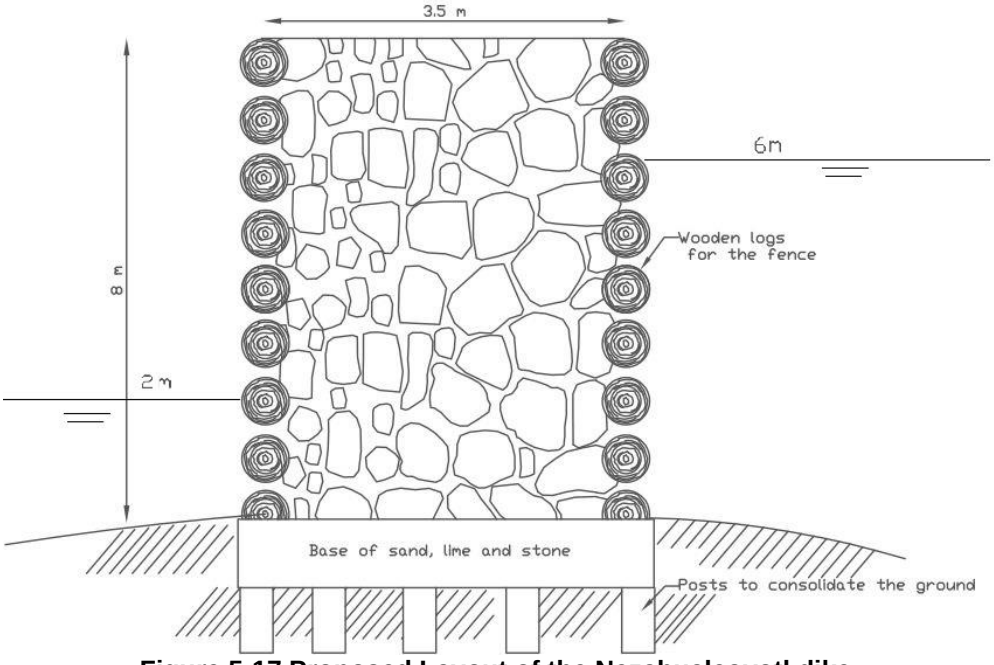


**Figure 5-17 Proposed Layout of the Nezahualcoyotl dike.**
Water depth in Lake Mexico and Tenochtitlan (Left side of the dike); Mean water depth in Lake Texcoco (Right side of the dike).

| Length [Km] | Height [m] | Width [m] |
|---|---|---|
| 16000.0 | 8 | 3.5 |

**Table 5-7: Proposal of the dimensions for the Nezahualcoyotl dike.**

Figure 5-16 and Figure 5-17 show the top and cross-section view of the Nezahualcoyotl dike that will be used for this thesis. This characterization was based on the analysis of water levels at the lakes presented in section 5.2 which led to the conclusion that the mean water level was approximately 2236 m.a.s.l. (6m water depth at the foot of the dike). In this way, the description provided by Hernández Cruz (2013) in Table 5-6 was appropriate given that the other sources in such table provide descriptions of a much smaller dike that would not have been able to stand water levels lower than the mean (3 to 4m water depth at the foot of the dike), which seem unreasonable given that the dike never failed during its lifetime.

# 6 Hydrological Model Results

This chapter presents the results obtained by following the hydrological model presented in Chapter 4. First, a description of the characterization of the wet seasons is provided, followed by an analysis of the generated synthetic data and finally, the resulting water levels at Lake Texcoco are presented.

## 6.1 Simulation of Wet seasons

In section 4.4.2 it was mentioned that in order to develop the copula model, the environmental variables (precipitation and evaporation) were fitted to probability distributions. Only data corresponding to the months within the wet season were considered, therefore, the results reflect the behavior of the variables during that time.

The fitted distribution functions were obtained by using a Matlab script: ALLFITDIST developed by Sheppard (2012) and are shown in Table 6-1.

| Station | Probability Distribution Function | |
|---|---|---|
| | $PR$ | $E$ |
| Atenco | Generalized Pareto | Generalized Extreme Value |
| La Grande | Generalized Pareto | Generalized Extreme Value |
| San Andres | Generalized Pareto | Generalized Extreme Value |
| El Tejocote | Generalized Pareto | Generalized Extreme Value |
| Chapingo (DGE) | Generalized Pareto | Generalized Extreme Value |

**Table 6-1 Results of the distribution fitting for the environmental variables.**

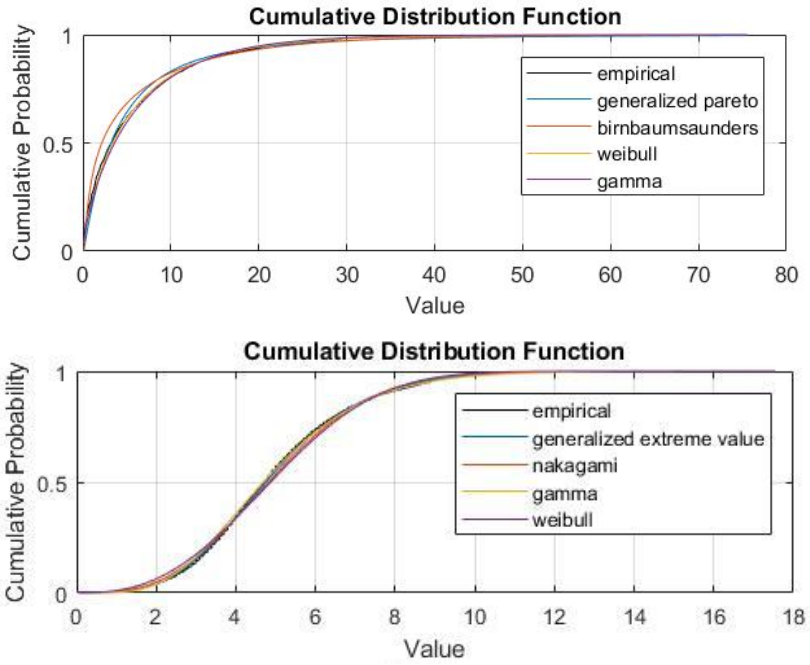


**Figure 6-1 CDF's for Precipitation and Evaporation data at Atenco Station.**
*X-axis units: Mm/day.

Figure 6-1 shows an example of the CDF's (Cumulative distribution function) computed for Atenco station for the environmental variables. Appendix C presents the CDF's of the other four stations and statistics of the goodness of fit. The results from Table 6-1 were obtained based on the negative log-likelihood method (NLogL) which is an equivalent of the maximum likelihood

estimation (MLE). The distribution with the lowest NLogL value was chosen as the best fit. This method allows estimating the parameters of the fitted probability distribution given the measurements of each variable. The computed parameters are presented in Appendix D.

The next step in the hydrological model was obtaining a description of the occurrence of rain in the basin. This was achieved by using a Markov Chain model -characterized by a transition matrix $P$ - (section 4.4.1). The values of the matrix for all five stations are shown in Table 6-2.

| Code | Name | $P_{00}$ | $P_{01}$ | $P_{10}$ | $P_{11}$. |
|---|---|---|---|---|---|
| 15008 | Atenco | 0.61 | 0.39 | 0.31 | 0.69 |
| 15044 | La Grande | 0.67 | 0.33 | 0.39 | 0.61 |
| 15083 | San Andres | 0.59 | 0.41 | 0.33 | 0.67 |
| 15167 | El Tejocote | 0.61 | 0.39 | 0.38 | 0.62 |
| 15170 | Chapingo (DGE) | 0.61 | 0.39 | 0.34 | 0.66 |

**Table 6-2 Transition Matrix $P$ for precipitation.**

The results of this table describe the probability of transitioning from state 0 (Dry day) to state 1 (Wet day), 0 to 1, 1 to 1 and 1 to 0. Notice that for all five stations, the probability that dry days will transition into dry days and the probability that wet days will transition into wet days is almost double the probability that a dry day will transition into a wet day or vice versa. Thus, is more probable that once it starts raining, it will keep raining and the same can be said once it is stopped raining. As the probabilities of all stations are very close to each other, the east region of Lake Texcoco has a similar spatial pattern of rain.

The resulting rain pattern was obtained in the form of vectors containing zeros and ones, representing dry and wet days as mentioned previously. Such a process was performed using the "simulate" tool in Matlab in combination with the transition matrix $P$ .

## 6.2 Generation of Synthetic Data

The synthetic time series for precipitation and evaporation were produced using bivariate copulas considering the pairs of data presented in section 4.4.2. From the copulas, it was possible to estimate the dependence and autocorrelation that characterize the data. See Table 6-3.

| Station | Spearman's rho correlation coefficient | | |
|---|---|---|---|
| | $PR-PR$ | $E-E$ | $PR-E$ |
| Atenco | 0.27 | 0.46 | 0.18 |
| La Grande | 0.25 | 0.41 | 0.19 |
| San Andres | 0.24 | 0.5 | 0.09 |
| El Tejocote | 0.18 | 0.44 | 0.16 |
| Chapingo (DGE) | 0.25 | 0.46 | 0.18 |

**Table 6-3 Correlation values for all stations and pairs.**

*Precipitation (PR), Evaporation (E).

The pairs of data sets were analyzed in order to find which copula describes best the dependence between them. The Gauss, Gumbel, and Clayton copula were considered in this study and two methods were used to verify the best fit: The Cramer von Mises and the Semi correlations method (Section 2.6. Eq. 10,Eq. 11 and Eq. 12). As an example, the results for the pair precipitation-evaporation at one of the stations (Atenco) are shown in Figure 6-2 to Figure 6-5.

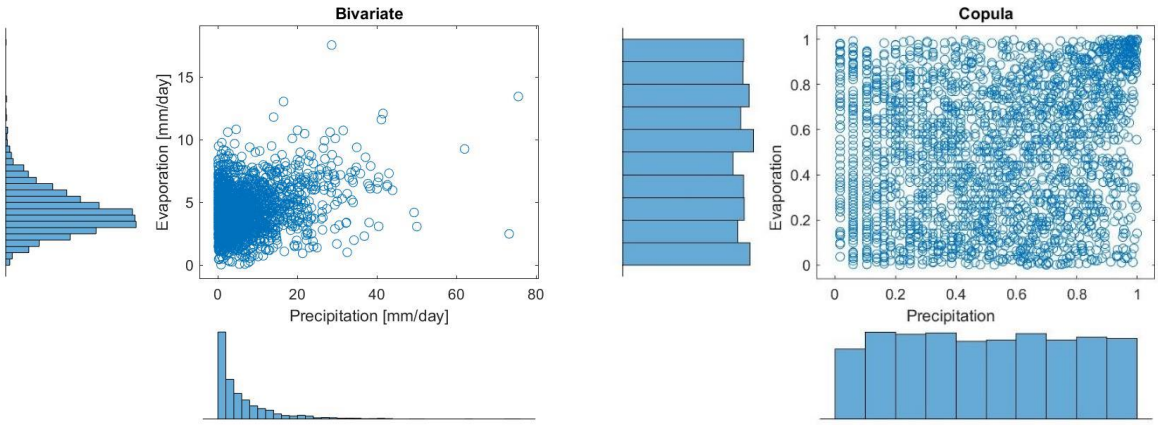


**Figure 6-2 Marginal data for Precipitation and Evaporation (Left). Pseudo-observations for precipitation and evaporation (Right). Atenco Station.**

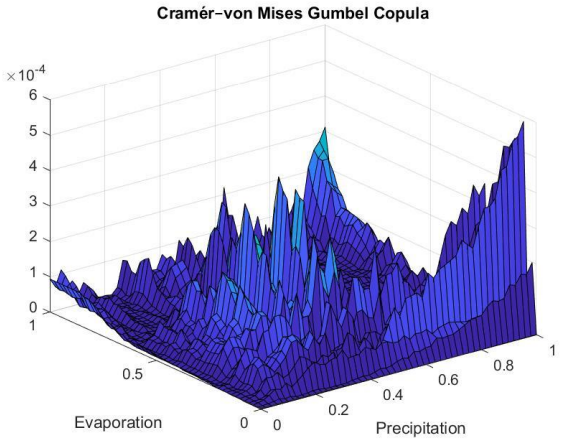


**Figure 6-3 Cramer von Mises results (Gumbel Copula) for the pair Precipitation-Evaporation. Atenco Station.**

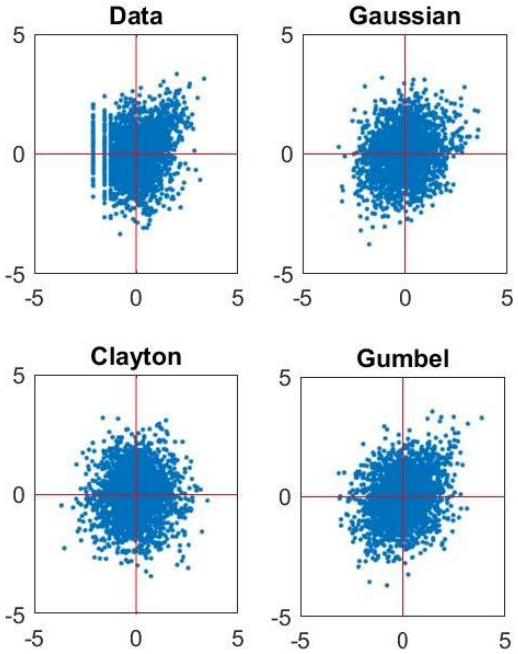


**Figure 6-4 Copula plot transformed to Standard Normal for the pair Precipitation-Evaporation. Atenco Station.**

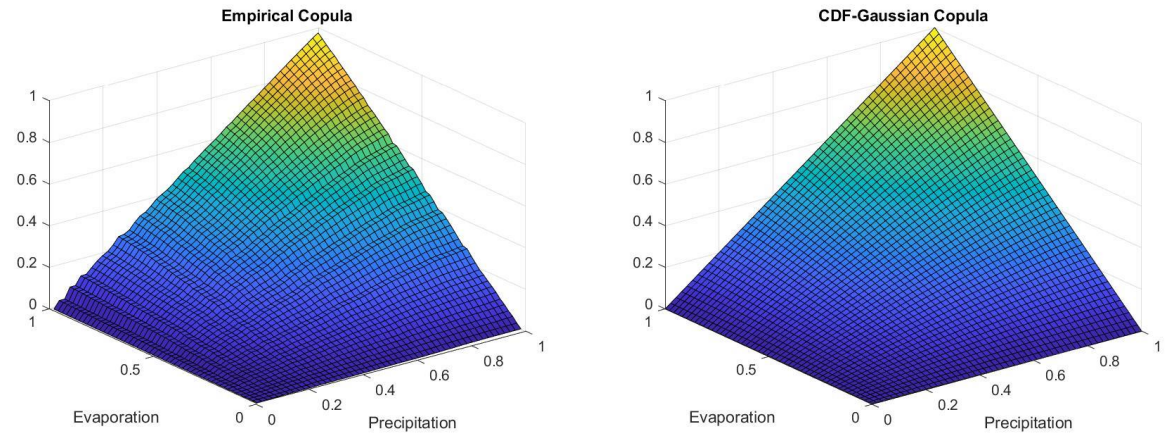


**Figure 6-5 Empirical (Left) and Gaussian (Right) copula for the pair Precipitation-Evaporation. Atenco station.**

Figure 6-2 presents a visualization of the variables in their original units and after the data has been transformed into pseudo-observations. The observations can be safely transformed to pseudo-observations using ranks and become uniformly distributed. Notice that the density of points at the upper right corner of Figure 6-2 (Right) appears to be slightly larger than the density at the lower left corner. This could be an indication of upper tail dependence. Figures of the other stations and pairs are presented in Appendix E.

Figure 6-3 shows the absolute difference between the Gumbel copula and the empirical copula (Eq. 10). This is the basis of the Cramer von Mises method ($S_n$). The Gumbel copula presented the lowest value of $S_n$ for Atenco Station (Table 6-4). However, before a decision is made for the best copula fit, the results from semi-correlation method needs to be analyzed. Table 6-4 presents the values of correlation for each quadrant at each copula considered:

| **Station** | $\rho$ | **Copula** | $\rho_{ne}$ | $\rho_{sw}$ | $S_n$ |
|---|---|---|---|---|---|
| Atenco | 0,18 | Gauss | 0.04 | 0.14 | 0.17 |
| | | Gumbel | 0.33 | 0.12 | 0.12 |
| | | Clayton | -0.05 | 0.01 | 0.58 |
| | | Data | 0.42 | -0.036 | - |

**Table 6-4 Cramer von Mises and Semi-correlation values for the pair precipitation-evaporation. Atenco Station.**

Based on the previous table, the values of semi correlations clearly show tail asymmetry (Figure 6-4). This suggests that a copula with upper tail dependence is preferred (Gumbel) and considering that the copula with the smallest value of square difference also belongs to the Gumbel copula, such model is chosen as the best (from the ones considered in this research) to describe the dependence between the variables. The results of Cramer von Mises and Semi-correlation for the other pairs and stations are presented in Appendix E.

A similar analysis was applied to all the considered pairs of all the stations, the results regarding the best fitting copula across different stations are shown in Table 6-5.

| Pairs | Atenco | La Grande | San Andres | El Tejocote | Chapingo (DGE) |
|---|---|---|---|---|---|
| $PR-PR$ | Gauss | Gauss | Gauss | Gauss | Gauss |
| $E-E$ | Gumbel | Gumbel | Gumbel | Gumbel | Gumbel |
| $PR-E$ | Gumbel | Gumbel | Gumbel | Gumbel | Gumbel |

**Table 6-5 Copula fit for all stations and pairs of variables.**

*Precipitation ( $PR$ ), Evaporation ( $E$ ).

The previous table shows that the copulas that best describes each pair of data are the same for all stations. Additionally, from Table 6-3, it was mentioned that the correlation value for each pair is very similar for all stations. This indicates that at different locations of the east side region of Lake Texcoco the variables have a similar dependence with each other, consequently, they can also be described by the same copula model (Table 6-5). Moreover, Table 6-1and Table 6-2 also showed that the variables of all five stations could be modeled by the same probability distribution function and that they have similar transition probabilities. Thus, all stations have an alike rain pattern. Based on these findings, is possible to choose the results from only one station (Preferably the station with the highest correlation values) to generate the time series of synthetic data. Therefore, Chapingo (DGE) station was selected. Hence, the pair was modeled with a Gaussian copula, while the pairs $E-E$ and $PR-E$ were modeled with a Gumbel copula. As an example, the synthetic time series of one wet season is shown below:

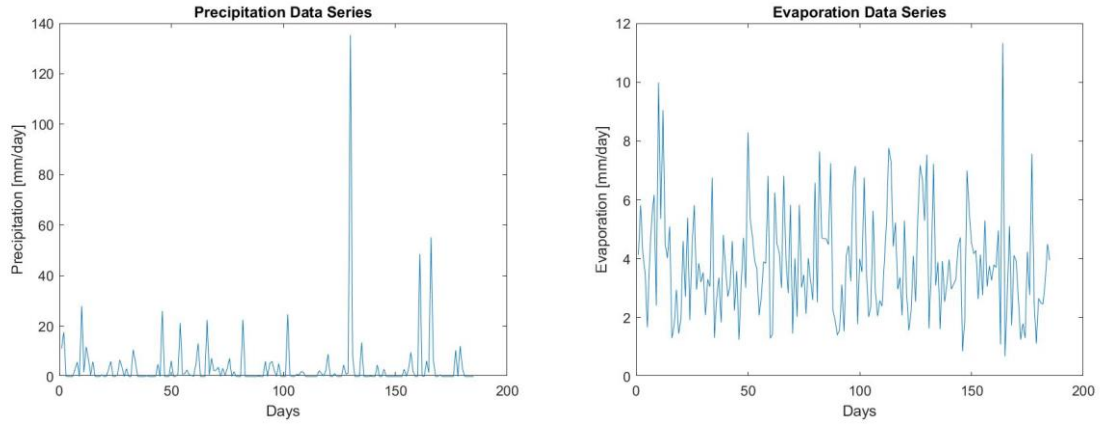


**Figure 6-6 Synthetic data series of Precipitation (Left) and Evaporation (Right) for one wet season.[mm/day]**

X-axis: Number of days within a wet season (185 Days).

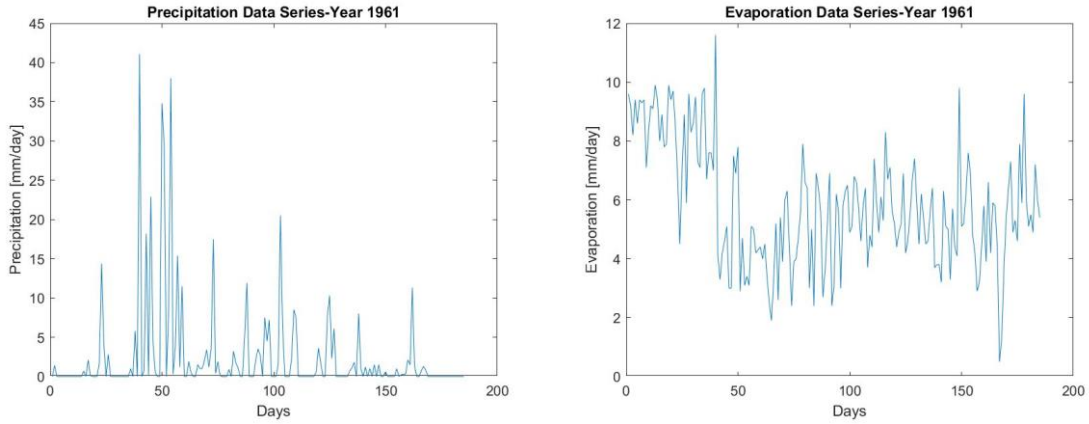


**Figure 6-7 Real data series of Precipitation (Left) and Evaporation (Right) for one wet season [mm/day]. Chapingo Station. Year 1961.**

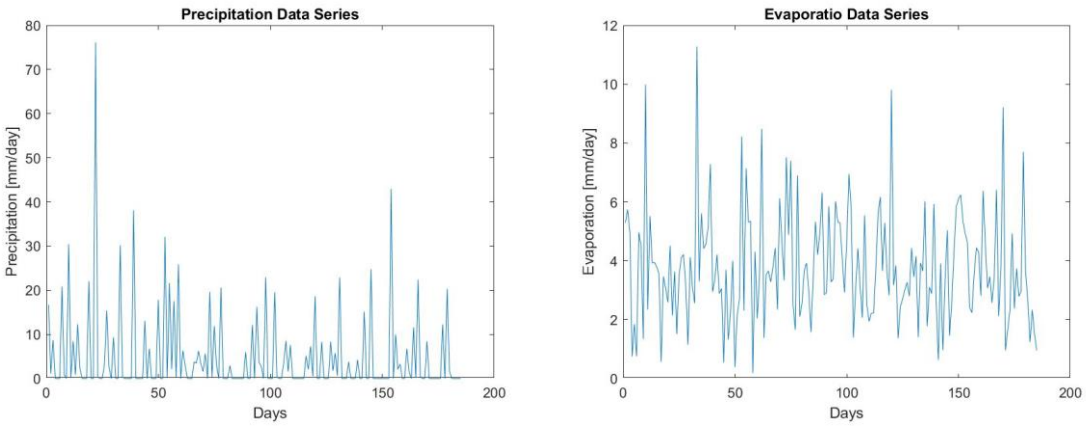


**Figure 6-8 Synthetic data series of Precipitation (Left) and Evaporation (Right) for one wet season with a higher correlation coefficient.**

The synthetic data was compared with real data of one wet season measured at Chapingo station (Figure 6-6 and Figure 6-7) Notice that the precipitation time series of real data has a higher number of peaks which are also close to each other, while the synthetic precipitation series shows fewer peaks with a bigger time between them and the values of the peaks in the synthetic series are much higher than in the actual measurements. These differences can be explained due to the low correlation coefficient (Table 6-3) between the variables, as described in the following paragraph. For evaporation data, the number and corresponding values of the peaks are similar between both series.

In order to explain this case further, another example of synthetic time series (Figure 6-8) was generated but in this case, the correlation coefficient was increased (to 0.8). In such series, notice that the precipitation data looks more similar to the real data in 6-7 (Lower values and more frequent peaks) while evaporation data does not show much difference. From this example, is important to highlight the role of dependence in precipitation data, it shows a noticeable improvement for a higher correlation coefficient. However, evaporation data shows no significant changes.

The analysis presented in the previous paragraphs indicate that the model is able to capture quite well the temporal distribution and estimation of precipitation and evaporation.

## 6.3 Water Levels

To recreate the water level fluctuation at Lake Texcoco a hydrological balance was performed in the region. The synthetic time series was used as an input. In section 4.4.3 it was stated that once the volume at the lake was computed, the elevation and surface area at the lake were obtained from the Volume-Elevation and Volume-Area curves ( fitted to a 2$^{nd}$-degree polynomial line) as shown in Figure 6-9 and Figure 6-10.

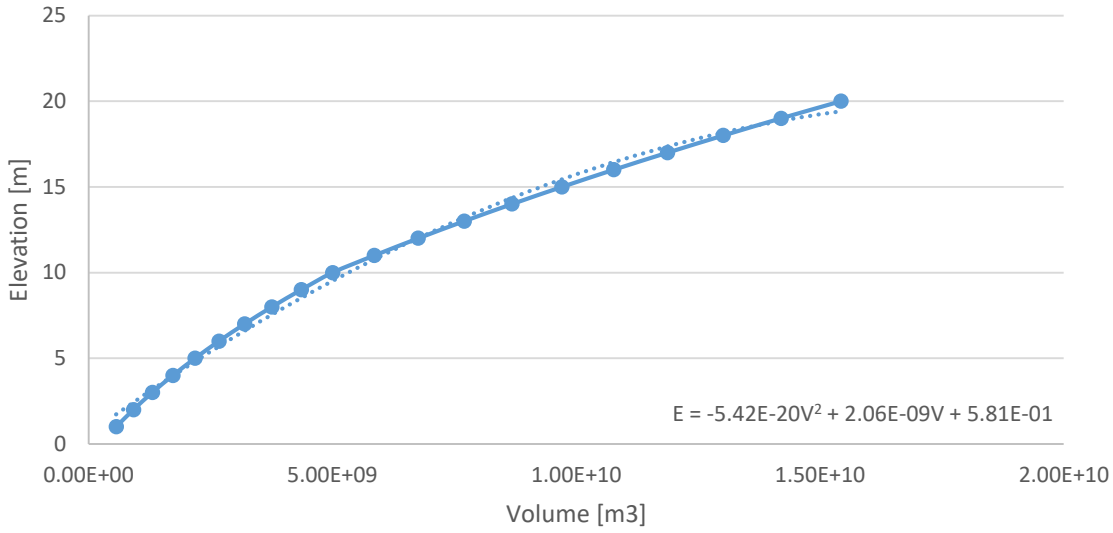


**Figure 6-9 Volume-Elevation Curve at Lake Texcoco (Continuous) and Trend Line (Dotted)**

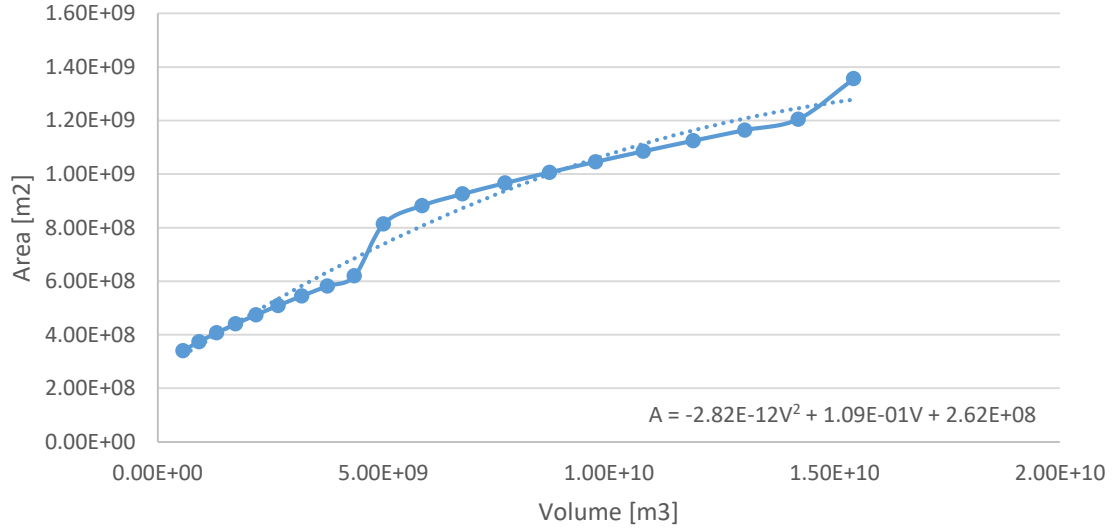


**Figure 6-10 Volume-Area Curve at Lake Texcoco (Continuous) and Trend Line (Dotted).**

The results from the hydrological balance are relative to the initial water level at the lake at the beginning of the wet season (Day 0 in Figure 6-11). The initial water level considered for this thesis is level 2231 (1m depth relative to the foot of the dike), considering that by the end of the dry season the lake was almost dry. The variation of the water level and the climate variables for one wet season is shown in Figure 6-11.

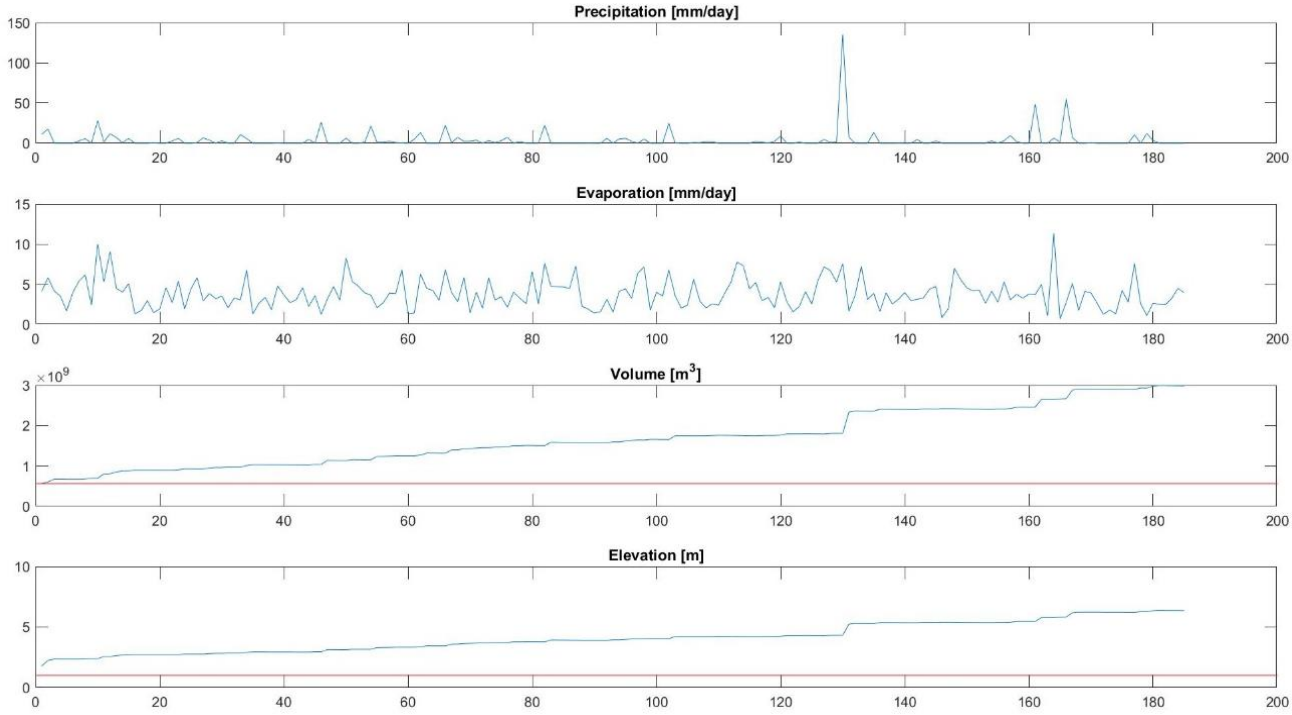


**Figure 6-11 Fluctuation of environmental data, volume and water elevation at Lake Texcoco in the wet season.**

X-axis: Number of days in the wet season (185 days).

The bottom plot of Figure 6-11 shows that the water level in the lake can increase approximately 5 to 6 meters (relative to the initial water depth) during the wet season, which is a significant water level growth. The procedure was performed for every water depth from the V-E curve with similar results. A close up of the water level fluctuation in Figure 6-11 is presented in Figure 6-12. Additionally, the hydrologic balance (Eq. 15) was tested using real data from Chapingo Station, the water level fluctuation at the lake in the wet season of the year 1961 is shown in Figure 6-12 as well.

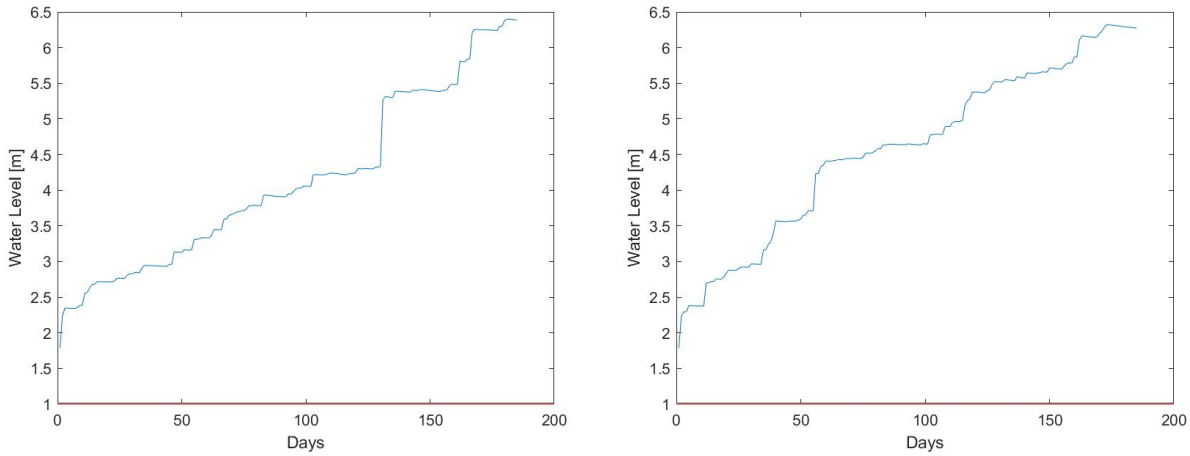


**Figure 6-12 Volume and water level fluctuation in Lake Texcoco during the wet season. Chapingo Station Data (Left) Simulated Data (Right).**

It is observed that the actual measurements of climate data result in a water level increase of approximately 5.5m respect to the initial water depth, very similar to the simulated data. Both graphs show a tendency of increasing water level through the wet season. Thus, the synthetic data provides a good estimation of water levels at the lake.

The hydrological balance was applied to the thousand years of synthetic data considering different initial water depths at the beginning of the wet season (from 1m to 20m) and the resulting water levels were added to their corresponding wind set up. A statistical analysis of the yearly maximum water levels over the thousand years of synthetic data was used to assess the reliability of the Nezahualcoyotl dike. The results from this procedure are presented in the following chapter.

# 7 Reliability Analysis

This chapter introduces an approach to assess the reliability of the Nezahualcoyotl dike.

## 7.1 Overflow

To estimate the probability of failure in the dike (PF), a frequency analysis was performed. This technique allows predicting water level values based on return periods or probabilities of exceedance. The annual maxima of water level for a given initial water depth were extracted from the thousand years of generated data (Section 6.3), then, this information was fitted to a General Extreme Value Distribution (GEV). The parameters for the fitted distribution are:

| Shape Parameter [k] | Scale Parameter [σ] | Location Parameter [μ] |
|---|---|---|
| 1.19 | 8.09e-12 | 20.04 |

**Table 7-1 GEV Distribution Parameters for extreme water levels at an initial depth of 1m.**

The frequency curves of the fitted probability distribution and the empirical data were plotted in the form of CDF's (Cumulative distribution functions).

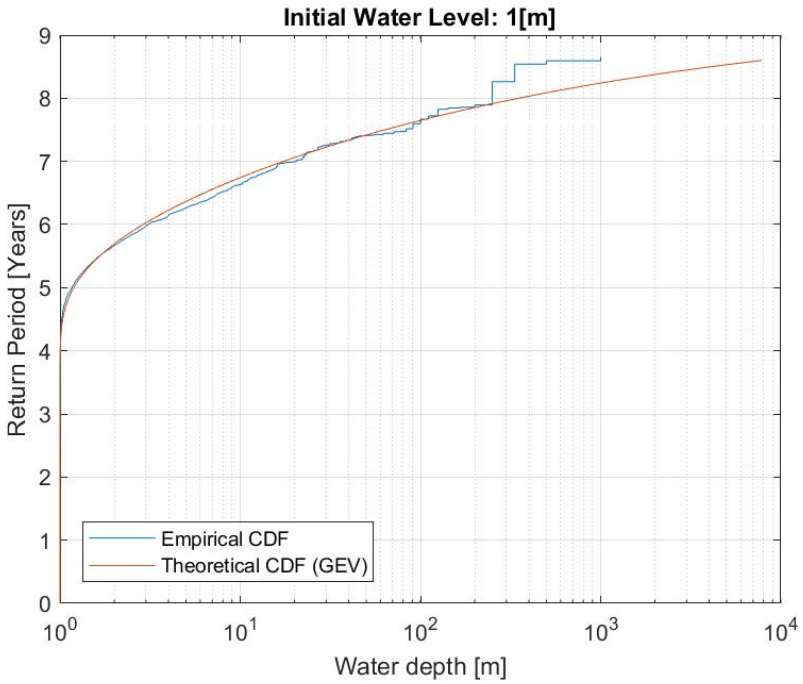


**Figure 7-1 Frequency Curve for an initial water depth of 1m.**

Figure 7-1 illustrates the case when the water level at the lake is approximately 1 meter at the start of the wet season (Figure 7-2). The return period for a water level exceeding 8 meters (Height of the Nezahualcoyotl dike) is approximately 300 years. It is important to be clear that if a water level with a 300 year return period occurs, it does not mean that another water level of that magnitude will not occur in the following 300 years. This probability is actually the first estimation of the probability of failure of the dike. In the following paragraphs, other values of the probability of failure will be presented as a result of variation in some of the model variables.

Table 7-2 shows the probability of failure (PF) of the dike for different depths at the beginning of the wet season at the foot of the dike.

| Water Depth at the foot of the dike [m] | M.a.s.l | PF (Without Set-up) | PF (With Set-up) |
|---|---|---|---|
| 1 | 2231 | 0.002 | 0.003 |
| 2 | 2232 | 0.013 | 0.018 |
| 3 | 2233 | 0.063 | 0.078 |
| 4 | 2234 | 0.222 | 0.261 |
| 5 | 2235 | 0.566 | 0.624 |
| 6 | 2236 | 0.918 | 0.943 |
| 7 | 2237 | 1 | 1 |
| 8 | 2238 | 1 | 1 |
| 9 | 2239 | 1 | 1 |
| 10 | 2240 | 1 | 1 |
| 11 | 2241 | 1 | 1 |
| 12 | 2242 | 1 | 1 |
| 13 | 2243 | 1 | 1 |
| 14 | 2244 | 1 | 1 |
| 15 | 2245 | 1 | 1 |
| 16 | 2246 | 1 | 1 |
| 17 | 2247 | 1 | 1 |
| 18 | 2248 | 1 | 1 |
| 19 | 2249 | 1 | 1 |
| 20 | 2250 | 1 | 1 |

**Table 7-2 Probability of failure (In any one year) given an initial water depth.**

Table 7-2 presents PF=P(Water level> 8 meters at Texcoco Lake) assuming that the water level of the lake at the start of the wet season has the meters indicated in the first column. For example, the second row of Table 7-2 can be read as follows: “If the water level at the lake at the start of the wet season is equal to 2 meters, the probability that the dike will be overflown is 0.013”. For levels higher than 5 meters it is clear that the dike would have failed every year assuming the model presented in previous sections is correct. Table 7-2 also shows the probability of failure for the case when wind set up is not taken into account (Column 3). Wind set-up was employed as a deterministic variable added to the computed water levels using Eq. 14.

Notice that the results from not considering wind set-up are not much different from the results of taking it into account (Probability of failure -PF- of 0.002 and 0.003 respectively). The contribution of wind set up does not have a large influence on this model. Figure 7-2 shows a schematic of the initial water depths at the beginning of the wet season relative the height of the dike.

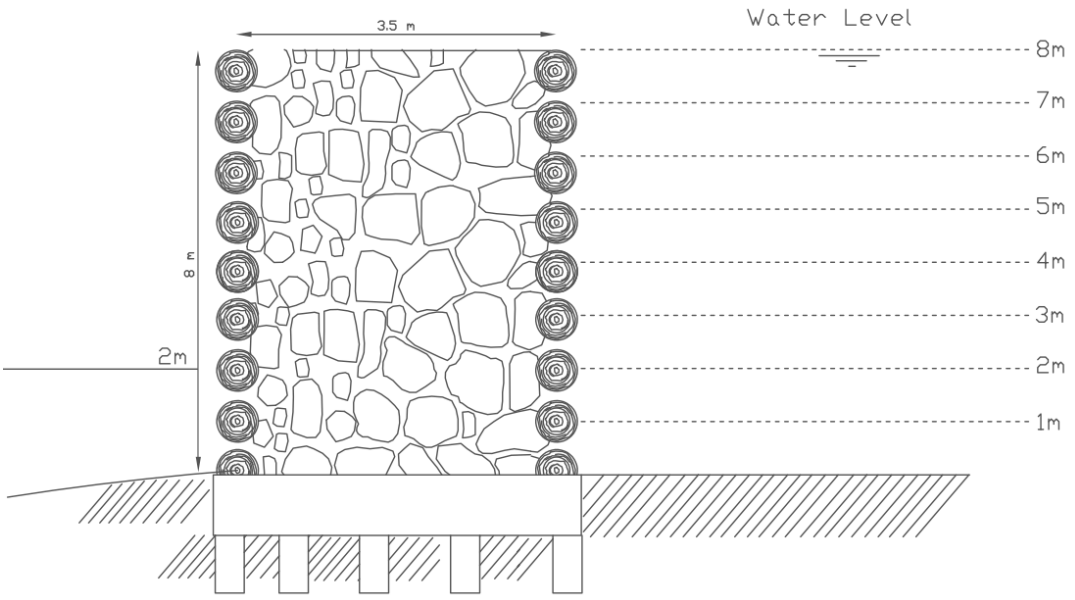


**Figure 7-2 Example of initial water levels at the start of the wet season.**
Water level at Lake Mexico (Left). Water Level at Lake Texcoco (Right).

The return period for the mean water level at Lake Texcoco (6 meters approximately. Figure 5-10 and Figure 7-2 ) corresponds to 3 years (PF=0.35) or a 35% chance that the dike will be overflown in any one year. Assuming a scenario without the dike and considering Lake Texcoco at mean conditions, the probability that the city of Tenochtitlan could be flooded is 110 times higher than a scenario with the dike. This result can explain why the city was constantly threatened by floods after the dike was destroyed, and highlights the inefficiency of the infrastructure available in colonial Mexico City. One could speculate why authorities of the time considered the drainage of the lakes as the only viable solution to deal with the problem of flooding after the conquer of Tenochtitlan.

It was noted that the computation of the probability of failure is sensitive to the tributary area of the basin used in the hydrological model (Eq. 15).

| Water Level [m] | Tributary Area [Km2] | PF | Return Period [Years] |
|---|---|---|---|
| 2250 | 3603.6 | 0.0003 | 3906.6 |
| 2245 | 3913.7 | 0.003 | 348.5 |
| 2240 | 4146.26 | 0.009 | 106.5 |
| 2236 | 4450.52 | 0.029 | 34.6 |
| 2232 | 4585.46 | 0.043 | 23.3 |
| 2231 | 4618.85 | 0.047 | 21.3 |
| 2230-Empty Lake | 4959.8 | 0.102 | 9.8 |

**Table 7-3 Probability of failure (in any other year) for different tributary areas of the basin.**

Table 7-3 shows that the tributary area of the basin influenced considerably the probability of failure of the dike. The major constraint is the Lake-Catchment Surface Area relationship. This relationship is determined by the size of the lake given that the area occupied by the lacustrine system is not considered as a tributary area but as the receptacle of water. See Eq. 16 and Figure 7-3.

$$A_{Tributary} = A_{Basin} - A_{Lake}$$

**Eq. 16**

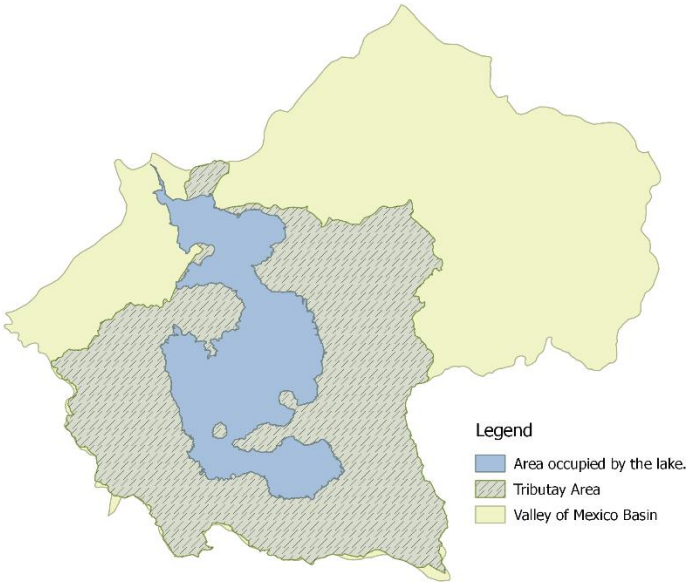


**Figure 7-3 Tributary Area.**

The surface area of the lake at different water levels was obtained from the V-E curve in Figure 5-9. The probability of failure presented in Figure 7-1 and Table 7-2 was obtained for the tributary area of the sub-basin minus the area occupied by the lakes at level 2245m (Eq. 16) as shown at the second row in Table 7-3. The first row in Table 7-3 corresponds to the area of the sub-basin minus the area occupied by the lakes at level 2250m (High-water mark), which results in a return period of 4000 years approximately (PF=0.0003). Notice that a 5-meter difference in water levels at the lake results in a dramatic reduction of the return period (3600 years). However, the gap between return periods gets smaller when lower water levels define the size of the lacustrine system. For example, between lake level 2250 and 2245m there is a reduction of approximately 3600 years for the return period, while between lake level 2245m and 2240m there is a reduction of 240 years.

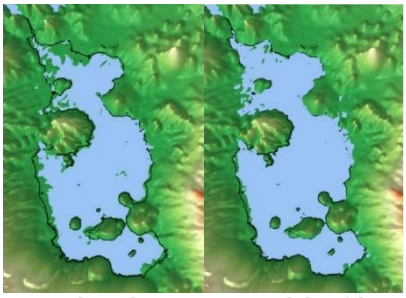

**Figure 7-4 Lake Texcoco at level 2245 m.a.s.l (Left) and 2250 m.a.s.l (Right).**

The model proved to be highly sensitive between levels 2240m and 2250m. Notice in Figure 7-4, that the biggest difference between those levels is the area reduction at Lake Zumpango (North). This could indicate the importance of this lake to provide water to the lacustrine system relative to other zones. Nevertheless, the topography employed could also be a factor that influenced these results. It is important to test the model for different topography sources in order to verify this hypothesis.

Finally, if the total area of the sub-basin is used as the tributary area (Empty lake), the resulting return period would be equal to 10 years (PF=0.1).

From the results presented in Table 7-3 together with the historical records of floods in Tenochtitlan (Section 3.5), is possible to provide an estimation of what could have been the tributary area of the basin:

The minimum tributary area corresponds to the high-water mark level of 2250m and is equal to 3603.60 $Km^2$, following in a probability of failure equal to 0.0003 (Return period of 4000 years approximately). The maximum tributary area is computed considering that no floods occurred while the Nezahualcoyotl dike was still standing (70 years approximately). Therefore, the probability of failure of the dike would have been of at least 0.014 (1/70), resulting in a tributary area close to 4250 $Km^2$ (for a lake level of approximately 2240m according to Table 7-3). These two areas set the lower and upper boundaries for the tributary area in the basin. Thus, assuming a tributary area between those two limits, for example, at level 2245 (as in Figure 7-1 and Table 7-2) is a reasonable choice given that the exact tributary area is uncertain.

The methodology and results presented in this thesis considered the contribution of precipitation and evaporation in the hydrological balance at the lacustrine system. Appendix F presents an alternative analysis by including river discharge into the hydrological balance (Eq. 15). In order to account for possible contributions of springs to the discharge of the rivers. This analysis was performed to estimate the influence of this variable in the probability of failure of the Nezahualcoyotl dike.

### 7.1.1 Scour

The flow over a hydraulic structure could lead to jets, which lifts the sediment particles and transport them downstream of the impacted area. The impact area is transformed into an energy dissipator and a scour hole is formed. Important parameters are the equilibrium scour depth and the length and width of the scour hole (Hoffmans & Verheij, 1997). For the case of the Nezahualcoyotl dike, a plunging jet would've been more likely to occur (Figure 7-5). This type of jet refers to the water that impinges on the free surface due to overflow discharge through a hydraulic structure.

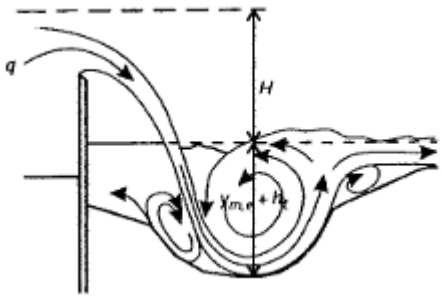


**Figure 7-5 Plunging Jet**

To calculate the equilibrium scour depth, the definition by Schoklitsch (1932) based on flume experiments was employed (Eq. 17).

$$y_{m,e} + h_t = \frac{c_s q^{0.57} H^{0.2}}{d_{90}^{0.32}}$$

**Eq. 17**

In which:

- $y_{m,e}$ : Equilibrium scour depth (m).
- $c_s$ : Coefficient with a dimension (=4.75).
- $q$ : Discharge per unit width ($m^2/s$)
- $H$ : Height between head and tail water levels (m).
- $d_{90}$ : Particle diameter for which 90% of the mixture is smaller than $d_{90}$ (m).

As rule of thumb, some of the variables of the previous equation were chosen in the following way:

- The overflow discharge was calculated using the formulation of discharge over a weir (Eq. 18).

$$q_w = \frac{2}{3}\sqrt{2g}R_c^{3/2}$$

**Eq. 18**

In which:

$q_w$ : Discharge over the dike [$m^2/s$].

$g$ : Gravity acceleration [$m/s^2$].

$R_c$ : Height of the crest relative to the water level. [m].

- The head over the dike was chosen as 0.1 m which correspond to an 8.1m water depth at Lake Texcoco (respect to the foot of the dike).
- The height between the head and tail water levels depend on the water depth at Lake Mexico. This lake was largely influenced by the chinampa system which needed a constant regulation of water levels. An estimation of the water level in Lake Mexico was presented at section 5.2 and is equal to 2 meters. Hence, $H = 8.10m - 2m = 6.10m$.
- The superficial layer of the soil in Lake Texcoco is described as a clayey silt to sandy silt, with a high content of sand (85%) (Díaz-Rodríguez, 2003). It was not possible to obtain a grain size distribution curve of the region. However, a $d_{90}$ equal to 0.5 mm was used based on the previous description.
-


**Figure 7-6 Scenario for scour.**

Finally, by introducing the previous data into Eq. 17 and Eq. 18, a scour depth of 18 meters was obtained. This result indicates that the water level at Lake Mexico would have not prevented a scour hole to occur, even for such a small head at the dike (10cm). A scour hole of such magnitude would most likely have provoked serious damage at the foot of the dike, leading to instability of the structure and eventually to its collapse.

### 7.1.2 Conclusion

Concerning overflow as the most relevant failure mechanism for the Nezahualcoyotl dike, the reliability analysis showed that the probability of failure is equal to 0.003 (or 300 years return period). This result corresponds to a lake area of 3913.70 $Km^2$ and a water depth of 1m at the beginning of the wet season. It is clear that the dike is more prone to fail if the initial level is higher at the beginning of the wet season (Table 7-2), given that generally, the water level at the lake increases 5 to 6 meters each wet season (Section 6.3).

The analysis of overflow presented in this chapter, provides positive results regarding the safety of the dike, an estimated value of the probability of failure equal to 0.003. However, the results are obtained with a model surrounded by great uncertainties, such as the water depth at the beginning of the wet season and the size of the tributary area of the basin relative to the surface area of the lakes. It is still important to highlight that the results from this approach agree with the historical description in which the dike never failed during its 70 years of lifetime. The results presented in section 7.1 confirmed that the dike was capable of protecting Tenochtitlan from rising water levels.

Section 7.1.1 presents an attempt to illustrate what would have been one of the effects of overflown at the dike. As result, a scour depth of approximately 18 meters could have formed at the foot of the dike at the side of Lake Mexico, putting at risk the stability of the dike and possibly leading to its collapse. This analysis has uncertainties related to the soil at the bottom of the lake. Hence, more information about this topic is needed.

## 7.2 Overtopping

In section 7.1 it was mentioned that wind set up did not have an important contribution to the estimation of the probability of failure at the dike. Nevertheless, wind waves could have also been present at the lake. In this section, an overtopping analysis is presented.

Wind waves are formed when the wind's energy is transferred to the surface of water. Several factors contribute to the formation of such waves: Wind speed, duration of the wind, fetch and water depth. The longer the fetch, the larger the waves. In lakes, waves can also cause a seiche, which means "a back and forth movement" of water. In this thesis, overtopping is not considered as the most relevant failure mechanism in the dike, however, is worth to analyze it.

At Lake Texcoco there is no data available of wave height and period, hence, it was generated using the equation proposed by Young and Verhagen (1996):

$$\tilde{H} = \tilde{H}_{\infty}\left\{\tanh\left(0.343\tilde{d}^{1.14}\right)\cdot\tanh\left(\frac{4.41\cdot10^{-4}\tilde{F}^{0.79}}{\tanh\left(0.343\tilde{d}^{1.14}\right)}\right)\right\}^{0.572}$$

$$\tilde{T} = \tilde{T}_{\infty}\left\{\tanh\left(0.10\tilde{d}^{2.01}\right)\cdot\tanh\left(\frac{2.77\cdot10^{-7}\tilde{F}^{1.45}}{\tanh\left(0.10\tilde{d}^{2.01}\right)}\right)\right\}^{0.187}$$

**Eq. 19**

In which:

- F: Fetch [m].
- d: Water depth [m].
- $U_{10}$ : Wind velocity at an altitude of 10m [m/s].
- $T_p$ : Peak wave period [s].
- $H_{mo}$ : Significant Wave Height [m].
- $\tilde{H}_{\infty}$ : Dimensionless wave height at deep water (0.24).
- $\tilde{T}_{\infty}$ : Dimensionless wave period at deep water (7.69).
- $g$ : Gravity acceleration [m/s$^2$].
- $\tilde{H} = \frac{gH_{mo}}{U_{10}^2}$
- $\tilde{T} = \frac{gT_p}{U_{10}}$
- $\tilde{d} = \frac{gd}{U_{10}^2}$
- $\tilde{F} = \frac{gF}{U_{10}^2}$

Wave data were computed for wind directions from the east side region of the lake. The main purpose of this analysis is to consider the worst case scenario possible. Overtopping was computed for a water level of 8 meters and a wind velocity of 8 m/s at the most vulnerable zone of the dike: The middle section (Figure 5-7), which is the lowest.

The mean overtopping discharges were calculated using Eq. 20 and the corresponding results are presented in Table 7-4.

$$\frac{q}{\sqrt{gH_{mo}^3}} = 0.047\cdot\exp\left[-\left(2.35\frac{R_c}{H_{mo}}\right)^{1.3}\right]$$

**Eq. 20**

In which:

- $q$ : Mean overtopping discharge [m$^3$/s/m].
- $R_c$: Height of the crest relative to the water level. [m].
- $H_{mo}$ : Significant wave height [m].

| Wind Direction | Water depth [m] * | Crest Level [m] | $R_c$ | $F$ [m] | $U_{10}$ [m/s] | $H_{mo}$ [m] | $T_p$ [s] | $q$ [m3/s/m] | $q$ [l/s/m] |
|---|---|---|---|---|---|---|---|---|---|
| N (0°) | 8 | 8 | 0 | 8389.23 | 8 | 0.47 | 2.59 | 0.05 | 47.51 |
| NNE (22.5°) | 8 | 8 | 0 | 22308.84 | 8 | 0.69 | 3.37 | 0.08 | 84.29 |
| NE (45°) | 8 | 8 | 0 | 25079.42 | 8 | 0.72 | 3.47 | 0.09 | 89.35 |
| ENE (67.5°) | 8 | 8 | 0 | 24288.78 | 8 | 0.70 | 3.45 | 0.09 | 87.96 |
| E (90°) | 8 | 8 | 0 | 21742.00 | 8 | 0.68 | 3.35 | 0.08 | 83.19 |
| ESE (112.5°) | 8 | 8 | 0 | 14410.77 | 8 | 0.58 | 3.00 | 0.07 | 66.24 |
| SE (135°) | 8 | 8 | 0 | 14972.22 | 8 | 0.59 | 3.03 | 0.07 | 67.74 |
| SSE (157.5°) | 8 | 8 | 0 | 14389.08 | 8 | 0.58 | 3.00 | 0.07 | 66.18 |

**Table 7-4 Overtopping mean discharges.**
*Relative to the foot of the dike.

The highest wave comes from the northeast direction and is approximately 0.72m height, which corresponds to a mean overtopping discharge of 89.35 l/s/m per meter. Is important to consider that this is not a continuous discharge. It depends on each wave reaching the dike. The resulting overtopping discharge can be considered slightly high. However, the dike had water at both sides so probably the influence of wind waves would not have been a serious factor.

## 7.3 Comparison to Modern Reliability Standards

The failure mechanisms considered in this thesis were based on failure mechanisms that are evaluated in the Netherlands and other countries. Consequently, the Aztecs' design criteria will be compared to the criteria applied by Dutch engineers nowadays.

Currently, there are two safety standards in the Netherlands: The "old" standard which is expressed as an acceptable return period of a hydraulic load to each section of a flood structure must be able to withstand (Jonkman et.al, 2017). The "new" safety standards are based on an acceptable probability of flooding in a dike trajectory.

The assessment presented previously for the Nezahualcoyotl dike (Section 7.1) is based in the exceedance of a determined water level. Thus, the old Dutch standard is more appropriate to be compared with the probability of failure of the Nezahualcoyotl dike.

Figure 7-7 shows the "old" safety standards at different regions of The Netherlands based on service limit state (SLS) criteria. Some sections show a probability of failure of 0.0008 or a return period of 1250 years. The highest (SLS) probability of failure in The Netherlands is, therefore, 60% smaller than the probability of failure in the Nezahualcoyotl dike. However, the safety standard that the Aztecs desired to achieve was based on an ultimate limit state (ULS), because no amount of water intrusion from Lake Texcoco was allowed due to its saline nature. The old Dutch standard for ULS is equal to 1/125000 (flooding probability originally derived as an optimum by the first Delta committee), corresponding to a probability of failure of 0.000008. Comparing this standard to the probability of failure of the Nezahualcoyotl dike (Section 7.1. PF=0.003), the probability of failure at the dike is 350 times bigger than the (ULS) old Dutch standard.

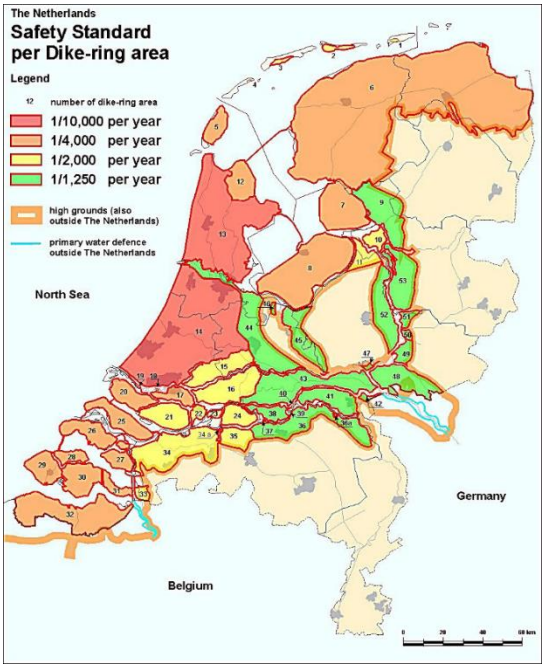


**Figure 7-7 Old Safety standards in The Netherlands.**

Furthermore, is worth to compare the safety of the Nezahualcoyotl dike to safety standards in other regions. For example, in the United States (U.S). A water level with a probability of exceedance of 1/100 or 1/200 per year is the current design level in California (Ammerlaan, 2007), which is higher than the probability of failure of the Aztec dike also computed under the assumption of exceeding water levels.

The safety standards for dikes in The Netherlands or in the US are based on completely different phenomena than the hazards that threatened Tenochtitlan. Most of the dikes in the Netherlands are designed to withstand hydraulic loads related to coastal conditions, while the Nezahualcoyotl dike considers conditions relevant for lakes. Moreover, we have no evidence to think that its design considered any statistical basis.

Additionally, in California and Mexico, there are earthquakes while The Netherlands does not encounter earthquakes of such magnitude. García Acosta & Suárez Reynoso (1996), describe two earthquakes during the lifetime of the Nezahualcoyotl dike. The first occurred in 1455. In this earthquake, the earth craked and the chinampa system collapsed. Considering that the chinampas were terrains built with humid materials (Section 3.4), their collapse shows a high-intensity seism (VIII according to the Cancani scale. Defined as “Ruinous”).

A second earthquake took place in 1475. This earthquake is described by the following description (García Acosta & Suárez Reynoso, 1996):

> “[…] several hills crackedd and buried the houses […] almost all the houses and buildings of the city were ruined. In some zones, the earth cracked and the top of some hills sank […]”.

The intensity of this earthquake is characterized between level VIII and X in the Cancani scale (Ruinous to Very Disastrous respectively). The previous descriptions show evidence that the Valley of Mexico was affected by strong earthquakes during the pre-hispanic era. However, these descriptions do not mention damage to the Nezahualcoyotl dike. It cannot be concluded that the

dike remained intact after these incidents. The resistance of the dike under earthquakes adds more uncertainties to its reliability, which is an important factor to take into account for future research. The criteria under which the levees in The Netherlands and California were constructed is also a factor to take into account. In the US, engineers design and evaluate levees based on levee design documents that are related to dam design manuals. In The Netherlands, dike safety is examined using special levee evaluation documents (Ammerlaan, 2007). For the case of the Nezahualcoyotl dike, there are no records that its safety was evaluated using guidelines of any type.

The probability of failure of the Nezahualcoyotl dike prove to be too high when compared to Dutch standards, but it is slightly lower than that of levees in California. Moreover, the Nezahualcoyotl dike never failed during its lifetime. With a PF=0.003 (Return period of 300 years) the reliability of the dike is equal to 0.997, which means a 99.7% chance that the dike did not fail in any one year.

# 8 Conclusions and Recommendations

This chapter presents the conclusions derived from the work conducted for this thesis, additionally, the answers to the research questions are provided and recommendations for further research are suggested based on the conclusions.

## 8.1 Conclusions

**Thesis goals** The main objective of this thesis was to assess the reliability of the Nezahualcoyotl dike considering the most relevant failure mechanism for this structure. With this premise in mind, the main effort was focused on the characterization of the dike itself and the lacustrine system. This task was challenging since there are no remains of the dike and the lakes were drained almost completely by the start of the 20th century. The probabilistic model presented in this thesis aimed to estimate the values of the variables necessary to test the most relevant failure mechanism in the dike: Overflow.

**Main findings**

An analysis of the flood history at the city of Tenochtitlan lead to the conclusion that the main hazard was the increase of water level in Lake Texcoco. There are no records of other types of flood-related hazards in the region, thus, overflow was selected as the most relevant failure mechanism. Additionally, as a consequence of overflow, an analysis of the equilibrium scour depth at the foot of the dike was performed. Finally, overtopping as failure mechanism was also included in the analysis. These last two failure mechanisms were not studied in the same detail as overflow.

The hydrological model presented in this thesis was selected to estimate overflow in order to generated data related to such failure mechanism. That is to investigate the water level fluctuation at Lake Texcoco. Only data during the wet season was used to create the model since approximately 90% of the yearly precipitation occurs during this season (Muciñio, 2001).

In this research, an important finding was the Volume-Elevation curve in Lake Texcoco (Section 5.2) using spatial analysis tools (ArcGIS). Such analysis allowed to confirm the proposals by Palerm (1973) and Bradbury (1971) (See Table 8-1). Additionally, this information allowed to provide a proposal for the layout of the Nezahualcoyotl dike.

| Level [M.a.s.l] | Water Depth [m] | Observations |
|---|---|---|
| 2230 | 0 | Level at the foot of the dike and also the level of the bottom of the lake. |
| 2232 | 2 | Water level at Lake Mexico. |
| 2236-2239 | 6-9. | Mean water level of Lake Texcoco. |
| 2240 | 10 | Level at which the all the Lakes joined as one body of water. |
| 2250 | 20 | High-water mark. |

**Table 8-1 Water levels at the lacustrine system.**

The mean water level in Lake Texcoco was approximately 6 meters relative to the foot of the dike. This information supported the description provided by Hernández Cruz (2013) in which the Nezahualcoyotl dike was 8 meters' height. 3.5 meters' width and 16 kilometers' long (Table 5-7 and Figure 5-17). The orientation of the dike was investigated using ArcGIS and it was found that the proposal given by Palerm (1973) did not comply with the dimensions provided by

Hernández Cruz (2013). The results from ArcGIS showed that the dike was 21 Km long. Thus, a new orientation was proposed for this thesis (Figure 5-16).

The cross-sectional and longitudinal view of the topography at Lake Texcoco (Figure 5-6 and Figure 5-7) showed that Tenochtitlan was located within the lowest region of the lacustrine system, between Km 4+000 and Km 9+000 of the dike. This can explain the importance of the Nezahualcoyotl dike for the Aztec empire.

To construct the hydrological model used to investigate the reliability of the Nezahualcoyotl dike, present-day data of precipitation, evaporation and river discharge was employed. A total of five stations were selected for their location at the east side of Lake Texcoco. The results of the model showed that all the stations could be fitted to the same probability distribution. For precipitation the data, all the stations fitted to a Generalized Pareto distribution, while data of evaporation, all the stations fitted to a Generalized Extreme Value distribution.

Moreover, all the stations proved to have similar rain pattern and a similar Spearman's rho correlation coefficient between the variables. For the rain pattern, the transition probabilities from state 0 (Dry days) to 1 (Wet days) and 1 to 0 showed to be around 0.3 to 0.4, while the transition probabilities for states 0-0 and 1-1 ranged between 0.6 to 0.69 (Table 6-2). The correlation coefficients between the pairs $PR - PR$ and $PR - E$ were in the order of 0.2, and the correlation coefficients for the pair $E - E$ were in the order of 0.4 (Table 6-3). Therefore, it is concluded that there is no spatial variation of the variables in this region, which allowed to simplify the model by focusing on data from only one station: Chapingo (DGE)

The hydrological model was able to capture quite well the temporal distribution and estimation of precipitation and evaporation values (Figure 6-6, Figure 6-7 and Figure 6-8). In general, the model overestimated values of precipitation, however, it was due to the low correlation coefficient between the variables (0.20 approximately), while evaporation values were not affected by this coefficient.

The synthetic water levels obtained from the hydrological balance (Section 6.3) showed the same behavior as the levels generated using actual measurements of the climate variables. Both results show an increase in water levels of 5 to 6 meters during the wet season (Figure 6-12).

After the water levels were obtained, the probability of failure due to overflow at the dike was computed. This was the most important result of this thesis. It was noted that the safety of the dike was greatly influenced by 2 factors: The water level at the start of the wet season and the tributary area of the basin. While the inclusion of wind set up in the analysis did not influence the results.

A higher initial water level increased the chance that the dike would fail (Table 7-2). Historical records mention that the lake decreased its volume during the dry season due to the high evaporation rates, sometimes to even dry the lake completely. Hence, focus was given to compute the probability of failure for an initial water depth of 1 meter.

The tributary area of the basin is mainly determined by the extent of the lacustrine system. In this thesis, an area between 3603.660 and 4250 $Km^2$ is proposed, which corresponds to the lake at level 2250 and 2240 m approximately (Table 7-3). Thus the probability of failure of the dike fluctuates between 0.0003 and 0.014. (Return periods of 300 and 70 years respectively). Finally, a tributary area between these limits was selected (3913.70 $Km^2$) corresponding to a lake level of

2245 meters. The resulting probability of failure is 0.003 (For an initial water depth of 1m at the beginning of the wet season).

The maximum overtopping discharge at the dike is equal to 89.35$m^3$/s/m for wind waves coming from the Northeast with a wave height of 0.72 meters and a wave period of 3.5 seconds. Such discharge is not constant, depends on the waves arriving at the dike. Even though the overtopping discharge is quite large, its effect on the inner wall of the dike could not be considered serious due to the presence of water in Lake Mexico.

The equilibrium scour depth was computed using an equation that described the flow over a weir (Eq. 18) since the flow over the dike could be described as a similar situation. The water depth at Lake Texcoco chosen for this analysis was 8.10m, which equals an overflow height of just 10cm. However, the resulting scour hole depth is equal to 18 meters (Section 7.1.1). The formation of such a hole would have also depended on the duration of the flood and influenced the stability of the dike. It can be concluded that overflow at the dike could have not only resulted in flooding Tenochtitlan but also with the possible collapse of the Nezahualcoyotl dike. Meaning that the presence of water in Lake Mexico would have not reduced the effect of scour.

In summary, the characterization of the lacustrine system, the Nezahualcoyotl dike, and the probabilistic model proposed in this thesis are surrounded by uncertainties. Nevertheless, the hydrological model provided good estimations for the values of precipitation, evaporation and, water levels. The results from the reliability analysis agree with the fact that the dike never failed during its lifetime (70 years approximately). The probability of failure of the dike is estimated as 0.003 equivalent to a return period of 300 years (given a water level of 1 meter at the beginning of the wet season and a tributary area of 3913.70 $Km^2$). In other words, a 0.33% chance that the water level will be exceeded in any one year. There is no evidence that the dike was built under statistical basis or that the Aztecs' followed construction guidelines as most of the designs of hydraulic structures nowadays. Regardless, the Aztecs' engineers had a deep understanding of the lacustrine system. This was evidenced by the description provided by all the sources used in this thesis and especially by the result of the reliability analysis in section 7.1. There is no doubt why the Aztecs were known as the great hydraulic engineers of pre-Hispanic Mexico.

## 8.2 Recommendations for further research

Throughout this thesis, three main topics are recommended for further investigation: Improving the hydrological balance, including the complex interaction between the lakes, and expanding the characterization of the Nezahualcoyotl dike.

Regarding the first topic, the methodology carried out in this thesis could be improved on the following issues:

- Including other fluxes into the hydrological balance, such as groundwater discharge, infiltration, and runoff.

  Obtaining groundwater volumes requires information of aquifer in the basin, such as the limits of the aquifer, area, fluctuation of piezometric levels, hydraulic conductivity and its storage capacity. These data can be downloaded from Mexico's national database INEGI.

  Infiltration volumes could be determined using an additional hydrological balance:

$$PR = E + Q_{Runoff} + Q_{Infiltrated}$$

The previous equation is only applicable when the volume of precipitation exceeds the volume of evapotranspiration (Gómez-Reyes, 2013). This condition agrees with the case of the basin during the wet season.

Runoff data is the percentage of superficial water that drains in the basin. It can be computed using hydrometric information. For this variable, data about vegetation cover and land use are crucial. However, more uncertainties will arise since the basin has been severely altered by humans in the last 350 years.

- Expanding the analysis of the climate variables considering stations located throughout the entire basin, in order to consider the rain pattern in other regions surrounding the lakes, as well as possible differences in the dependencies between the variables.

- Computation of precipitation volumes can be improved by estimating their contribution to each lake through Thiessen polygons or Isohyets (The latter could require Kriging algorithms). While evaporation volumes can be checked using Penman Monteith's equation if the relevant data for this method such as net irradiance, ground heat flux, specific humidity or conductivity of air are available.

- As mentioned in section 7.1, the water level at Lake Texcoco at the beginning of the wet season is an important factor that influences the probability of failure of the dike. Upgrading the generation of water levels at the lake by including data during the dry season will allow estimating the water level at the beginning of each wet season. Thus, a more realistic characterization of the lake could be obtained.

This thesis generated the water level fluctuation only in Lake Texcoco, the model can be expanded to the entire lacustrine system by exploring the following ideas:

- Generating Volume-Elevation and Area-Elevation curves for each of the six lakes in the lacustrine system. In order to get a more realistic layout of the complex interaction between the lakes, considering that the lakes at higher altitudes filled first and then their surplus water was deposited in Lake Texcoco. Perhaps such filling process could have slowed down the speed at which Lake Texcoco grew over during the wet season.

- Taking into account the role of the entire hydraulic organization developed by the Aztecs in all the lakes. Figure 5-13 shows the extent of such organization in the lacustrine system. Additionally, in section 5.3 is described how these structures already had an impact on the regulation of water levels in the lakes. Therefore, it is important to estimate the influence of these structures on the safety of the empire and to the probability of failure of the dike.

- Computing and comparing the results of the hydrologic model employing Volume-Elevation curves for topographies from other sources, in order to measure the influence of this information in the results. It is also recommended to study the influence of land subsidence in current topography in Mexico City (because current topography could be affected by it), to have a better estimation of the water levels in the lakes.

Reconstruction of the Nezahualcoyotl dike can be improved by considering the following points:

- Investigating the construction materials of the dike. This could be achieved by consulting documents of other Aztec's ancient structures, such as temples or aqueducts that still remain to this day. An analysis of this type could allow performing a reliability analysis of the dike for failure mechanisms such as micro stability.

- A failure mechanism that was not mentioned in Table 2-1 is the failure due to non-closure of gates. In historical sources, it is mentioned that the Nezahualcoyotl dike would have had gates to regulate the flow between the two lakes. The reliability of closure, the number of demands and the storage capacity of inflow water behind the dike has to be considered. This is an important failure mechanism to take into account for future research.

Finally, some extra remarks:

- The methodology employed in this thesis to compute wave heights and wave periods at the lake is very simple. It is proposed to use different formulations or to elaborate a model to improve its estimation.
- Developing a probabilistic model to characterize wind throughout the wet season, so its influence in the water levels at the lake could be more realistic.
- Given that the dike has water at both its sides it can also be modeled as a dam. Hence, different failure mechanism related to such type of structure can be studied.

# References


Aguilar, A. G., Ezcurra, E., Garcia, T., Mazari Hiriart, M., & Pisanty, I. (1995). The Basin of Mexico. In R. E. Jeanne X. Kasperson, *Regions at risk: comparisons of threatened environments.* Tokyo-New York-Paris: United Nations University Press.

Aire CDMX. (n.d.). *Sistema de Monitoreo Atmosférico Ciudad de Mexico (System of Atmospheric Monitoring Mexico City).* Retrieved from http://www.aire.cdmx.gob.mx/

Ammerlaan, P. (2007). *Levees and levee evaluation. The Dutch and US practice compared* . Master Thesis, TU Delft, Hydraulic Engineering, Delft.

Aranguren Rojas, I. (2017, November). Flood Risk Evaluation of Netzahualcoyotl Dike (Additional Graduation Work). Delft, South Holland, The Netherlands.

Armillas, P. (1971). Gardens on Swamps. *Science, 174*(4010), 653-661. Retrieved from http://science.sciencemag.org/content/174/4010/653

Bagowsky, I. (1961). Reliability Theory and Practise. Prentice-Hall.

Billinton, R., & Allan, R. (1983). Introduction. In *Reliability Evaluation of Engineering Systems.* Boston, MA: Springer.

Birkle, P., Torres, V., & González-Partida, E. (1998). The water balance for the Basin of the Valley of Mexico and implications for future water consumption. *Hydrogeology Journal, 6*, 500-517.

Bradbury, J. (1971, March). Paleolimnology of Lake Texcoco, Mexico. Evidence from Diatoms. *Paleolimnology of Lake Texcoco, Mexico. Evidence from DIATOMS1, 16*, 180-200. doi:10.4319/lo.1971.16.2.0180

British Standards Institutions. (2001). *Eurocode-Basis of Structural Design.* London: British Standards Institution.

Caballero, M., & Ortega Guerrero, B. (1998). Lake Levels since about 40,000 Years Ago at Lake Chalco, near Mexico City. *Quaternary Research, 50*(1), 69–79. doi:10.1006/qres.1998.1969

Christopher Caran, S., & Neely, J. (2006). Hydraulic Engineering in Prehistoric Mexico. *Scientific American*(295), 78-85.

CIRIA. (2013). *The International Levee Handbook.* CIRIA. Retrieved from https://books.google.nl/books?id=h6wsnwEACAAJ

CLICOM. (n.d.). *CICESE.* Retrieved from http://clicom-mex.cicese.mx/

CONAGUA. (n.d.). *Banco Nacional de Datos de Aguas Superficiales (National Bank of Data of Superficial Water).* Retrieved from http://www.conagua.gob.mx/conagua07/contenido/documentos/portada%20bandas.htm

Daou, D. (2011). Synthetic Ecology: Revisiting Mexico City's Lakes Project (Master Thesis). Massachusetts Institute of Technology. Dept. of Architecture. Retrieved from http://hdl.handle.net/1721.1/67223

Díaz-Rodríguez, J. (2003). Characterization and engineering properties of Mexico City lacustrine soils. *Characterization and engineering properties of natural soils*, 725-755.

Fitts, C. (2013). *Groundwater Science.* Academic Press. Retrieved from https://books.google.nl/books?id=AJPL3Z2k2hQC

FLOODsite-Consortium. (2005). *Language of Flood Risk.* Retrieved from www.floodsite.net.

García Acosta, V., & Suárez Reynoso, G. (1996). *Los Sismos en la Historia de México: El Analisis Social.* Mexico City: Universidad Nacional Autonoma de Mexico. Retrieved from https://books.google.nl/books?id=vAF-9pNtpg8C

Genest, C., & Favre, A.-C. (2007, 07). Everything You Always Wanted to Know about Copula Modeling but Were Afraid to Ask. *Journal of Hydrologic Engineering - J HYDROL ENG*, *12*.

Gobierno del Estado de Mexico. (2018). *Secretaria del Medio Ambiente*. Retrieved from http://sma.edomex.gob.mx/distribucion_de_cuencas

Gómez-Reyes, E. (2013). *Valoración de las Componentes del Balance Hídrico usando información estadística y geográfica: La Cuenca del Valle de México.* Instituto Nacional de Estadística y Geografía, Mexico City.

Hernández Cruz, G. M. (2013). *Hidrología de los Ríos del Oriente del Valle de México y Funcionamiento Hidráulico en Conjunto con el Lago de Texcoco (Hydrology of the Rivers of the Mexico Valley East Side and Hydraulic Operation Together with the Texcoco Lake ).* Mexico City: Post Graduate Thesis.

Hoffmans, G., & Verheij, H. (1997). *Scour Manua.* Taylor \& Francis. Retrieved from https://books.google.nl/books?id=44VNuHmNWGUC

INEGI. (n.d.). *Instituto Nacional de Estadística y Geografía (National Institute of Statistics and Geography).* Retrieved from http://www.beta.inegi.org.mx/temas/mapas/topografia/

Joe, H. (2014). *Dependence Modeling with Copulas.* Vancouver, Canada: CRC Press, Taylor & Francis Group.

Jonkman, N. S., Jorissen, E., Schweckendieck, T., & van den Bos, P. (2017). *Flood Defenses.Lecture Notes CIE5314* (2 ed.). Delft.

Jonkman, S., Steenbergen, R., Morales-Nápoles, O., Vrouwenvelder, A., & Vrijling, J. (2016). *Probabilistic Design: Risk and Reliability Analysis in Civil Engineering. Lecture notes CIE4130.* Delft.

Lafrance, A. (2015, August 31). A Brief History of Levees. Manmade embankments are an ancient technology, modeled from nature. *The Atlantic*. Retrieved July 23, 2018, from https://www.theatlantic.com/technology/archive/2015/08/a-brief-history-of-levees/402119/

LEAD. (2004, December). *Mexico City: Opportunities and Challenges for Sustainable Management of Urban Water Resources*. Retrieved March 19, 2018, from https://web.archive.org/web/20081207190625/http://casestudies.lead.org/index.php?cscid=100

Legorreta, J. (2006). El agua y la Ciudad de Mexico. De Tenochtitlan a la megápolis del siglo XXI. Mexico City: Artes Impresas.

Lehner, B., Verdin, K., & Jarvis, A. (n.d.). HydroSHEDS Technical Documentation. (W. W. Fund, Ed.) Washington, DC, US. Retrieved from http://hydrosheds.cr.usgs.gov

Lemieux, C. (2009). *Monte Carlo and Quasi-Monte Carlo Sampling.*

Leontaris, G., Morales-Nápoles, O., & Wolfert, A. (2016). Probabilistic scheduling of offshore operations using copula based environmental time series – An application for cable installation management for offshore wind farms",. *Ocean Engineerin, 125*, 328-341. doi:https://doi.org/10.1016/j.oceaneng.2016.08.029.

Lewis, A. C., & Torres, J. (2013). The Ghosts of Lake Texcoco Still Haunting Mexico City. *The Drop, Water Management and Hydrological Science Program, 5*.

Lombardo de Ruiz, S. (1973). *Desarrollo Urbano de México-Tenochtitlán según las fuentes históricas (Urban Development of Mexico-Tenochtitlan According Historical Sources ).* Mexico City: Instituto Nacional de Antropología e Historia.

Medina A, M. (2010). *Nezahualcóyotl. Su Legado como Arquitecto y Constructor del Paisaje* (1st ed.). Mexico: Programa Editiorial Compromiso.

Merriam-Webster, Inc. (1997). *Merriam-Webster's geographical dictionary.*

Molenaar, W., & Voorendt, M. (2016). *Manual Hydraulic Structures.* Delft.

Muciñio, D. (2001). *Estudio General del Caso Lago de Texcoco, Mexico. Proyecto Regional, Sistemas Integrados de Tratamiento y Uso de Aguas Residuales en America Latina: Realidad y Potencial Convenio: IDRC- OPS/HEP/CEPIS 2000-2002.* Mexico.

Munich Reinsurance Company. (1997). *Flooding and insurance.* Munich: Münchener Rückversicherungs-Gesellschaft.

Nelsen, R. B. (2006). *An Introduction to Copulas* (Second ed.). (I. Springer Publishing Company, Ed.)

Niederberger, C. (1987). *Paléopaysages et archéologie pré-urbaine du bassin de México (Mexique).* Centre d'études mexicaines et centraméricaines.

Olivas Solano, J. C. (2010). *Ciudades de Agua. Tenochtitlan (Cities of Water. Tenochtitlan).* Valparaiso.

Oxford Dictionary. (2018). *OxfordDictionaries.com*. Retrieved July 11, 2018, from https://en.oxforddictionaries.com/definition/us/markov_chain

Palerm, A. (1973). *Pre-Hispanic Hydraulic Works in the Lacustrine System of the Mexico Valley.* Mexico City: Sep Inah.

Peña Santana, P., & Levi, E. (1989). *History of Hyadraulics in Mexico. Water supply since the Pre-Hispanic time until the Porfiriato.* Mexico City.

Pereira, D. (2015, June 22). Wind Rose Matlab script.

Petroski, H. (2006, 01). Levees and Other Raised Ground. *American Scientist - AMER SCI, 94*.

R. Gabriel, K., & Neumann, J. (1962, 01). A Markov Chain Model for Daily Rainfall Occurrence at Tel Aviv. *Quarterly Journal of the Royal Meteorological Society, 88*, 90 - 95.

Rabiela, T., Ruiz, J., Licea, D., & Social, C. d. (2009). *Cultura Hidráulica y Simbolismo Mesoamericano del Agua en el México Prehispánico.* México: Instituto Mexicano de Tecnología del Agua.

*Reliability Engineering Resources.* (2018). Retrieved March 13, 2018, from http://www.weibull.com/

Remillard, B. (2010, 12 22). Goodness-of-Fit Tests for Copulas of Multivariate Time Series. *Econometrics, 5*, 13. doi: http://dx.doi.org/10.2139/ssrn.1729982

Rip, J. (2016). *Probabilistic Downtime Analysis for Complex Marine Projects.* Delft: (Master Thesis).

Sarewitz, D. P. (2003). Vulnerability and Risk: Some Thoughts from a Political and Policy Perspective. *Risk Analysis, 23*, 805–810.

Schanze, J. a. (2007). *Flood Risk Management: Hazards, Vulnerability and Mitigation Measures.* Springer Netherlands.

Schmidt, T. (2007). Coping with copulas. In *Copulas - From Theory to Application in Finance.*

Schneider, J. (2006). *Introduction to Safety and Reliability of Structures.* IABSE-AIPC-IVBH. Retrieved from https://books.google.nl/books?id=Mszw6-2PPP4C

Sheppard, M. (2012). *Allfitdist-Fit all parametric probability distributions to data: MATLAB Central.* Retrieved from http://www.mathworks.com/matlabcentral/fileexchange/34943-fit-all-valid-parametric-probability-distributions-to-data/content/allfitdist.m

Sistema de Aguas de la Ciudad de Mexico. (2012). *El Gran Reto del Agua en la Ciudad de Mexico. Pasado, presente y prospectivas de solucion para una de las ciudades mas complejas del mundo.* Mexico City.

Sklar, A. (1959). Fonctions de Réparition à n Dimensions et Leurs Marges 8. *Institut statistique de l' Université de Paris*, 229–231.

Skrzypczak, I. &.-O. (2017). The Application of Reliability Analysis in Engineering Practice-Reinforced Concrete Foundation. *Procedia Engineering, 193*, 144-151.

van Rinsum, G. (2015). *Accuracy wind set-up formula for irregularly shaped lakes with a strong varying water depth.* Bachelor Thesis, Delft.

WBGU. (1998). *World in Transition-Strategies for Managing Global Environmental Risks.* Berling and others: Springer.

Wilby, R. L., & Keenan, R. (2012). Adapting to flood risk under climate change. *Progress in Physical Geography*, 348-378.

Young, I., & Verhagen, L. (1996). The growth of fetch limited waves in water of finite depth. Part 1: Total energy and peak frequency. *Coastal Engineering, 29*, 47-78.

# Appendix A: Wind Roses

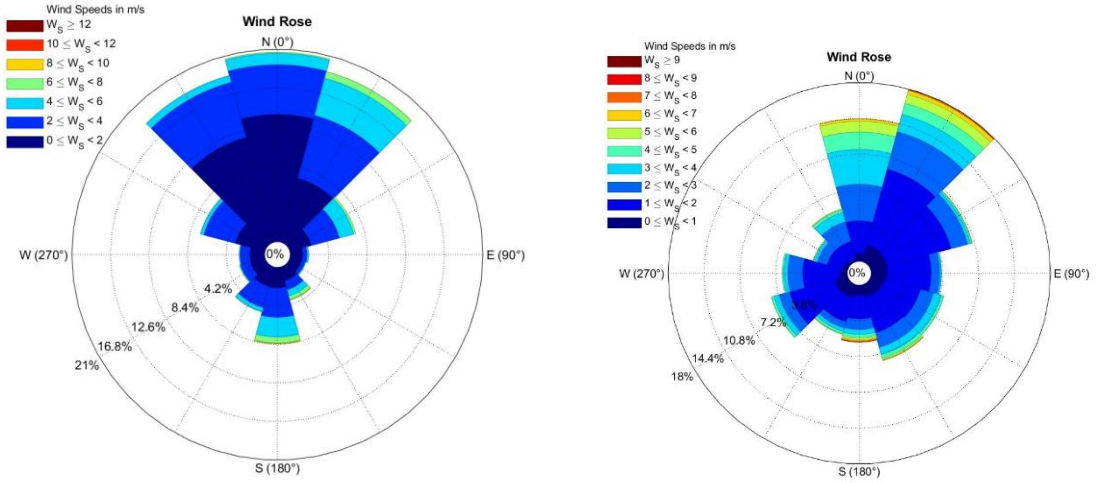


**Figure A- 1 Left: Acolman Station. Right: Gustavo A. Madero Station.**

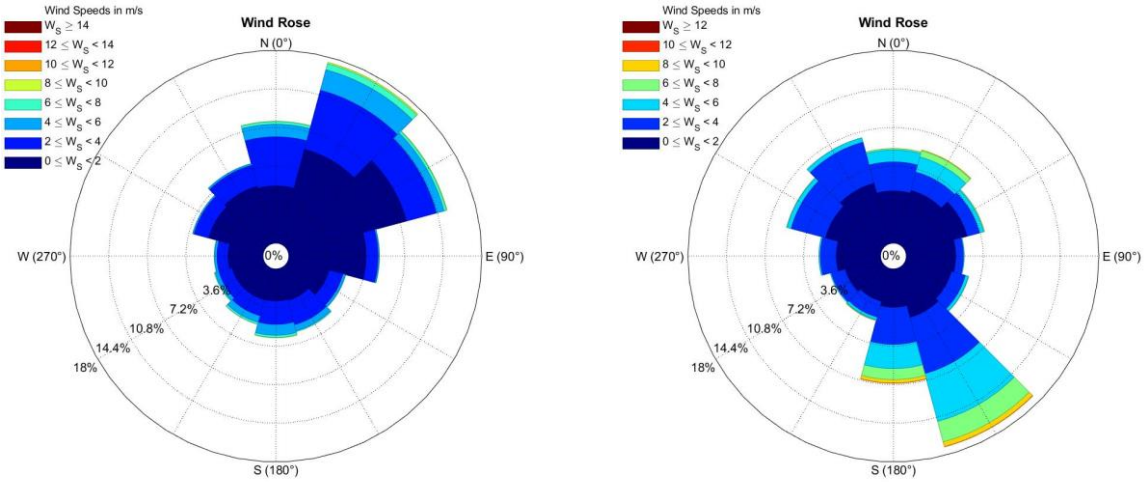


**Figure A- 2 Left: Hangares Station. Right: Montecillo Station.**

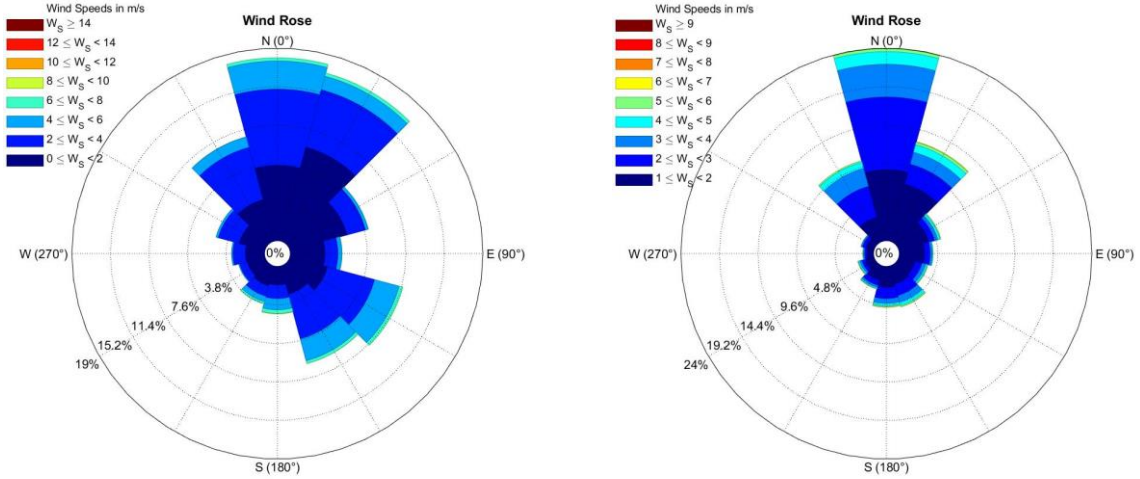


**Figure A- 3 Left: Nezahualcoyotl Station. Right: San Agustin Station.**

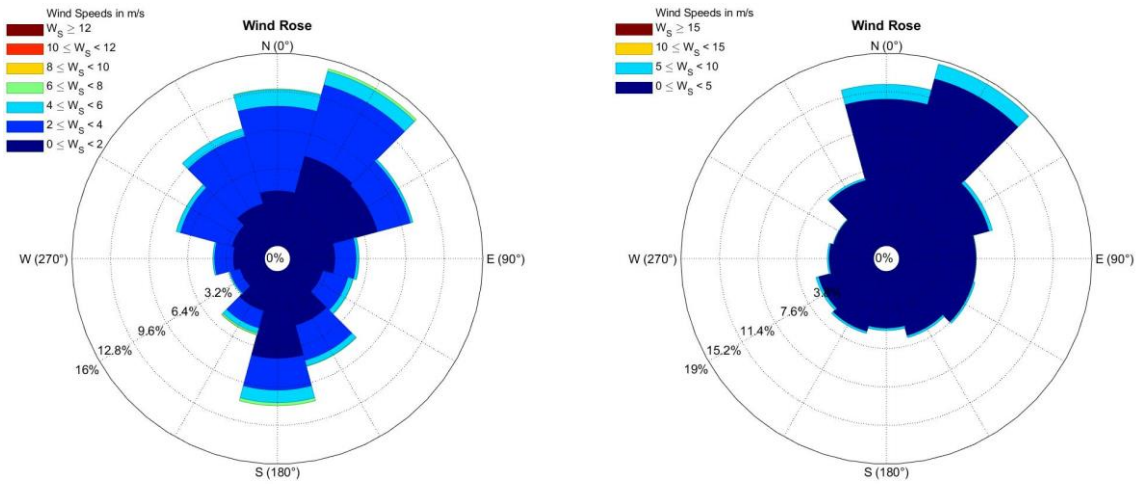


**Figure A- 4 Left: UAM Iztapalapa Station. Right: Xalostoc Station.**

# Appendix B: Water Level Evolution

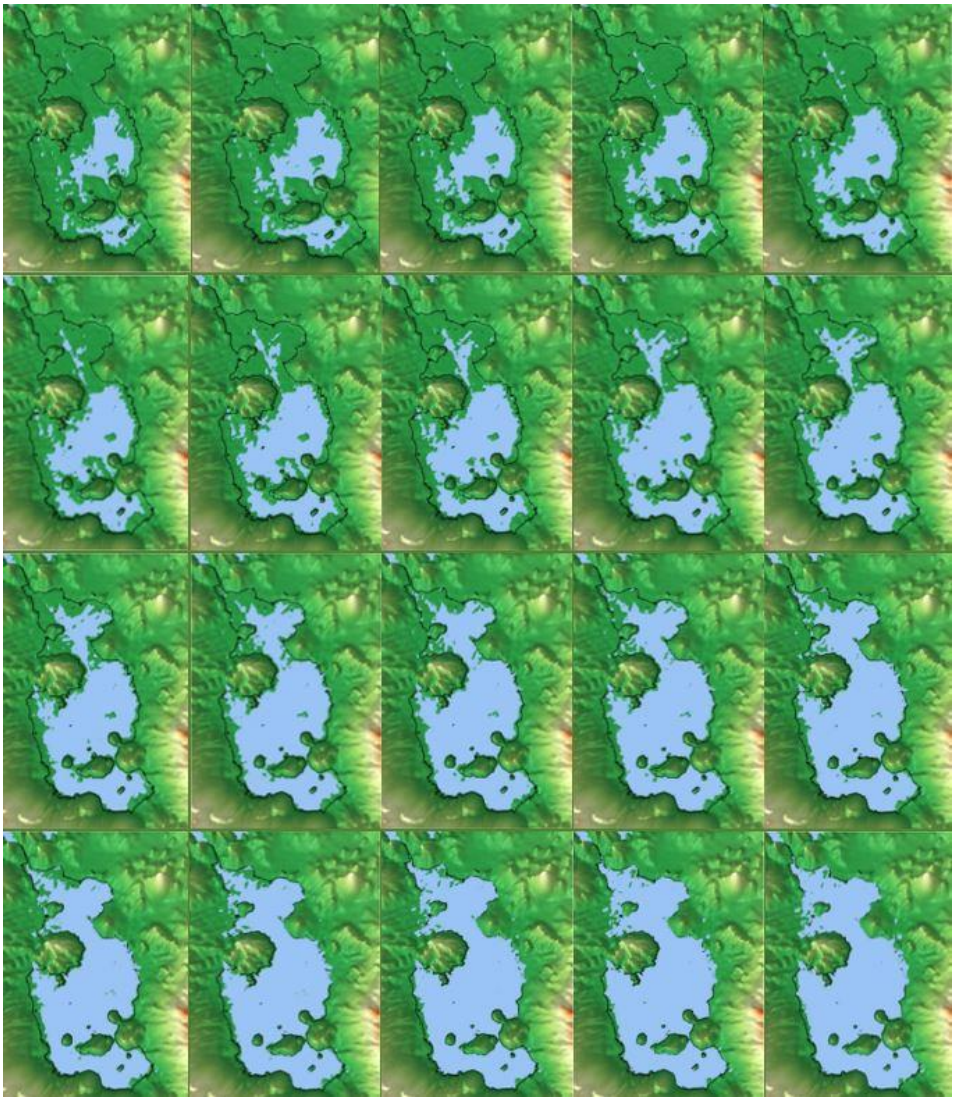

**Figure B- 1 Appearance of the lacustrine system for the data of the V-E curve.**

# Appendix C: Cumulative Distribution Functions and Goodness of Fit

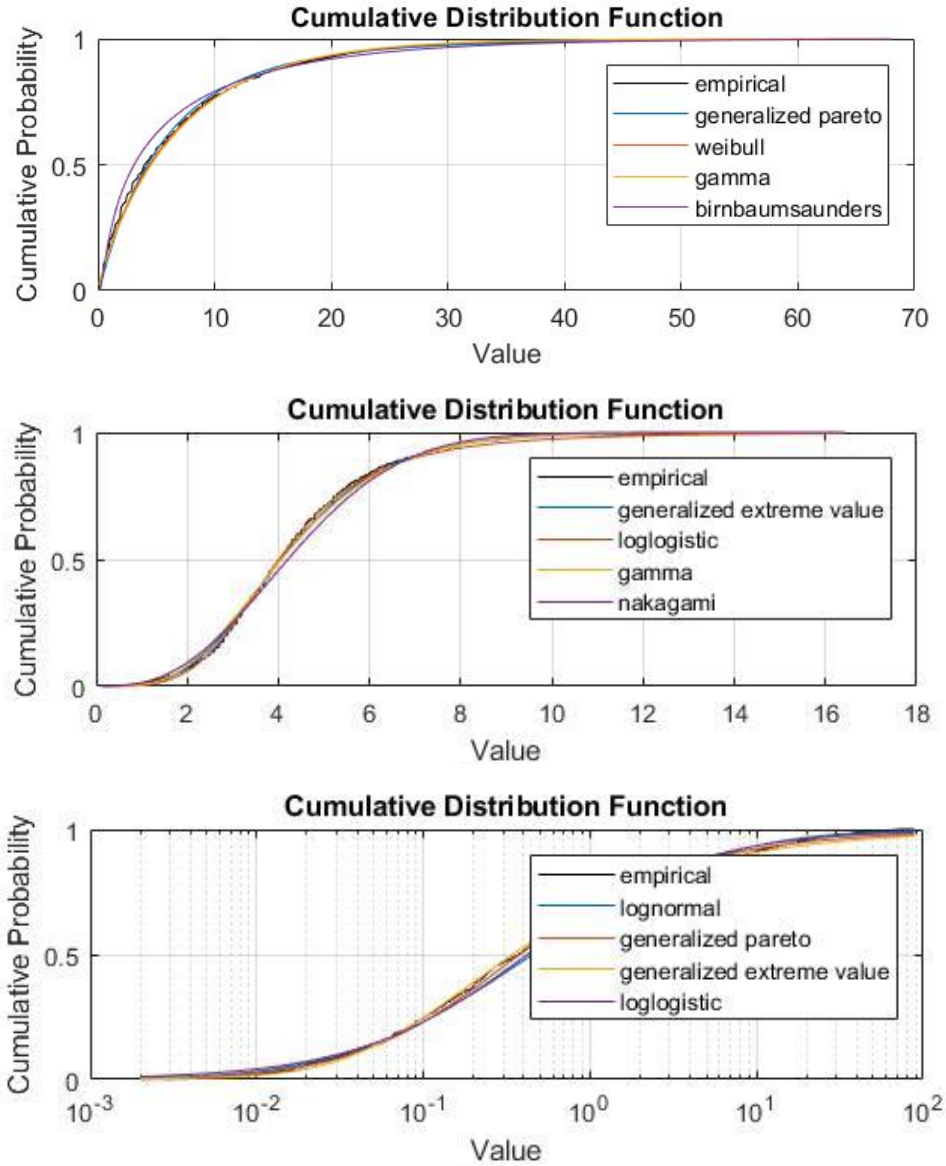


**Figure C- 1 CDF's for precipitation, evaporation and river discharge data at La Grande station.**
*X axis units: Mm/day for precipitation and evaporation and m3/s for river discharge.

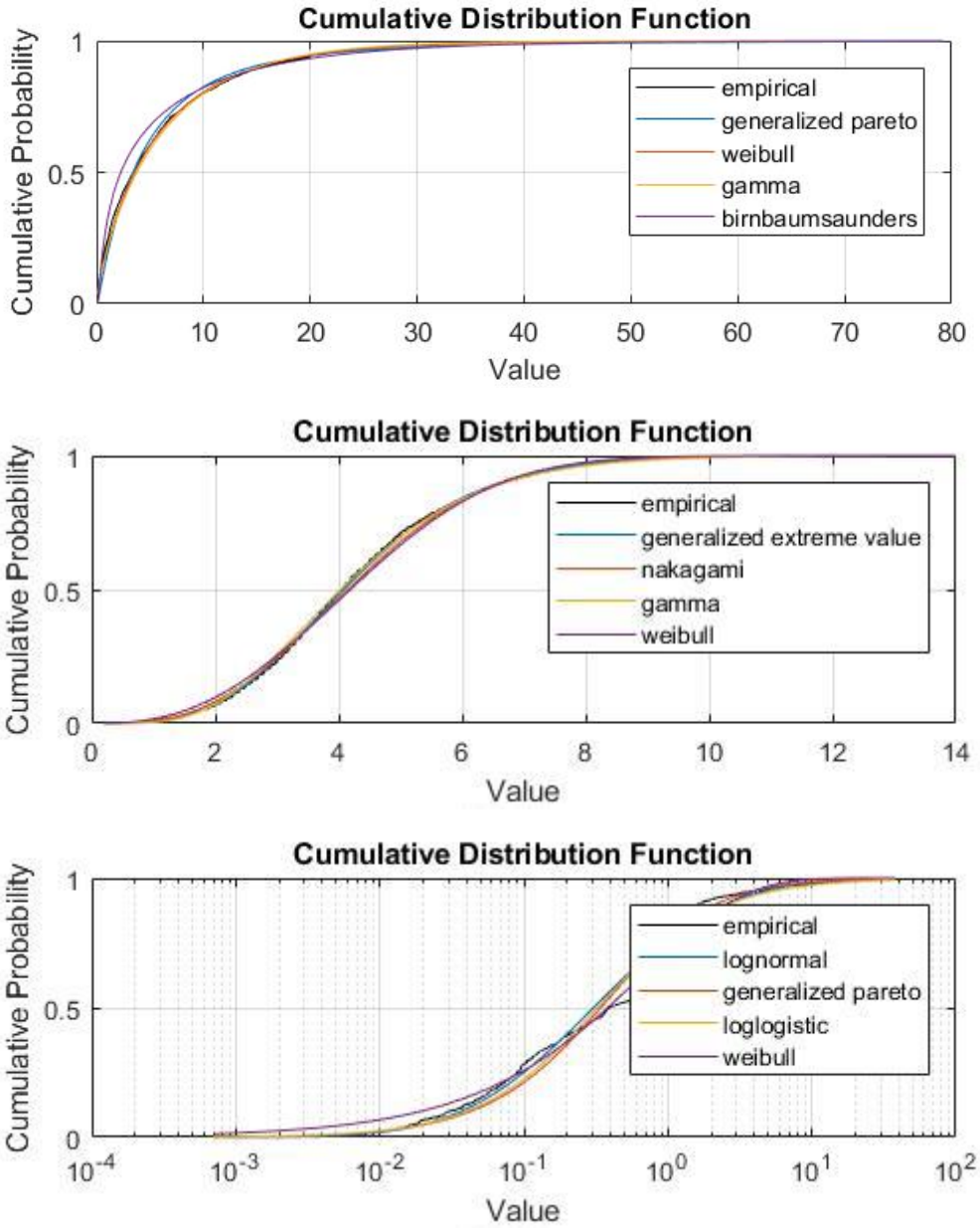


**Figure C- 2 CDF's for precipitation, evaporation and river discharge data at San Andres Station.**
*X axis units: Mm/day for precipitation and evaporation and m3/s for river discharge.

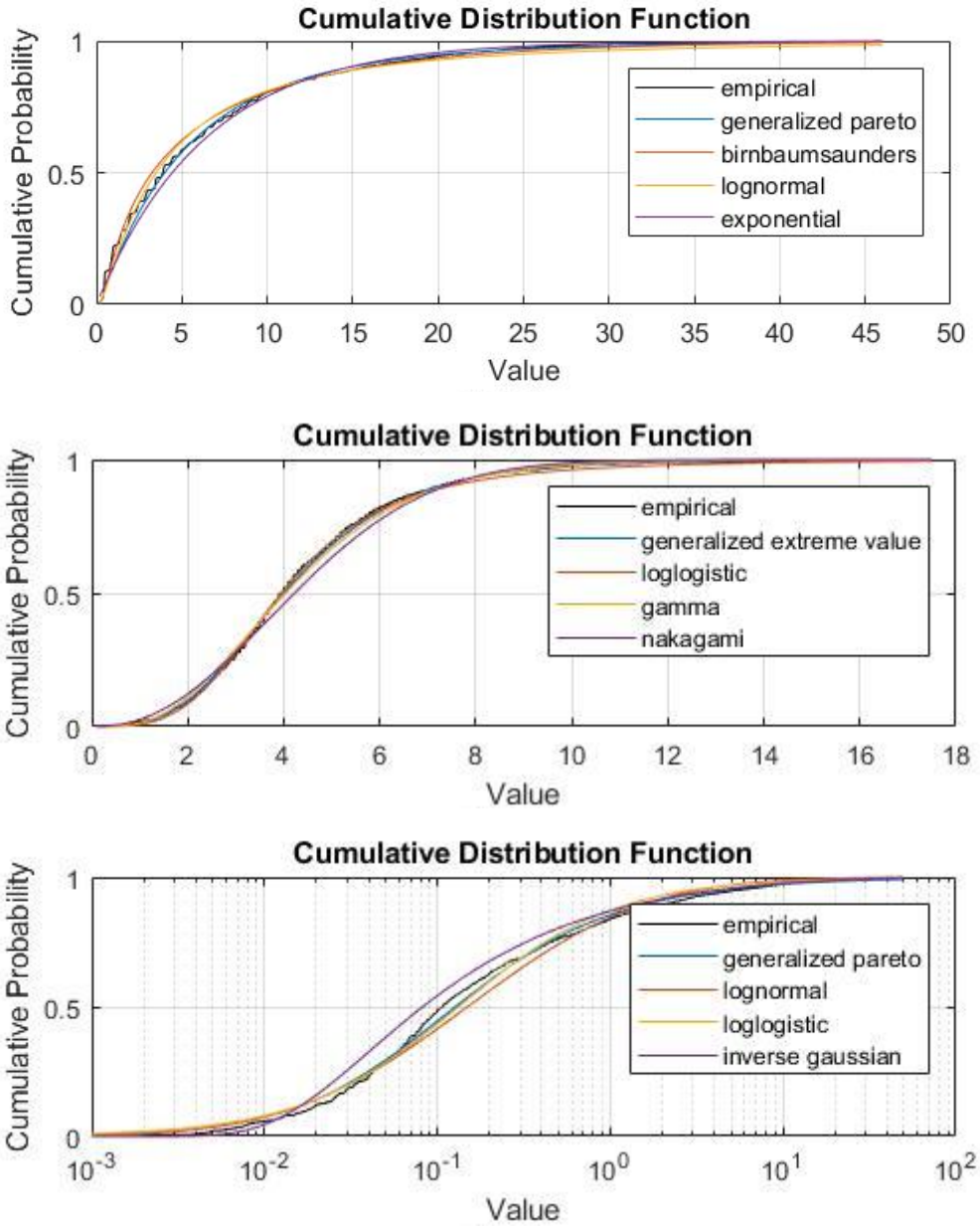


**Figure C- 3 CDF's for precipitation, evaporation and river discharge data at El Tejocote station.**
*X axis units: Mm/day for precipitation and evaporation and m3/s for river discharge.

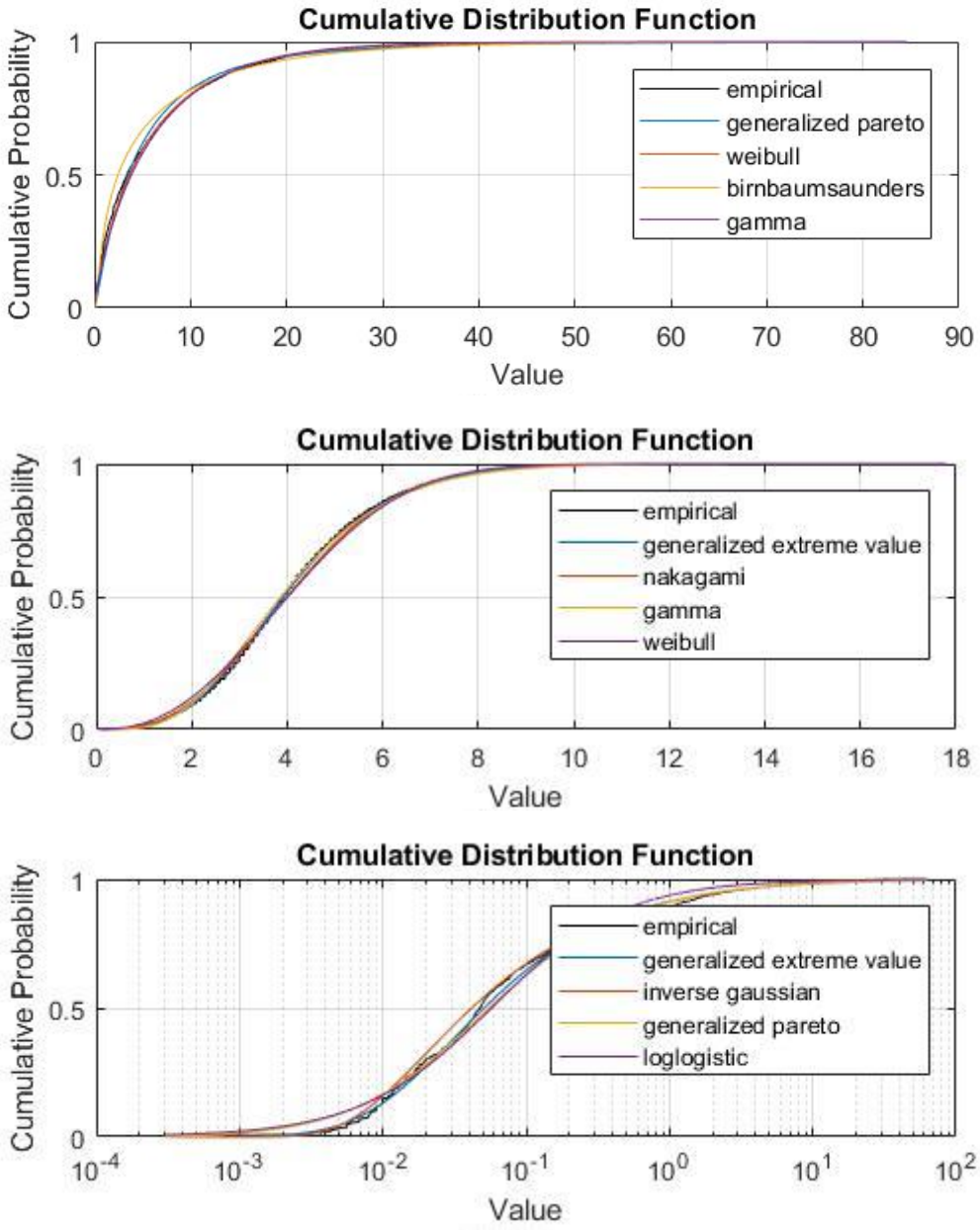


**Figure C- 4 CDF's for precipitation, evaporation and river discharge data at Chapingo (DGE) station.**

*X axis units: Mm/day for precipitation and evaporation and m3/s for river discharge

| Atenco | | La Grande | | San Andres | | Tejocote | | Chapingo (DGE) | |
|---|---|---|---|---|---|---|---|---|---|
| G.E.V | 12696.0 | G.E.V | 9110.9 | G.E.V | 13495.4 | G.E.V | 6107.4 | G.E.V | 19012.7 |
| Nakagami | 12750.3 | Loglogistic | 9151.7 | Nakagami | 13541.7 | Loglogistic | 6137.9 | Nakagami | 19104.0 |
| Gamma | 12800.1 | Gamma | 9168.2 | Gamma | 13566.7 | Gamma | 6148.9 | Gamma | 19150.1 |
| Weibull | 12808.0 | Nakagami | 9238.9 | Weibull | 13612.6 | Nakagami | 6227.6 | Weibull | 19189.9 |
| Rician | 12829.0 | Tlocationscale | 9295.4 | Rician | 13650.8 | Rayleigh | 6246.5 | Rician | 19241.5 |

**Table C- 1 Evaporation data goodness of fit.**

| Atenco | | La Grande | | San Andres | | Tejocote | | Chapingo (DGE) | |
|---|---|---|---|---|---|---|---|---|---|
| G. Pareto | 6508.5 | G. Pareto | 5009.0 | G. Pareto | 7244.3 | G. Pareto | 2991.1 | G. Pareto | 9469.1 |
| Birnbaum-saunders | 6543.6 | Weibull | 5044.2 | Weibull | 7288.2 | Birnbaum-saunders | 2998.5 | Weibull | 9538.5 |
| Weibull | 6544.9 | Gamma | 5050.6 | Gamma | 7302.8 | Lognormal | 3025.2 | Birnbaum-saunders | 9547.8 |
| Gamma | 6561.4 | Birnbaum-saunders | 5052.5 | Birnbaum-saunders | 7324.2 | Exponential | 3036.6 | Gamma | 9558.9 |
| Lognormal | 6592.9 | Exponential | 5059.7 | Lognormal | 7349.3 | Weibull | 3033.97 | Lognormal | 9586.0 |

**Table C- 2 Precipitation data goodness of fit.**

.

| Atenco | | La Grande | | San Andres | | Tejocote | | Chapingo (DGE) | |
|---|---|---|---|---|---|---|---|---|---|
| G.E.V | -297.0 | G.E.V | 3936.1 | G.E.V | 3277.6 | G.E.V | 262.8 | G.E.V | -4267.2 |
| G. Pareto | -228.3 | G. Pareto | 3965.0 | G. Pareto | 3289.5 | Lognormal | 296.5 | Inverse Gaussian | -4114.9 |
| Loglogistic | -198.0 | Lognormal | 3981.9 | Loglogistic | 3339.3 | Loglogistic | 301.7 | G. Pareto | -4051.1 |
| Lognormal | -191.1 | Loglogistic | 3997.0 | Weibull | 3506.9 | Inverse Gaussian | 348.6 | Loglogistic | -3906.8 |
| Inverse Gaussian | -37.3 | Birnbaumsaunders | 4074.2 | Lognormal | 3530.6 | G. Pareto | 357.7 | Lognormal | -3895.2 |

**Table C- 3 River discharge data goodness of fit**

# Appendix D: Distribution Parameters

| Station | | Parameters | | |
|---|---|---|---|---|
| Code | Name | Shape [κ] | Scale [σ] | Location [θ] |
| 15008 | Atenco | 0.40 | 3.66 | 0.10 |
| 15044 | La Grande | 0.22 | 5.28 | 0.10 |
| 15083 | San Andres | 0.34 | 3.94 | 0.10 |
| 15167 | El Tejocote | 0.18 | 5.04 | 0.20 |
| 15170 | Chapingo (DGE) | 0.32 | 4.08 | 0.10 |

**Table D- 1 General Pareto's distribution parameters for precipitation.**

| Station | | Parameters | | |
|---|---|---|---|---|
| Code | Name | Shape [κ] | Scale [σ] | Location [θ] |
| 15008 | Atenco | -0.10 | 1.73 | 4.13 |
| 15044 | La Grande | -0.05 | 1.43 | 3.49 |
| 15083 | San Andres | -0.09 | 1.51 | 3.54 |
| 15167 | El Tejocote | 0.02 | 1.64 | 3.32 |
| 15170 | Chapingo (DGE) | -0.06 | 1.54 | 3.41 |

**Table D- 2 Generalized Extreme Value's distribution parameters for evaporation.**

| Station | | Parameters | | |
|---|---|---|---|---|
| Code | Name | Shape [κ] | Scale [σ] | Location [θ] |
| HD26178 | Atenco | 1.25 | 0.09 | 0.07 |
| HD26193 | La Grande | 1.70 | 0.32 | 0.18 |
| HD26184 | San Andres | 1.24 | 0.24 | 0.16 |
| HD26195 | Tejocote | 1.76 | 0.20 | 0.11 |
| HD26183 | Chapingo (DGE) | 1.45 | 0.04 | 0.03 |

**Table D- 3 Generalized Extreme Value's distribution parameters for river discharge.**

# Appendix E: Copula Fitting

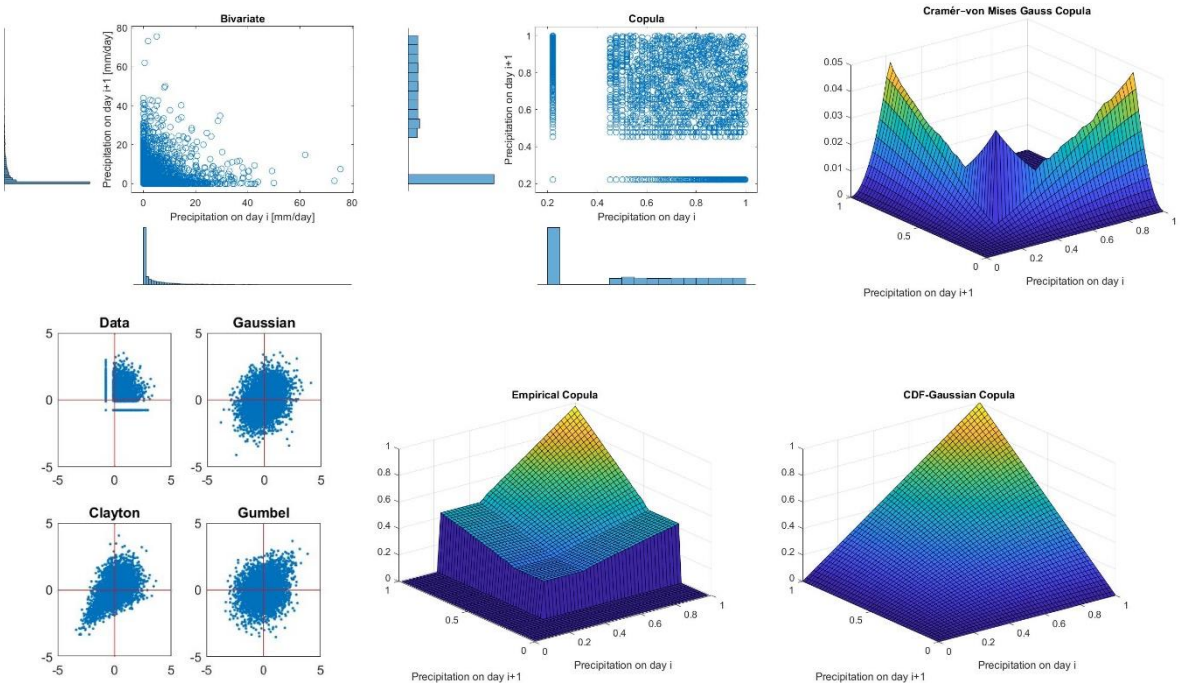


**Figure E- 1 Copula fitting of the pair P-P. Atenco Station.**

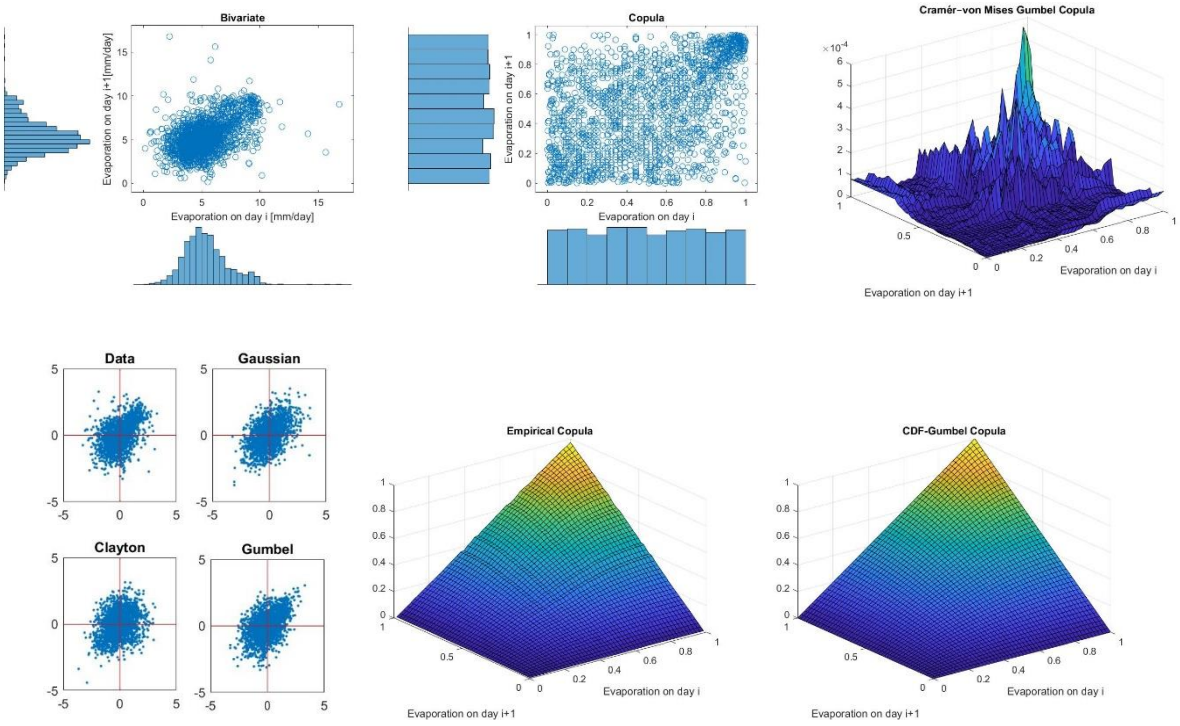


**Figure E- 2 Copula fitting of the pair E-E. Atenco Station.**

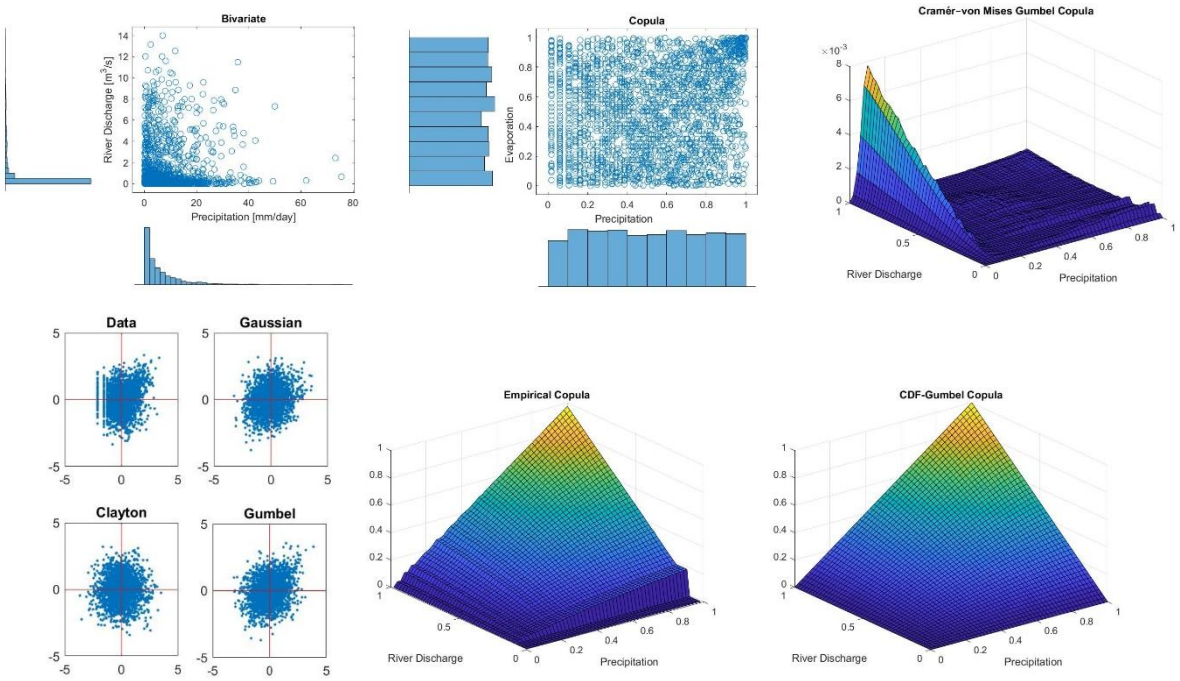


**Figure E- 3 Copula fitting of the pair P-E. Atenco Station.**

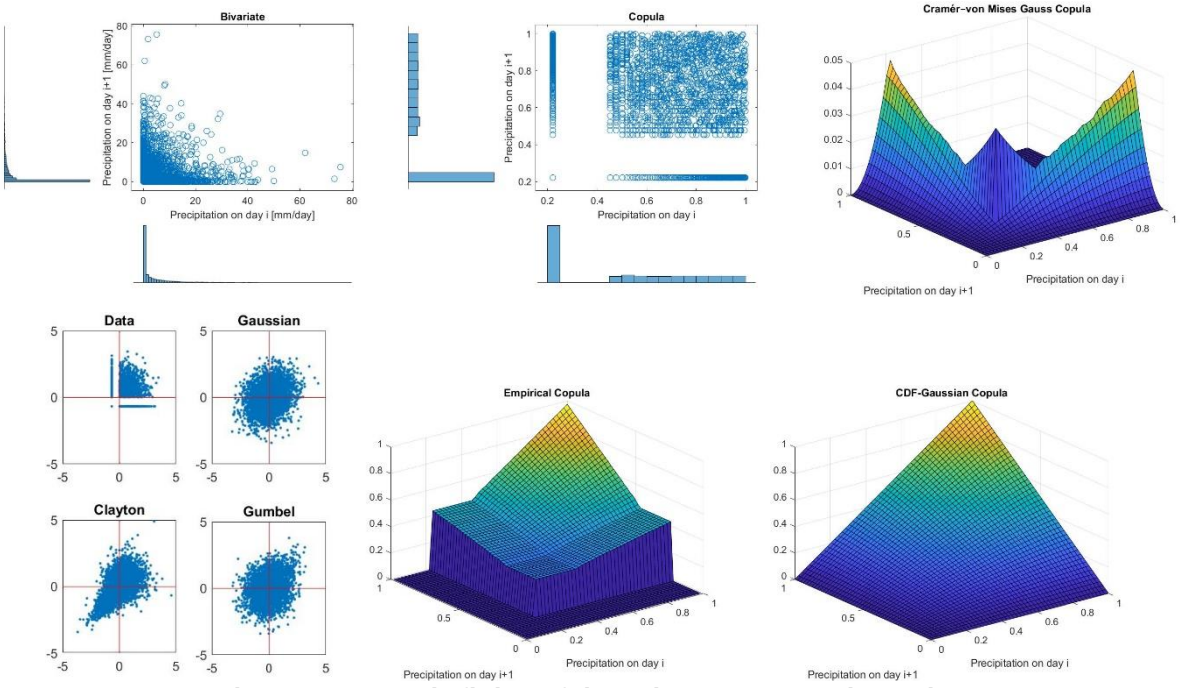


**Figure E- 4 Copula fitting of the pair P-P. La Grande Station.**

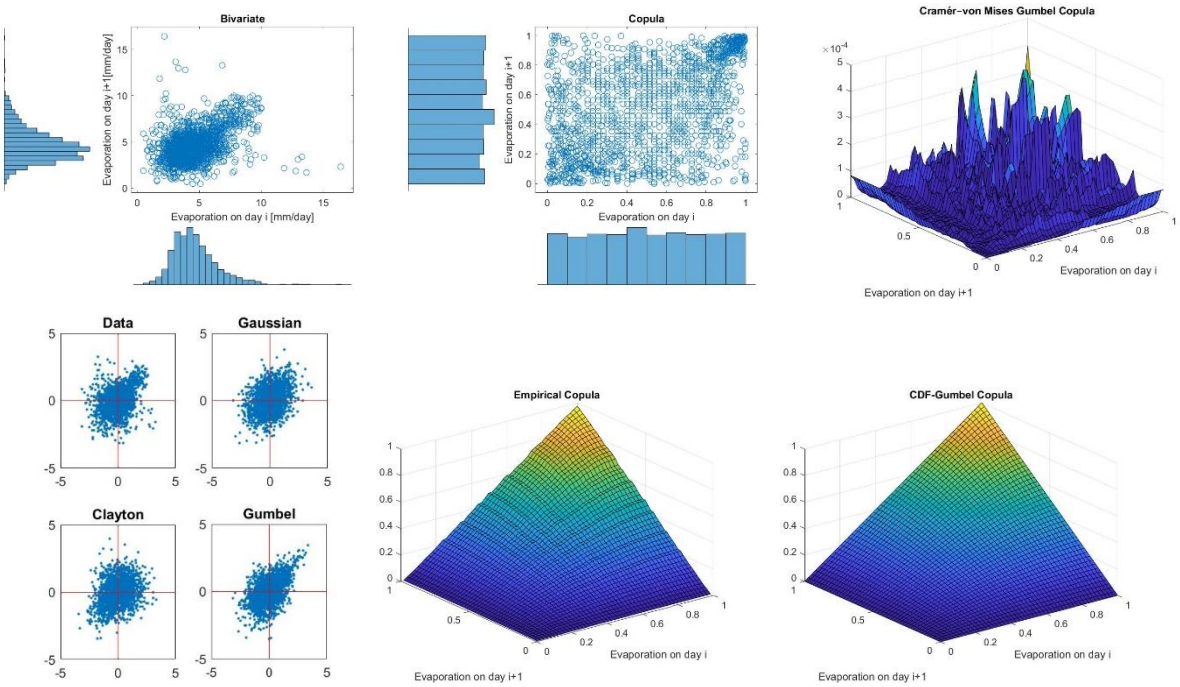


**Figure E- 5 Copula fitting of the pair E-E. La Grande Station.**

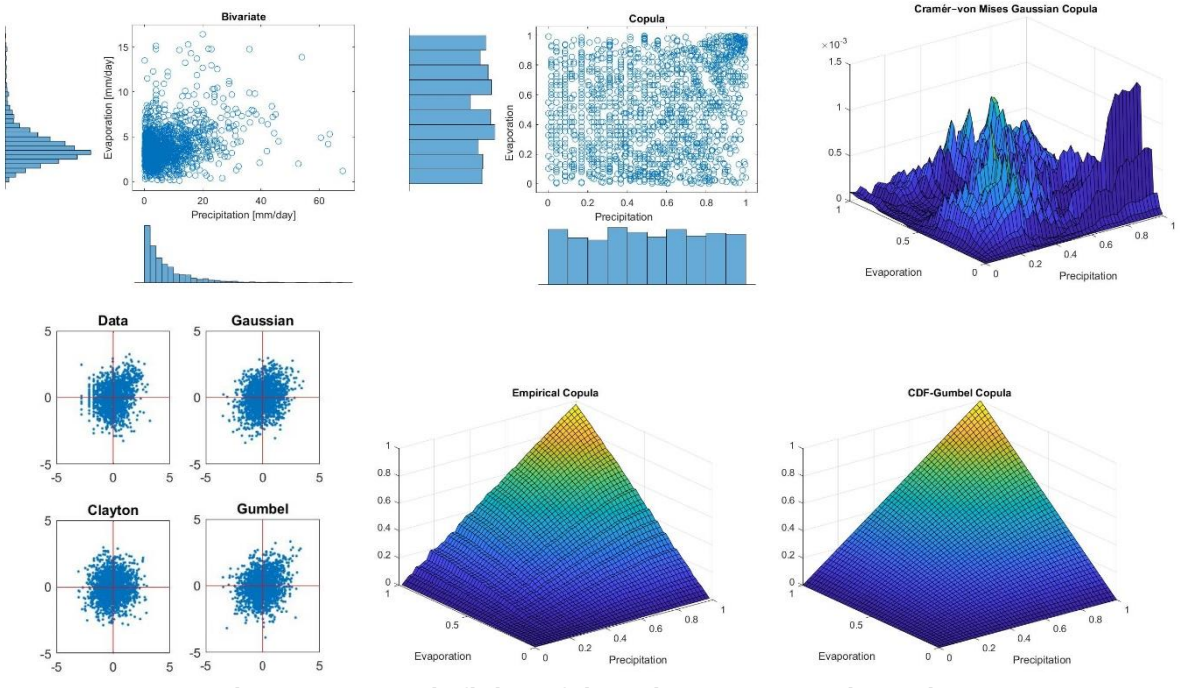


**Figure E- 6 Copula fitting of the pair P-E. La Grande Station.**

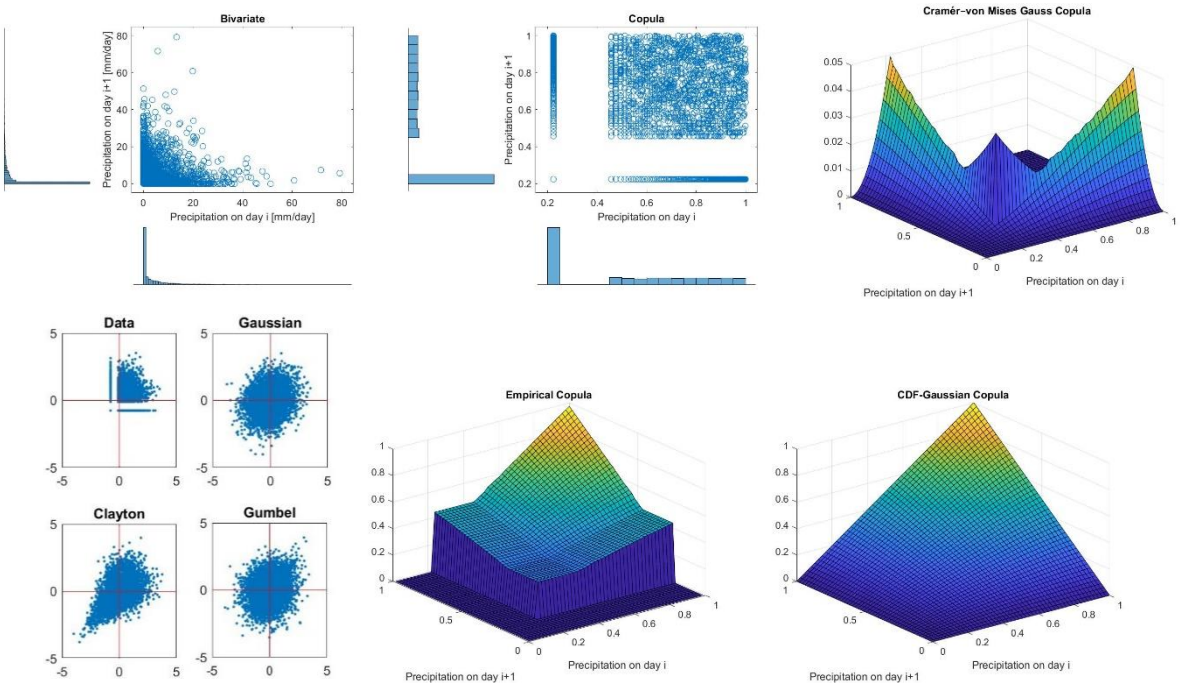


**Figure E- 7 Copula fitting of the pair P-P. San Andres Station.**

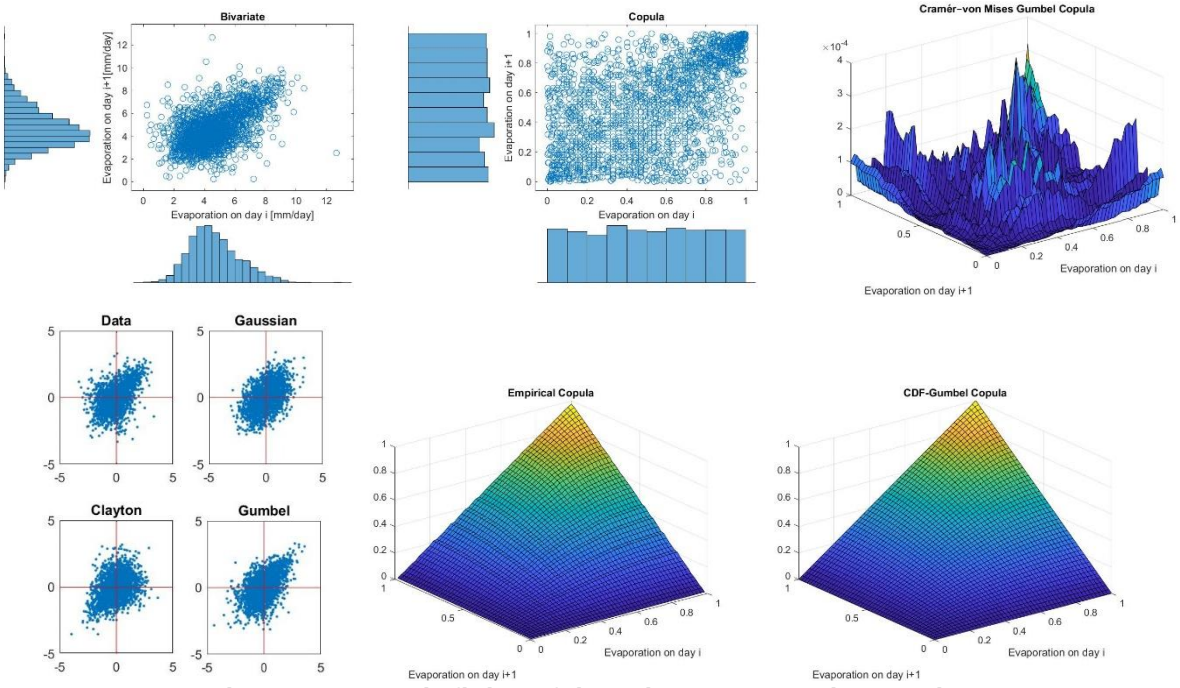


**Figure E- 8 Copula fitting of the pair E-E. San Andres Station.**

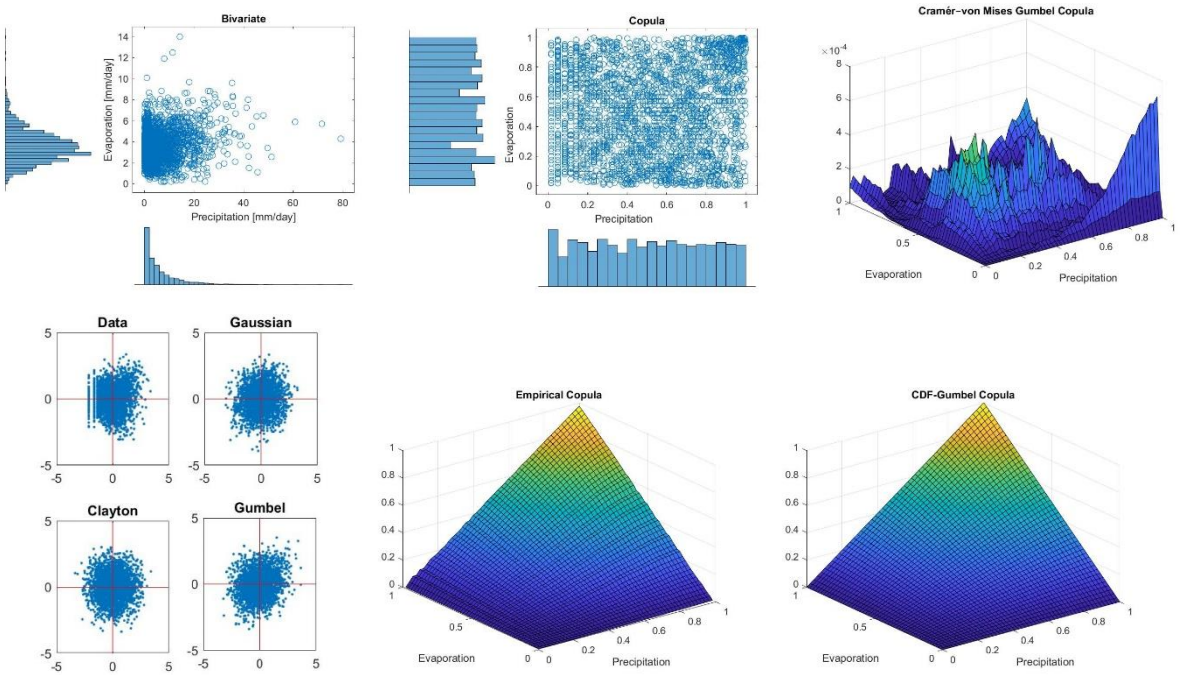


**Figure E- 9 Copula fitting of the pair P-E. San Andres Station.**

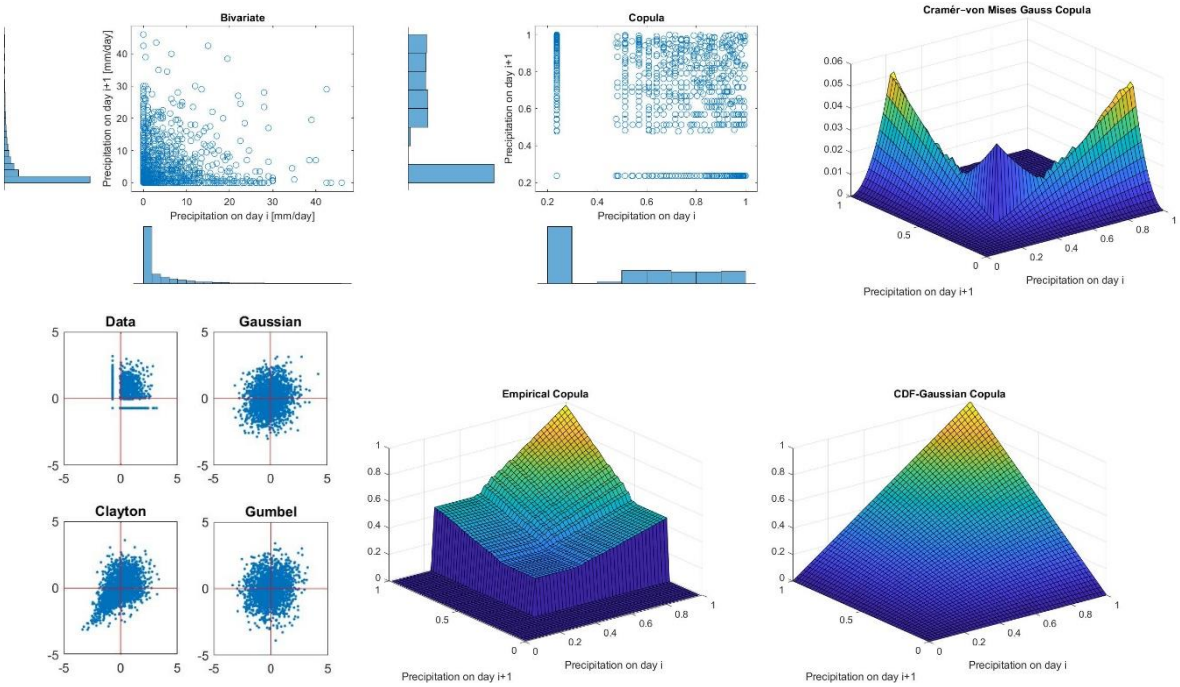


**Figure E- 10 Copula fitting of the pair P-P. El Tejocote Station.**

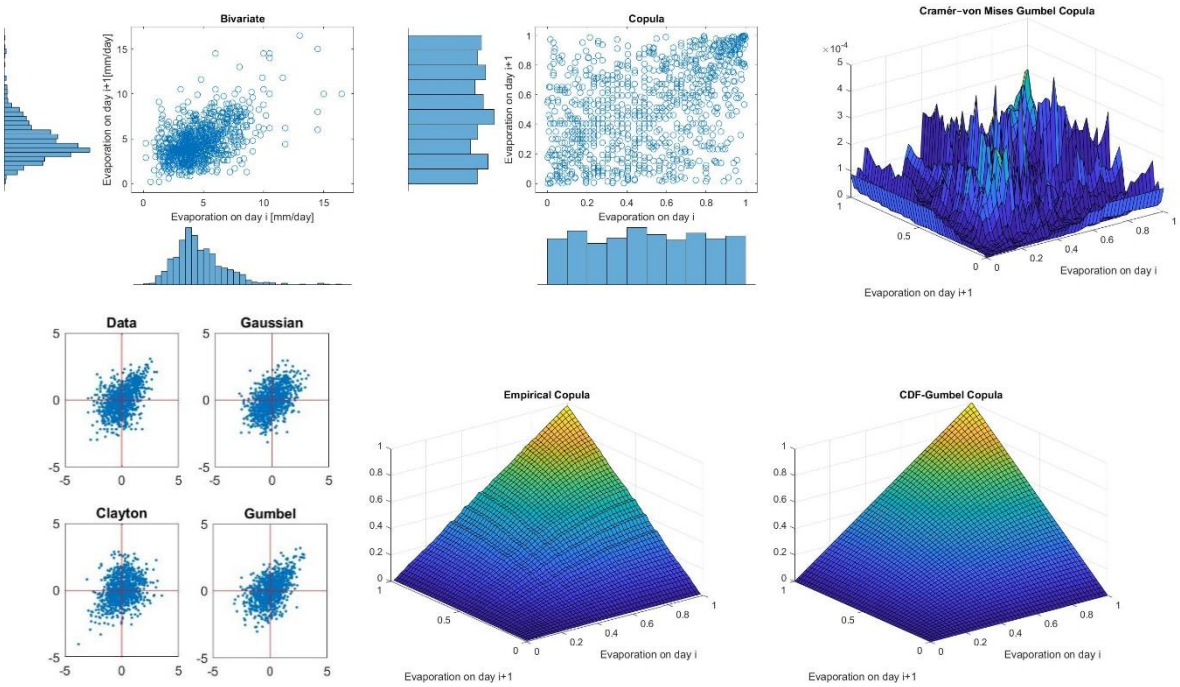


**Figure E- 11 Copula fitting of the pair E-E. El Tejocote Station.**

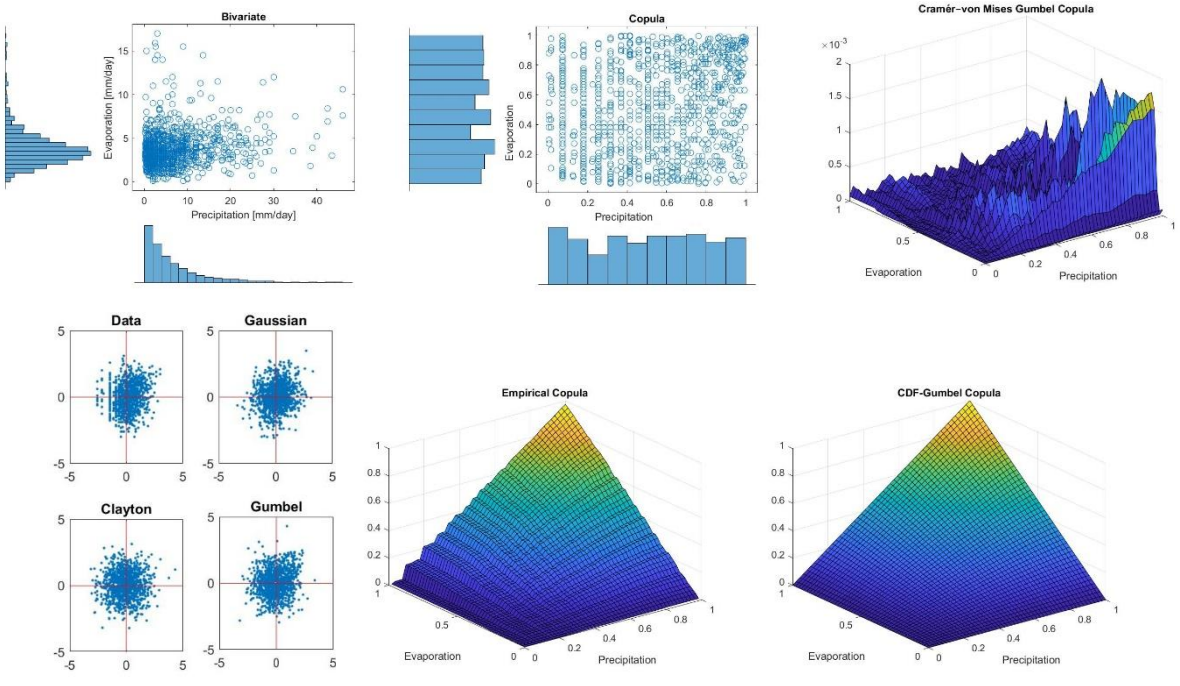


**Figure E- 12 Copula fitting of the pair P-E. El Tejocote Station.**

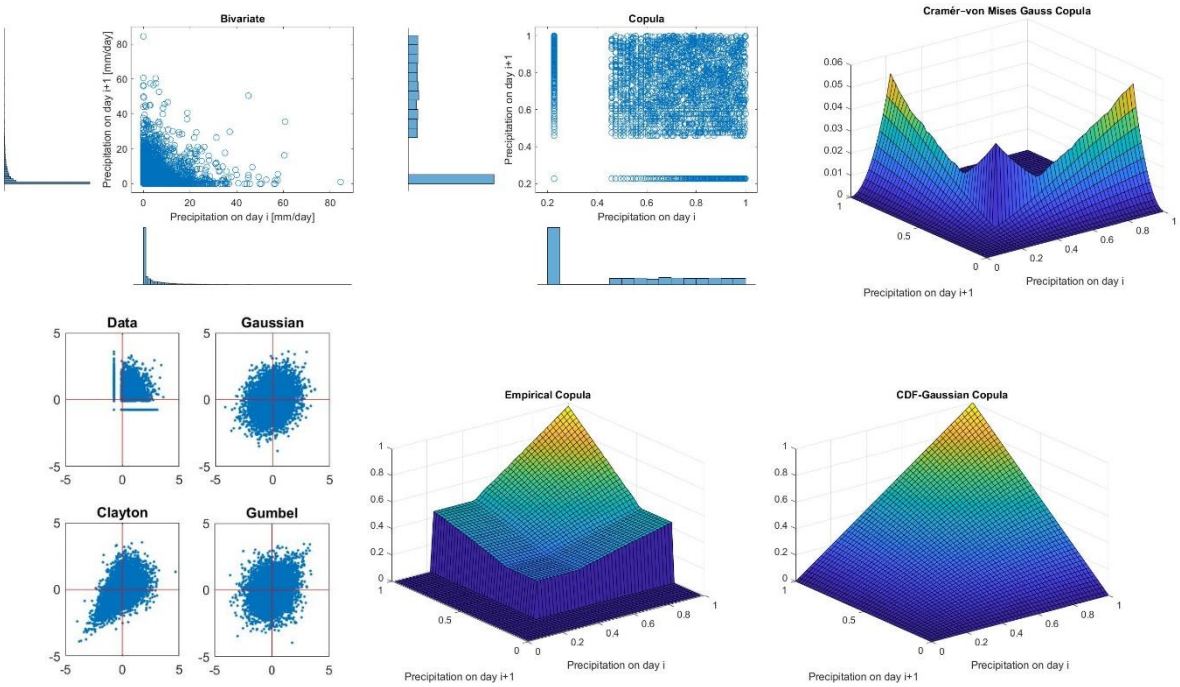


**Figure E- 13 Copula fitting of the pair P-P. Chapingo Station.**

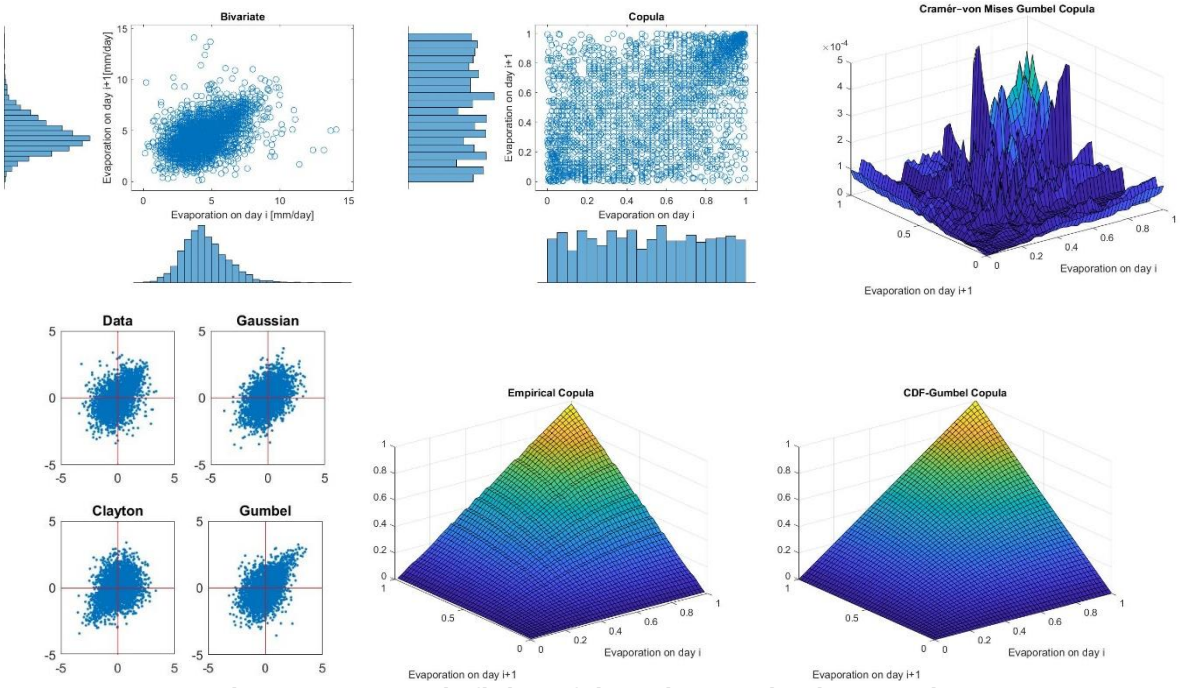


**Figure E- 14 Copula fitting of the pair E-E. Chapingo Station.**

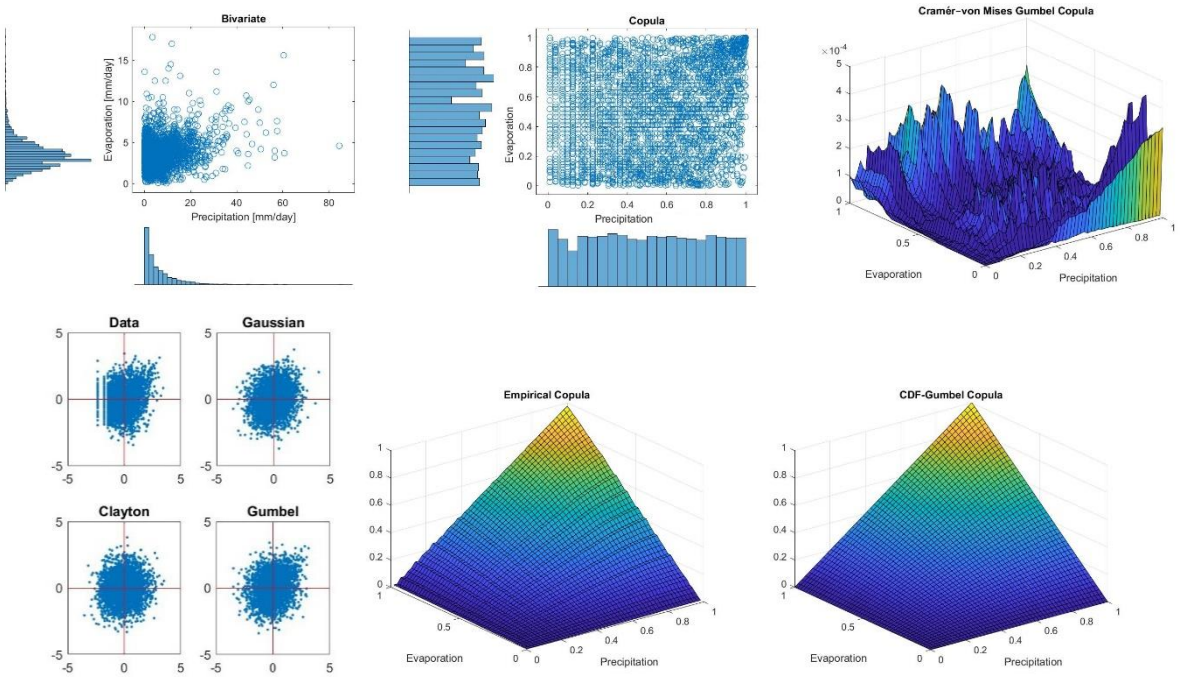


**Figure E- 15 Copula fitting of the pair P-E. Chapingo Station.**

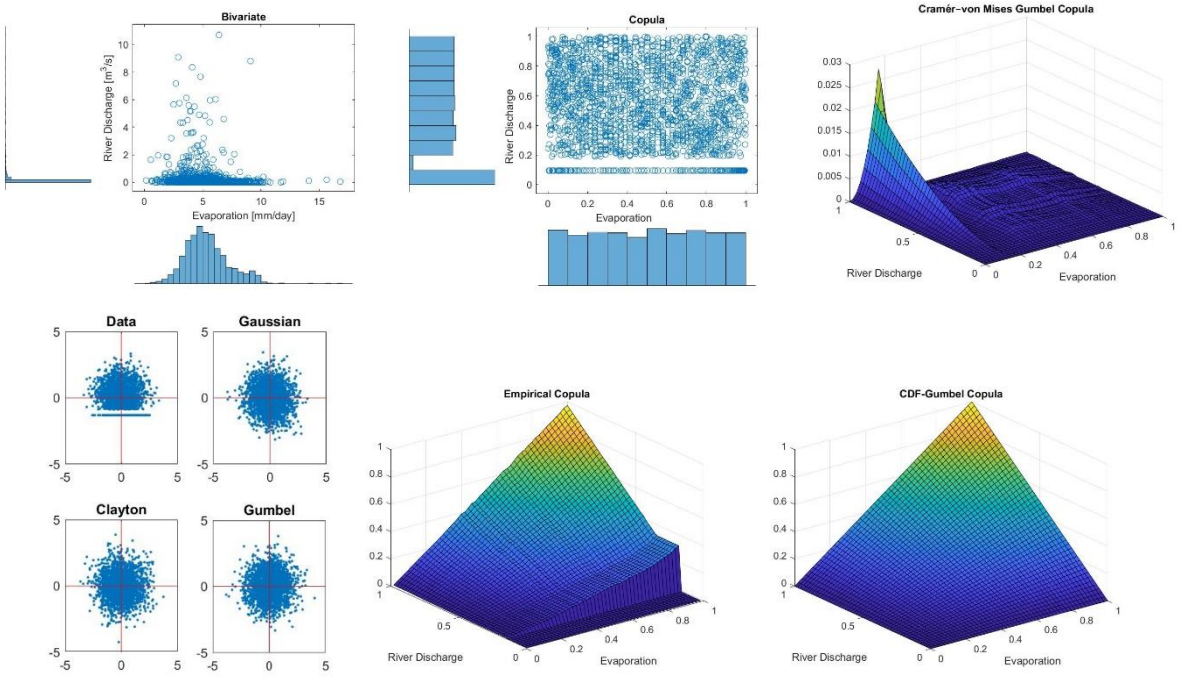


**Figure E- 16 Copula fitting of the pair E-Q. Atenco Station.**

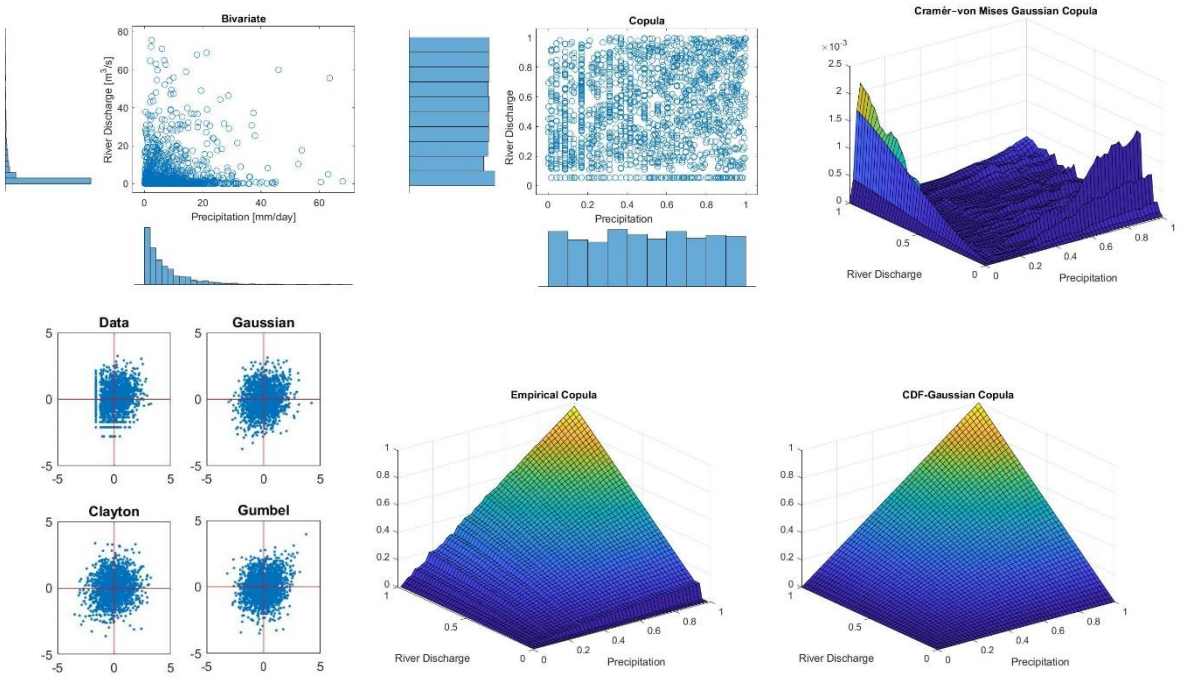


**Figure E- 17 Copula fitting of the pair P-Q. La Grande Station.**

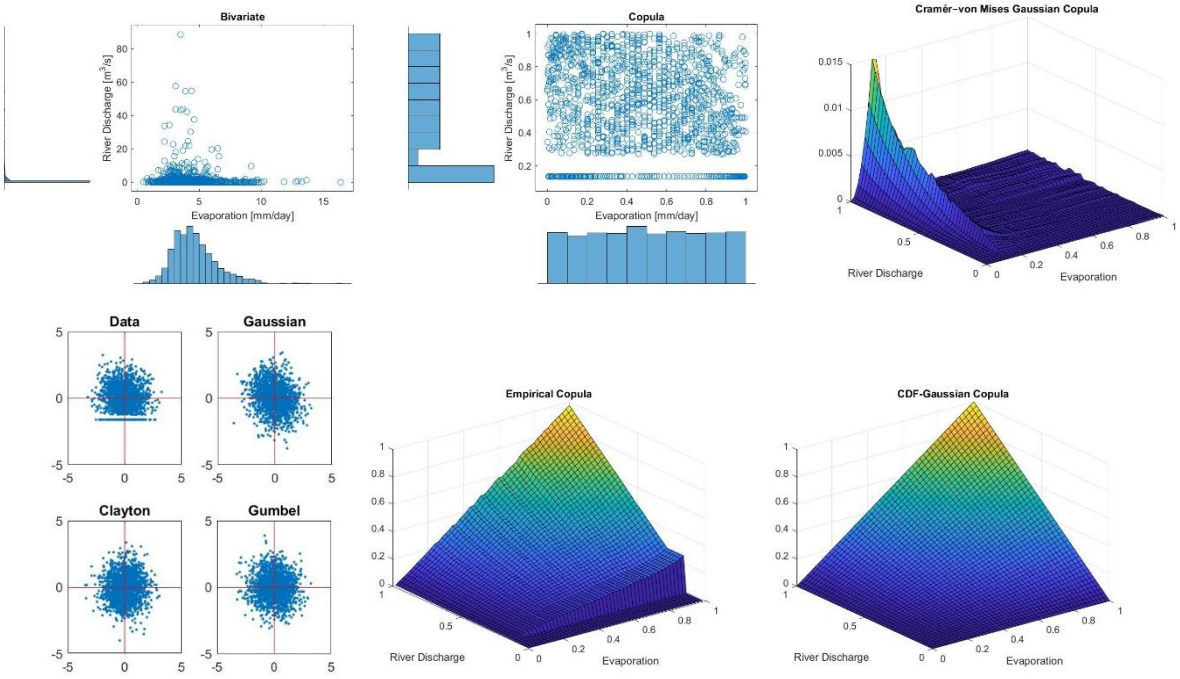


**Figure E- 18 Copula fitting of the pair E-Q. La Grande Station.**

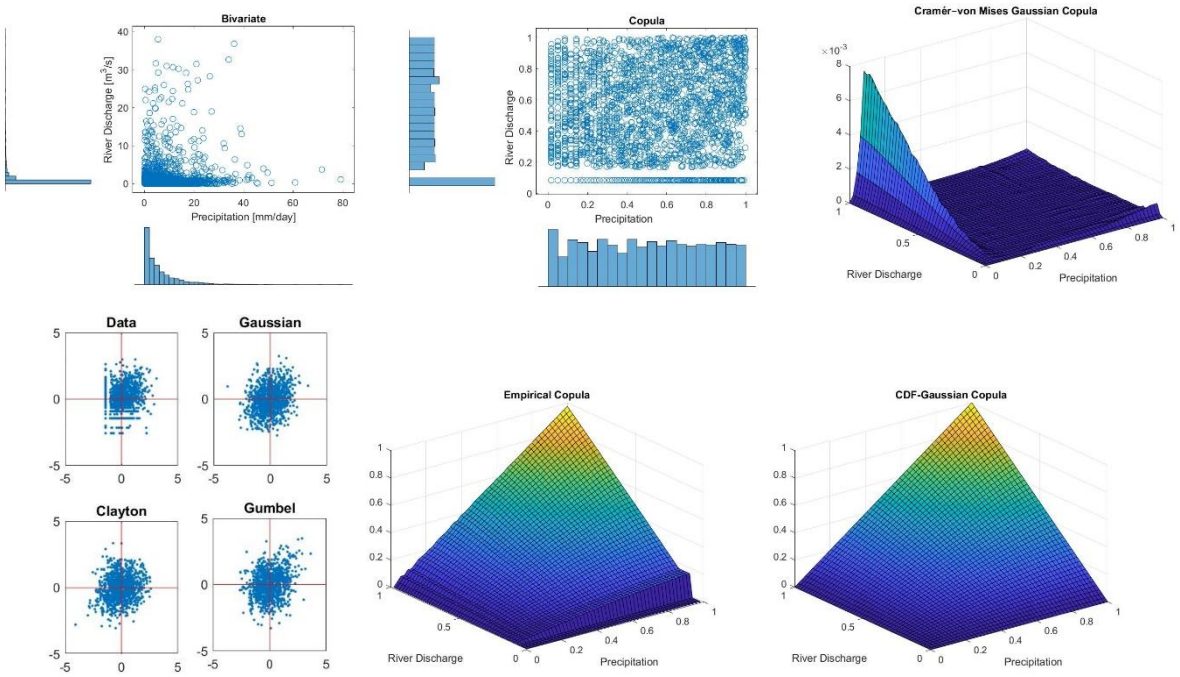


**Figure E- 19 Copula fitting of the pair P-Q. San Andres Station.**

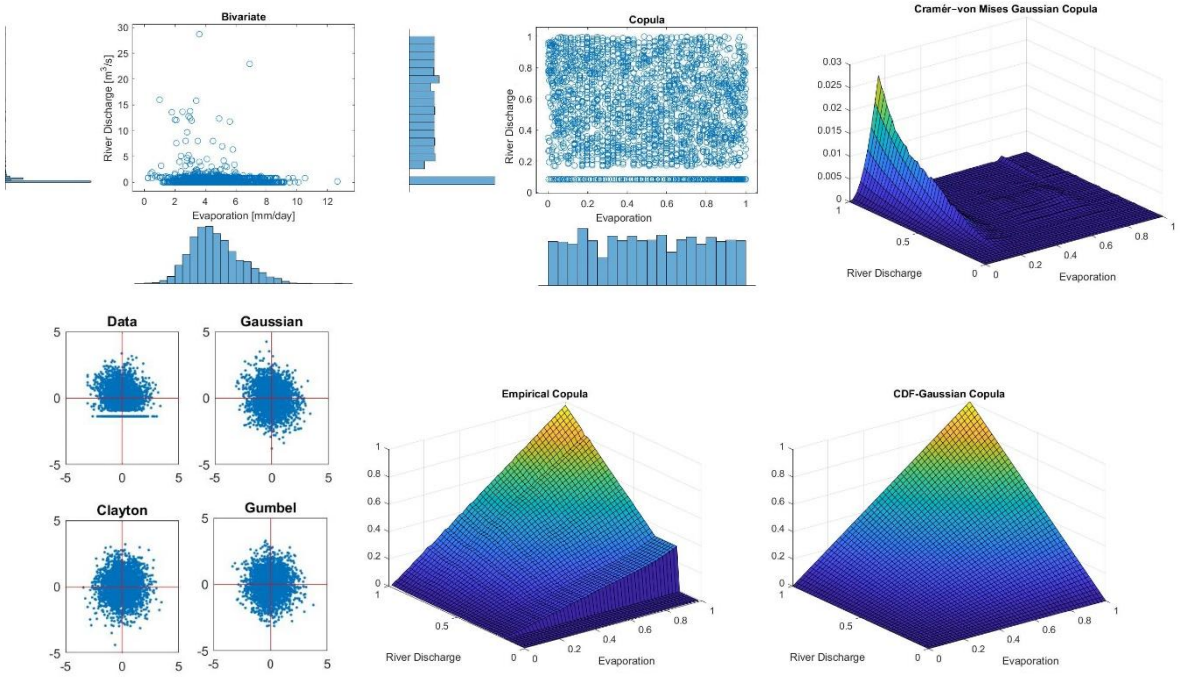


**Figure E- 20 Copula fitting of the pair E-Q. San Andres Station.**

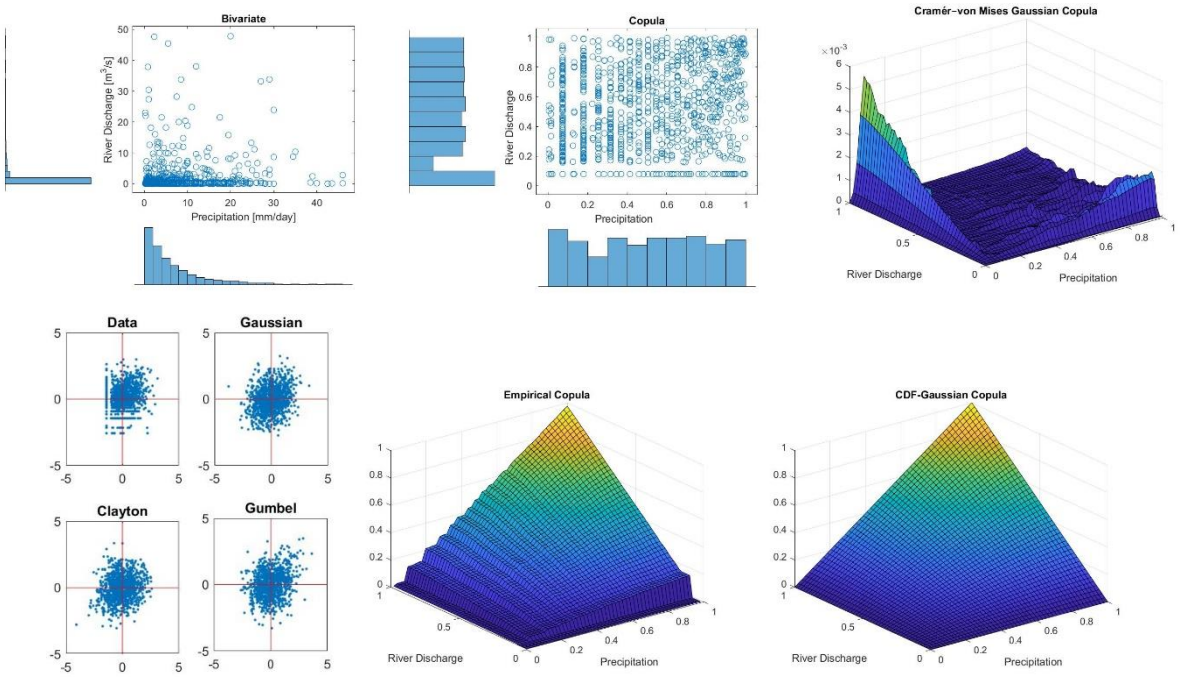


**Figure E- 21 Copula fitting of the pair P-Q. El Tejocote Station.**

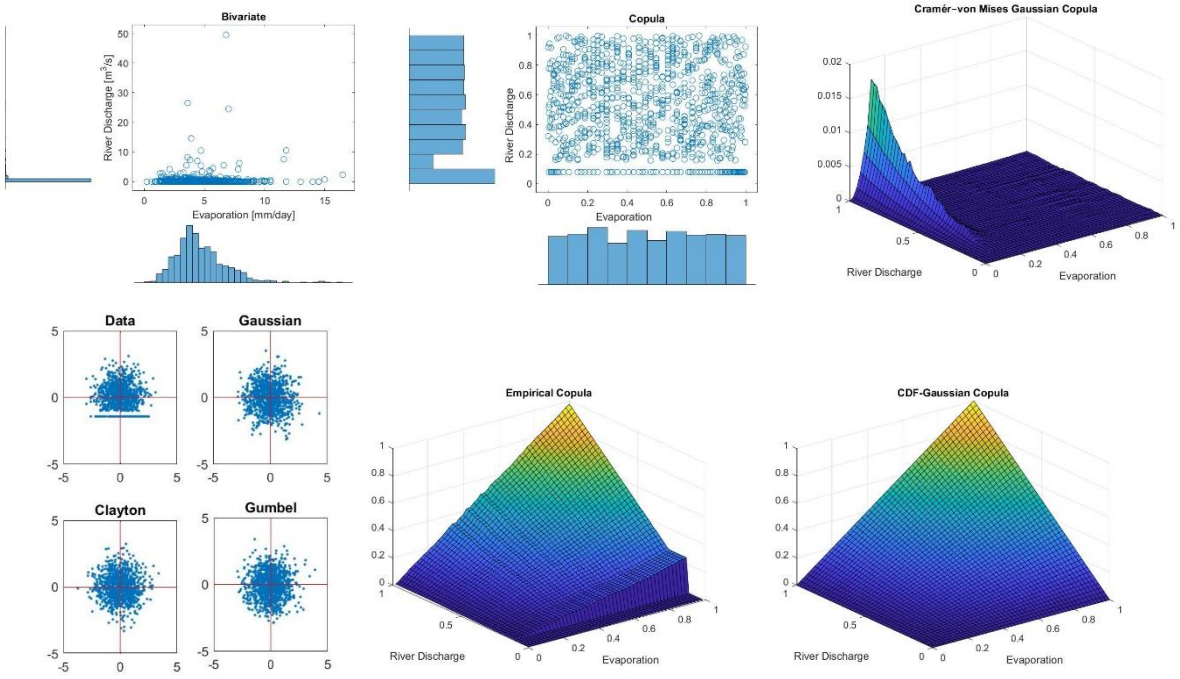


**Figure E- 22 Copula fitting of the pair E-Q. El Tejocote Station.**

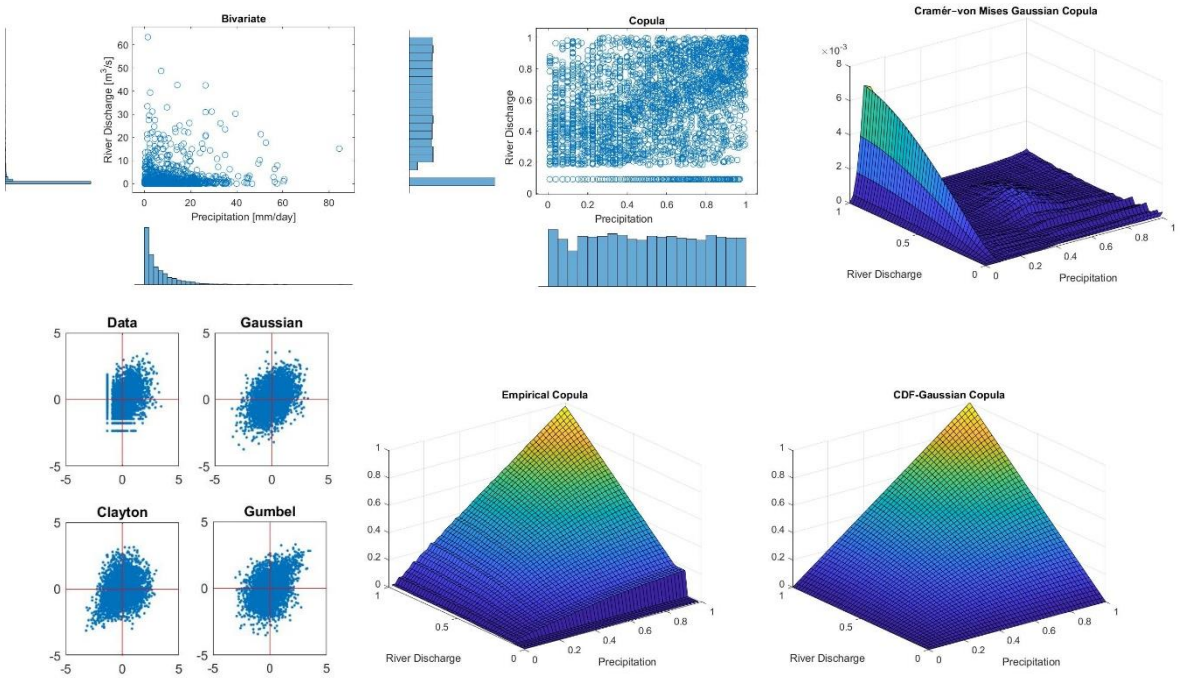


**Figure E- 23 Copula fitting of the pair P-Q. Chapingo Station.**

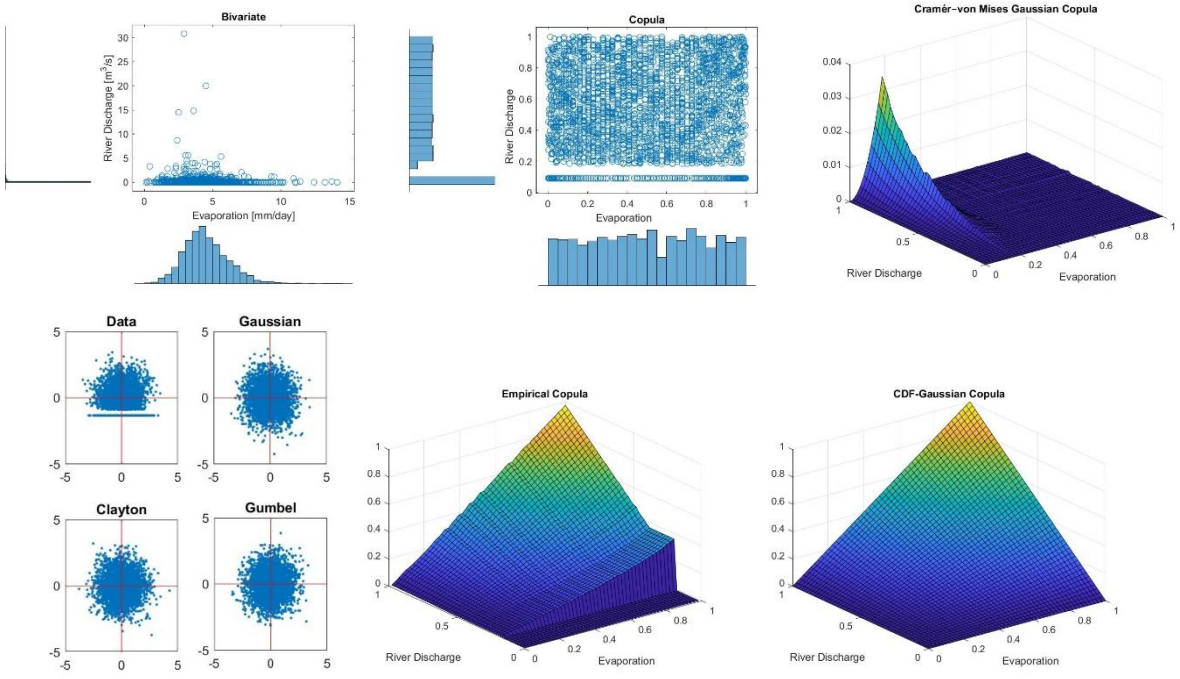


**Figure E- 24 Copula fitting of the pair E-Q. Chapingo Station.**

| Station | Overall $\rho$ | Copula | $\rho_{ne}$ | $\rho_{sw}$ | $S_n$ |
|---|---|---|---|---|---|
| Atenco | 0.27 | Gauss | 0.14 | 0.10 | 17.26 |
| | | Gumbel | 0.26 | 0.07 | 17.64 |
| | | Clayton | 0.12 | 0.10 | 17.00 |
| La Grande | 0.25 | Gauss | 0.08 | 0.07 | 23.86 |
| | | Gumbel | 0.33 | 0.09 | 23.84 |
| | | Clayton | 0.08 | 0.06 | 24.94 |
| San Andres | 0.24 | Gauss | 0.08 | 0.08 | 17.12 |
| | | Gumbel | 0.00 | 0.07 | 17.45 |
| | | Clayton | 0.00 | 0.06 | 16.88 |
| El Tejocote | 0.18 | Gauss | 0.13 | -0.01 | 18.51 |
| | | Gumbel | -0.03 | 0.07 | 18.59 |
| | | Clayton | -0.01 | 0.06 | 19.18 |
| Chapingo (DGE) | 0.25 | Gauss | 0.07 | 0.10 | 18.05 |
| | | Gumbel | 0.02 | 0.08 | 18.41 |
| | | Clayton | 0.01 | 0.13 | 17.51 |

**Table E- 1 Cramer von Mises and semi-correlation results for the pair P-P. All stations.**

| Station | Overall $\rho$ | Copula | $\rho_{ne}$ | $\rho_{sw}$ | $S_n$ |
|---|---|---|---|---|---|
| Atenco | 0.46 | Gauss | 0.19 | 0.17 | 0.24 |
| | | Gumbel | 0.40 | 0.16 | 0.09 |
| | | Clayton | 0.16 | 0.19 | 1.41 |
| La Grande | 0.41 | Gauss | 0.24 | 0.18 | 0.18 |
| | | Gumbel | 0.45 | 0.21 | 0.09 |
| | | Clayton | 0.12 | 0.13 | 1.00 |
| San Andres | 0.50 | Gauss | 0.24 | 0.31 | 0.26 |
| | | Gumbel | 0.54 | 0.25 | 0.10 |
| | | Clayton | 0.16 | 0.22 | 1.57 |
| El Tejocote | 0.44 | Gauss | 0.24 | 0.24 | 0.23 |
| | | Gumbel | 0.46 | 0.17 | 0.13 |
| | | Clayton | 0.18 | 0.12 | 1.24 |
| Chapingo (DGE) | 0.458 | Gauss | 0.27 | 0.29 | 0.17 |
| | | Gumbel | 0.54 | 0.17 | 0.09 |
| | | Clayton | 0.17 | 0.17 | 1.06 |

**Table E- 2 Cramer von Mises and semi-correlation results for the pair E-E. All stations.**

| Station | Overall $\rho$ | Copula | $\rho_{ne}$ | $\rho_{sw}$ | $S_n$ |
|---|---|---|---|---|---|
| Atenco | 0.18 | Gauss | -0.01 | 0.10 | 0.167 |
| | | Gumbel | 0.27 | 0.06 | 0.124 |
| | | Clayton | 0.00 | 0.06 | 0.579 |
| La Grande | 0.19 | Gauss | 0.06 | 0.15 | 0.388 |
| | | Gumbel | 0.29 | 0.18 | 0.281 |
| | | Clayton | 0.10 | 0.06 | 1.061 |
| San Andres | 0.09 | Gauss | 0.07 | -0.02 | 0.192 |
| | | Gumbel | 0.21 | 0.10 | 0.192 |
| | | Clayton | -0.02 | 0.04 | 0.358 |
| El Tejocote | 0.16 | Gauss | 0.07 | 0.03 | 0.439 |
| | | Gumbel | 0.22 | 0.02 | 0.383 |
| | | Clayton | -0.08 | -0.04 | 0.919 |
| Chapingo (DGE) | 0.181 | Gauss | 0.07 | 0.12 | 0.164 |
| | | Gumbel | 0.21 | 0.07 | 0.121 |
| | | Clayton | 0.01 | 0.07 | 0.607 |

**Table E- 3 Cramer von Mises and semi-correlation results for the pair P-E. All stations.**

| Station | Overall $\rho$ | Copula | $\rho_{ne}$ | $\rho_{sw}$ | $S_n$ |
|---|---|---|---|---|---|
| Atenco | 0.20 | Gauss | 0.01 | 0.02 | 0.66 |
| | | Gumbel | 0.23 | 0.12 | 0.72 |
| | | Clayton | 0.05 | 0.09 | 0.78 |
| La Grande | 0.17 | Gauss | 0.19 | 0.05 | 0.23 |
| | | Gumbel | 0.16 | 0.00 | 0.31 |
| | | Clayton | 0.00 | -0.02 | 0.29 |
| San Andres | 0.18 | Gauss | 0.04 | 0.10 | 0.49 |
| | | Gumbel | 0.24 | 0.03 | 0.57 |
| | | Clayton | 0.03 | 0.02 | 0.54 |
| El Tejocote | 0.23 | Gauss | 0.14 | 0.06 | 0.55 |
| | | Gumbel | 0.03 | 0.07 | 0.60 |
| | | Clayton | 0.11 | 0.12 | 0.66 |
| Chapingo (DGE) | 0.379 | Gauss | 0.24 | -0.01 | 0.78 |
| | | Gumbel | 0.13 | 0.13 | 0.85 |
| | | Clayton | 0.01 | 0.36 | 1.28 |

**Table E- 4 Cramer von Mises and semi-correlation results for the pair P-Q. All stations.**

| Station | Overall $\rho$ | Copula | $\rho_{ne}$ | $\rho_{sw}$ | $S_n$ |
|---|---|---|---|---|---|
| Atenco | -0.27 | Gauss | -0.193 | -0.11 | 1.86 |
| | | Gumbel | -0.028 | 0.01 | 1.25 |
| | | Clayton | -0.048 | -0.11 | 1.10 |
| La Grande | -0.21 | Gauss | -0.07 | -0.09 | 3.08 |
| | | Gumbel | 0.01 | 0.10 | 2.13 |
| | | Clayton | -0.10 | -0.02 | 1.29 |
| San Andres | -0.12 | Gauss | -0.08 | -0.11 | 1.93 |
| | | Gumbel | -0.02 | 0.04 | 1.29 |
| | | Clayton | -0.01 | -0.01 | 1.11 |
| El Tejocote | -0.10 | Gauss | -0.03 | -0.05 | 3.08 |
| | | Gumbel | 0.05 | -0.04 | 2.13 |
| | | Clayton | -0.15 | -0.08 | 1.29 |
| Chapingo (DGE) | -0.219 | Gauss | -0.01 | -0.10 | 1.92 |
| | | Gumbel | 0.04 | -0.01 | 1.27 |
| | | Clayton | -0.04 | -0.02 | 1.12 |

**Table E- 5 Cramer von Mises and semi-correlations results for the pair E-Q. All stations.**

# Appendix F: Reliability Analysis including River Discharge

In this appendix, an alternative reliability analysis is presented. The difference of this procedure consists of including river discharge data into the hydrological balance (Eq. 15). This data was collected from stations located in rivers that flowed directly towards the east region of Lake Texcoco (Figure F- 1). These rivers are The Papalotla, Xalapango, Coxcacuaco, Texcoco, San Bernardino, Chapingo, Coatepec, and Santa Monica River.

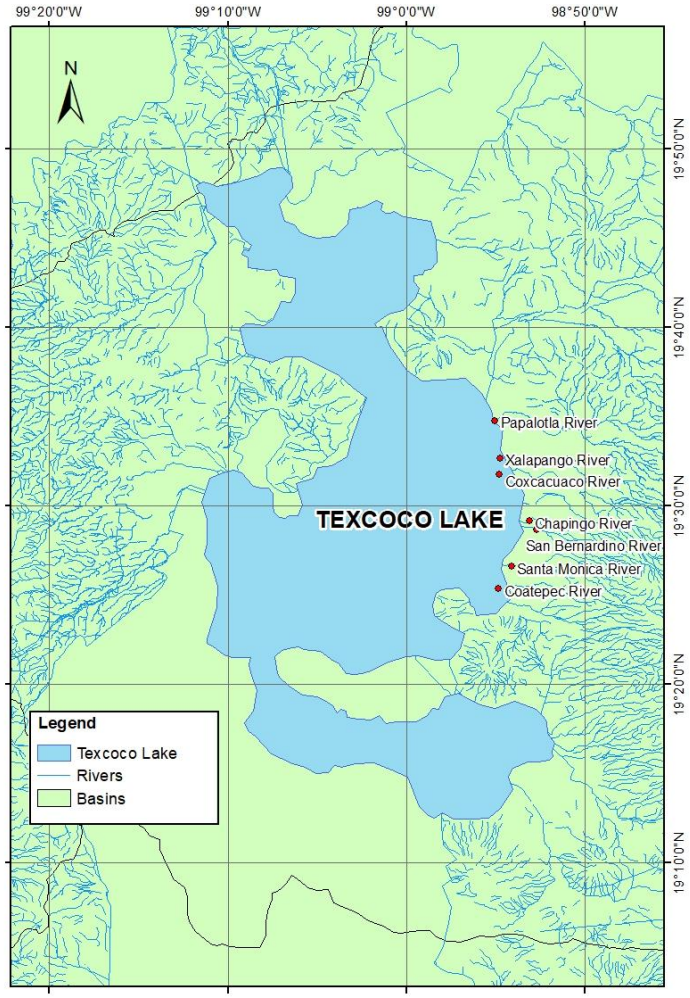


**Figure F- 1 Rivers at the east side of Lake Texcoco.**

The filtering process to choose the stations for river discharge data was the same as for evaporation and precipitation data (Section 4.3.2). A total of 5 stations were chosen based on their proximity to the stations selected for precipitation-evaporation and by their data availability. See Table F- 1and Figure F- 2.

| Code | Name | River | Timeline |
|---|---|---|---|
| HD26178 | Atenco | Xalapango | 1/1/1944-22/8/2013 |
| HD26183 | Chapingo | Chapingo | 1/8/1944-31/12/2014 |
| HD26184 | San Andres | Coxcacoaco | 1/8/1944-31/12/2014 |
| HD26193 | La Grande | Papalotla | 1/1/1945-01/01/2007 |

**Table F- 1 River Discharge Stations.**

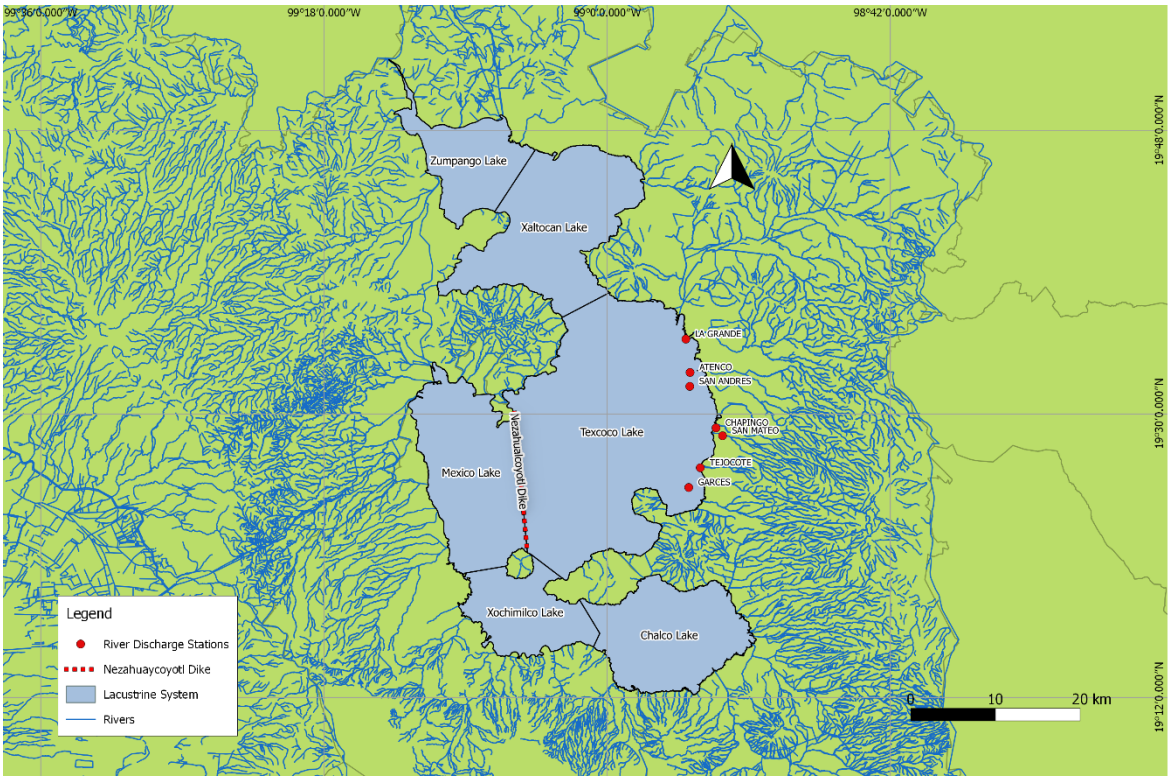


**Figure F- 2 River discharge stations.**

As mentioned in section 6.1, only data corresponding to the wet season were considered. The fitted marginal distributions for river discharge are shown in Table F- 2.

| Station | Probability Distribution Function |
|---|---|
| | $Q$ |
| Atenco | Generalized Extreme Value |
| La Grande | Generalized Extreme Value |
| San Andres | Generalized Extreme Value |
| El Tejocote | Generalized Extreme Value |
| Chapingo (DGE) | Generalized Extreme Value |

**Table F- 2 Fitting distribution results for river discharge data.**

The previous table indicates that the data from all the stations can be described by the same probabilistic distribution function: The general extreme value distribution. The CDF's (Cumulative distribution function) plots for each station are presented in Appendix C.

By following the methodology presented in Chapter 4, the next step in this analysis is the Markov Chain model (Section 4.4.1). However, this model remains unchanged and so its results (Table 6-2).

The inclusion of river discharge data in this alternative analysis is reflected in the generation of the synthetic data series. Thus, the copula model expanded as shown in Figure F- 3.

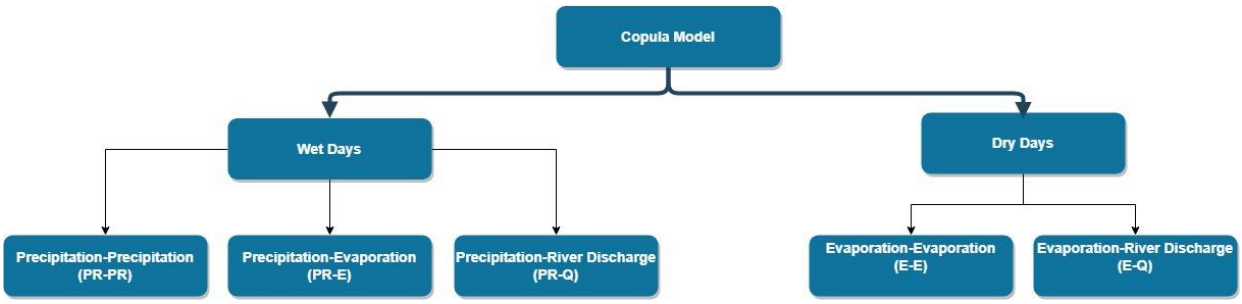


**Figure F- 3 Flowchart for the generation of synthetic data through a copula model (including river discharge).**

The pairs of data were divided into two groups according to two conditions: Wet days and dry days as shown in section 4.4.2. The pairs for wet days are Precipitation-precipitation (PR-PR), Precipitation-Evaporation (PR-E), and Precipitation-River discharge (PR-Q). The pairs for dry days are Evaporation- Evaporation (E-E) and Evaporation-Discharge (E-Q). Now the synthetic time series includes precipitation, evaporation and river discharge data. Precipitation and evaporation data was generated in the same manner as presented in section 4.4.2. The generation of discharge data is illustrated as follows:

The $PR-Q$ copula or $C\left(Q_t \middle| PR_t\right)$, which is the conditional copula of river discharge in time $t$ given precipitation on time $t$, generates data of river discharge given a wet day. The generated datasets for river discharge given a dry day were generated based on the $E-Q$ copula. Where the conditional copula of river discharge in time $t$ given evaporation in time $t$ is denoted as $C\left(Q_t \middle| E_t\right)$.

As result from the copula model (Section 2.5), the dependence between the pairs $PR-Q$ and $E-Q$ was obtained. See Table F- 3.

| Station | Spearman's rho correlation coefficient | |
|---|---|---|
| | $PR-Q$ | $E-Q$ |
| Atenco | 0.2 | -0.27 |
| La Grande | 0.17 | -0.21 |
| San Andres | 0.18 | -0.12 |
| El Tejocote | 0.23 | -0.1 |
| Chapingo (DGE) | 0.38 | -0.22 |

**Table F- 3 Correlation values for all stations for the pairs with river discharge.**

*Precipitation (P), Evaporation (E), River Discharge (Q).

The pairs of data sets from the previous table were also fitted to a copula following the same procedure as in section 6.2. The results are shown in Table F- 4.

| Pairs | Atenco | La Grande | San Andres | El Tejocote | Chapingo (DGE) |
|---|---|---|---|---|---|
| $PR-Q$ | Gumbel | Gauss | Gauss | Gauss | Gauss |
| $E-Q$ | Gumbel | Gauss | Gauss | Gauss | Gauss |

**Table F- 4 Copula fit for all stations and pairs *PR-Q* and *E-Q*.**

The previous table shows that the copulas that best describes each pair of data are the same for all stations, for the exception at Atenco station in which the best fit corresponds to a Gumbel copula instead of a Gauss copula as the other stations. River discharge data shows similar

correlation values for both pairs $PR-Q$ and $E-Q$ between all the stations (Table F- 3). Additionally, the marginal distributions and pairs can be described by the same marginal distributions and copulas (Table F- 2 and Table F- 4 respectively). Therefore, river discharge data can also be described by the data of one station. Thus, Chapingo (DGE) station was chosen in order to keep in accordance with the results shown in section 6.2.

In total, one thousand wet seasons were generated. The resulting time series of one wet season for river discharge is shown in Figure F- 4.

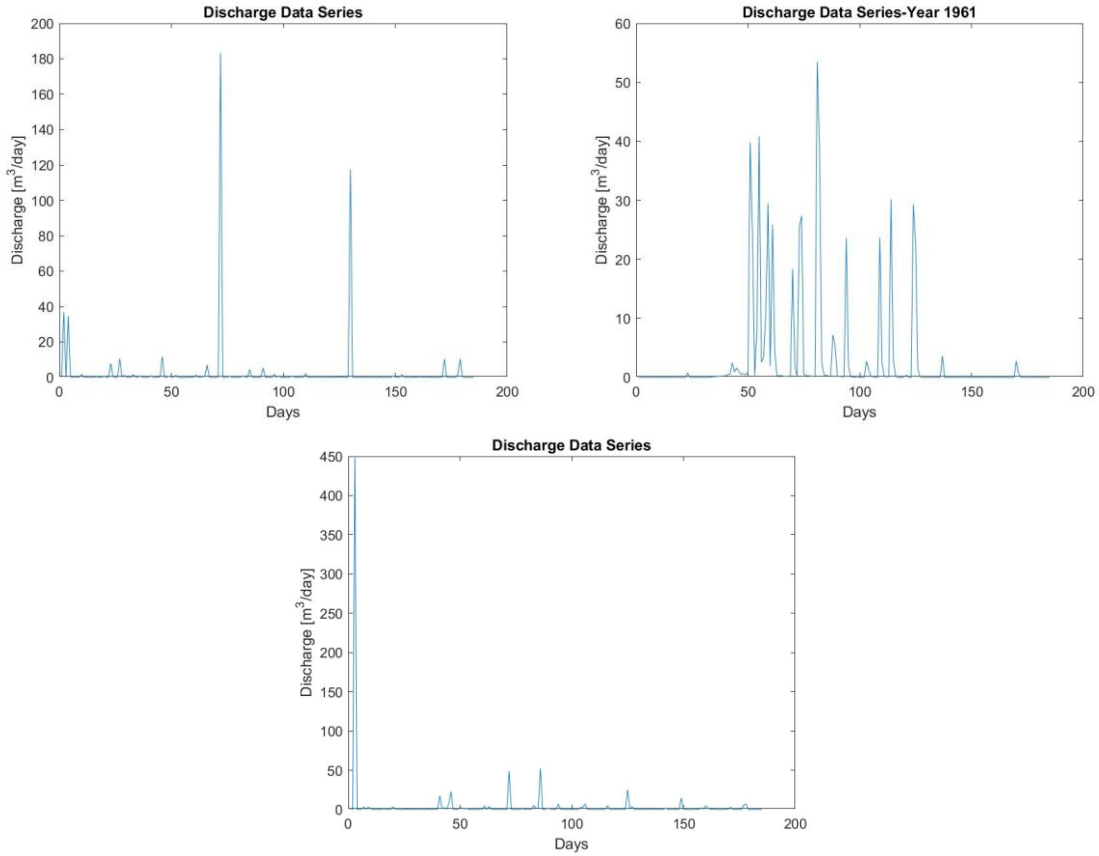


**Figure F- 4 Discharge data: (a) Synthetic data series (Top Left); (b) Real data series at Chapingo Station. Year 1961 (Top Right); (c) Synthetic data series with a higher correlation coefficient (Bottom).**

The river discharge synthetic data were compared with real data of one wet season measured at Chapingo station (Figure F- 4a and Figure F- 4b). Notice that the time series of real data has a slightly higher number of peaks which are also close to each other, while the synthetic series shows fewer peaks with a bigger time between them. The values of the peaks in the synthetic series are much higher than in the actual measurements. A similar pattern was observed for the precipitation time series in section 6.2.

Another example of the synthetic time series (Figure F- 4c) was generated with a correlation coefficient of 0.8. Notice that in this case, river discharge data show a small number of peaks throughout the wet season, where one peak is much bigger than the rest of the series. The data does not show improvements from increasing the correlation value.

Moreover, a correlation curve between precipitation and lagged versions of river discharge was computed. In order to estimate if river discharge had a delayed reaction to precipitation events, which could explain the high and isolated peaks. See Figure F- 5.

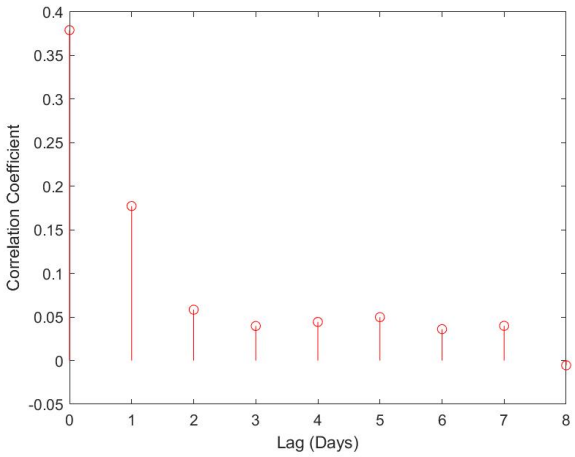


**Figure F- 5 Correlation Curve for the pair P-Q.**

The previous figure shows that the dependence of river discharge after a precipitation event decreases as the number of days after such event increases. This means that the initial correlation factor (Table F- 3) is still most adequate to model river discharge data.

The analysis presented in the previous paragraphs indicate that the model overestimates the values of river discharge. It is important to remember that the copula model did not include groundwater or infiltration data that could improve the generation of river discharge data.

Once the synthetic time series for the three variables were generated, the hydrological balance at Lake Texcoco was computed (Eq. F- 1).

$$PR_i \cdot A_{Tributary} + Q_i - E_i \cdot A_{lake_j} = \frac{dV}{dt}_{ij} \text{ [m}^3\text{/day]}$$

**Eq. F- 1**

In which:

- $PR_i$ : the ith value of precipitation on the lake surface [m$^3$/day].
- $E_i$ : the ith value of evaporation from the lake surface [m$^3$/day].
- $Q_i$ : ith value of inflow (River discharge) [m$^3$/day].
- $A_{Tributary}$ : Tributary area of the basin [m2].
- $A_{lake_j}$ : Surface area of the lake j [m2].
- $\frac{dV}{dt}_{ij}$ : the ith rate of change of volume at the lake at depth j [m$^3$/day].

The steps to obtain the water level in Lake Texcoco are the same as presented in section 4.4.3. The resulting water levels in Lake Mexico from the application of Eq. F- 1 are presented in Figure F- 6 and Figure F- 7.

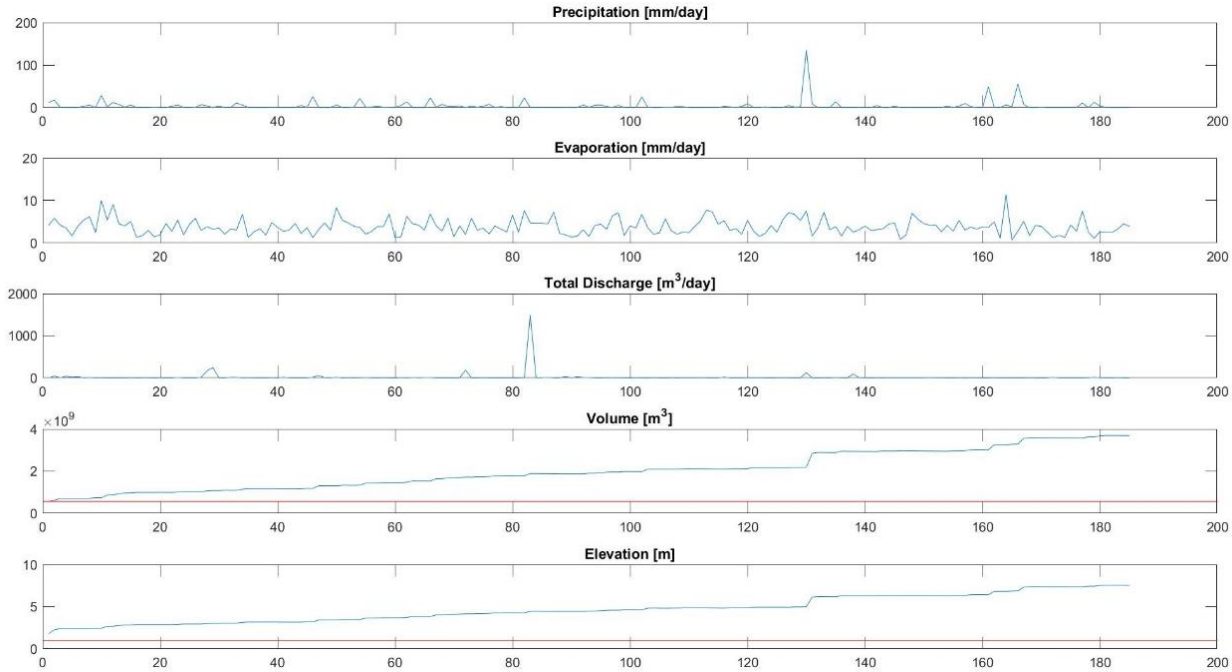


**Figure F- 6 Fluctuation of environmental data, volume and water elevation at Lake Texcoco in the wet season.**

X axis: Number of days in the wet season.

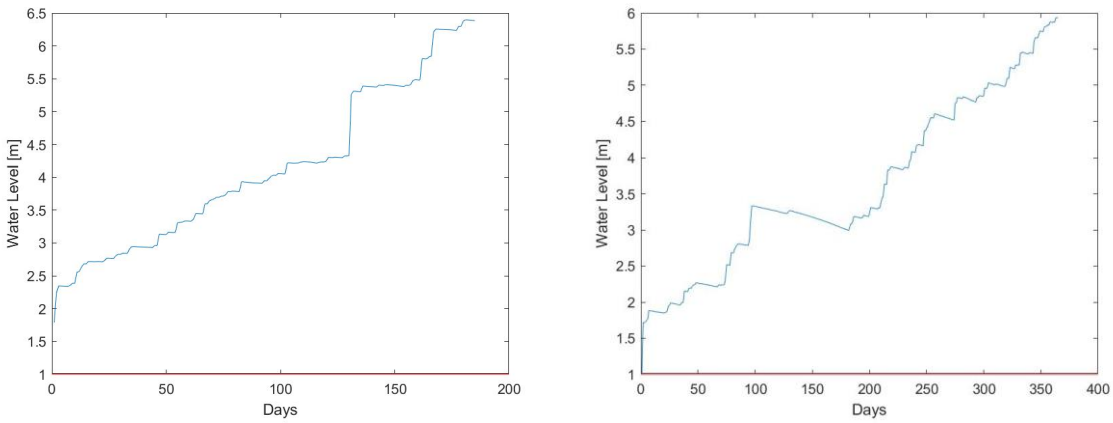


**Figure F- 7 Volume and water level fluctuation in Lake Texcoco during the wet season. Chapingo Station Data (Left) Simulated Data (Right).**

The bottom plot of Figure F- 6 shows that the water level at Lake Texcoco can increase approximately 5 or 6 meters (relative to the initial water depth), same as the results from section 6.3. A close up of the water level fluctuation in Figure F- 6 shows the same tendency as presented in Figure 6-12. It appears that adding river discharge data into the hydrological balance does not have a big influence in the generated water levels in Lake Texcoco.

The Probability of failure of the Nezahualcoyotl dike was then obtained by following the same procedure presented in sections 4.5 and 7.1. This procedure consisted in fitting the maximum water levels to a general extreme value distribution. The probability of failure was also computed for the case with and without wind set up. See Table F- 5.

| Water Depth at the foot of the dike [m] | M.a.s.l | PF (Without Set-up) | PF (With Set-up) |
|---|---|---|---|
| 1 | 2231 | 0.002 | 0.003 |
| 2 | 2232 | 0.013 | 0.018 |
| 3 | 2233 | 0.063 | 0.078 |
| 4 | 2234 | 0.223 | 0.261 |
| 5 | 2235 | 0.567 | 0.624 |
| 6 | 2236 | 0.918 | 0.943 |
| 7 | 2237 | 1 | 1 |
| 8 | 2238 | 1 | 1 |
| 9 | 2239 | 1 | 1 |
| 10 | 2240 | 1 | 1 |
| 11 | 2241 | 1 | 1 |
| 12 | 2242 | 1 | 1 |
| 13 | 2243 | 1 | 1 |
| 14 | 2244 | 1 | 1 |
| 15 | 2245 | 1 | 1 |
| 16 | 2246 | 1 | 1 |
| 17 | 2247 | 1 | 1 |
| 18 | 2248 | 1 | 1 |
| 19 | 2249 | 1 | 1 |
| 20 | 2250 | 1 | 1 |

**Table F- 5 Probability of failure (in any one year) given an initial water depth.**
*Including discharge data.

The previous table shows almost no difference with the results in Table 7-2 (Section 7.1). From these results, it is clear that including river discharge in the analysis does not influence the probability of failure of the Nezahualcoyotl dike.